High Precision QCD Calculation by Renormalon Subtraction and Applications to Heavy Quark Systems

Ph.D.Thesis

High Precision QCD Calculation by Renormalon Subtraction and Applications to Heavy Quark Systems

(リノーマロン除去による高精度QCD計算法の開発と
重いクォーク系への応用)

Yuuki Hayashi

令和4年

Abstract

In order to validate the Standard Model of particle physics with high accuracy in experiments such as LHC and Belle II, precise calculations of QCD effects on physical observables are highly demanded. In recent decades, it has become clear that the higher-order perturbative calculations have uncertainties due to renormalons which disrupt convergence of perturbative expansion. In this thesis, we develop a method for subtracting renormalons in the framework of the operator product expansion (OPE). The method utilizes the properties of the inverse Laplace transform to construct a convergent series, which enables a simultaneous separation of multiple renormalons from the perturbative expansion, systematically with a finite number of known expansion coefficients. This method is applied to observables of heavy quark systems such as the masses of the B and D mesons, and the inclusive semileptonic B decay width, by which we determine the parameters of EFT and one of the CKM matrix elements, $|V_{cb}|$, respectively. In both determinations subtraction of the next-order renormalons in $\overline{\text{MS}}$ mass scheme has been performed for the first time. The results are given by $\left[\bar{\Lambda}\right]_{\text{PV}} = 0.486\,(54)$ GeV, $\left[\mu_\pi^2\right]_{\text{PV}} = 0.05\,(22)$ GeV^2, and $|V_{cb}| = 0.04147\,(^{+98}_{-117})$, which are consistent with previous studies. These results indicate that the renormalon uncertainties are well suppressed, but that higher-order perturbative calculations are required in order to determine the parameters more accurately than the current precision. In particular, for the latter determination, the scheme dependence and the input parameter dependence of $|V_{cb}|$ are discussed in depth, in order to examine how the value of $|V_{cb}|$ will be determined as both theory and experiment progress in the future.

Contents

1 Introduction **3**

2 Theoretical framework for high precision QCD calculation **9**
2.1 **Operator Product Expansion** 9
2.2 **Renormalons in QCD** 10
2.3 **Renormalon subtraction based on OPE** 15

3 Method for renormalon subtraction using dual space **18**
3.1 **Basic concept of dual space** 18
3.2 **Formula for renormalon subtraction** 19
3.3 **Renormalon subtraction with simple cases** 23

4 Renormalon subtraction in heavy quark systems **32**
4.1 **OPE for Heavy Quark Systems** 32
4.1.1 **Heavy Quark Effective Theory** 32
4.1.2 **Renormalons of quark pole mass** 34
4.1.3 **Masses of B and D mesons** 35
4.1.4 **Inclusive semileptonic decay of B meson** 39
4.2 **Application I: Masses of B and D mesons** 41
4.2.1 **PV mass determination from $\overline{\rm MS}$ mass** 41
4.2.2 **Determination of HQET parameters** 50
4.3 **Application II: Inclusive semileptonic B decay** 52
4.3.1 **Renormalon cancellation using the DSRS method** 52
4.3.2 **$|V_{cb}|$ determination** 57

5 Conclusions and discussion **63**

A Perturbative coefficients **69**

B Relation between Borel transform and Dual transform **73**

C Including logarithmic corrections to DSRS method **79**

D Resummation of UV renormalons in DSRS method **84**

E Derivation of Eq. (4.51) **86**

F Renormalon cancellation in $B \to X_c \ell \bar{\nu}$ in the large-β_0 approximation 88

G Determination of $|V_{cb}|$ at N^{3}LO level using 1S state mass of bottomonium 90

Chapter 1

Introduction

To overcome renormalon problem in QCD

Frontier experiments at the LHC and Belle II have validated the Standard Model (SM) of particle physics to a high degree of accuracy, which has required theorists to accurately calculate observables. Perturbation theory is a powerful method to systematically calculate physical quantities in general quantum field theory. In particular in quantum chromodynamics (QCD), recent improvements in computational techniques and algorithms have made it possible to achieve higher-order calculations for various quantities. For example, the 5-loop (next-to-next-to-next-to-next-to leading order ($\mathrm{N^4LO}$) level) correction to the QCD beta function [1], the 3-loop ($\mathrm{N^3LO}$ level) correction to the static QCD potential [2, 3, 4], and the 4-loop ($\mathrm{N^3LO}$ level) correction to the heavy quark mass relation (pole-$\overline{\mathrm{MS}}$ mass relation) [5, 6, 7] were calculated. As a property of QCD, the QCD effects give important contributions to observables on a wide range of scales. Due to the asymptotic freedom of QCD, the higher-order perturbative calculations make the theoretical predictions more precise for the high-scale observables. On the other hand, for systems with a scale of about $\mathcal{O}(1-10)$ GeV, specifically those involving bottom or charm quarks, the theoretical uncertainties caused by 'renormalons' have limited the accuracy of perturbative calculations.

Renormalon [8, 9, 10, 11] is a concept that originates from an IR gluon in a particular loop diagram, which is known to cause the perturbative coefficients to factorially diverge. This is one of the reasons why perturbative expansion is asymptotic series, indicating that it is impossible to calculate the true value of observables by perturbative calculations alone in principle. Considering renormalons, the best prediction accuracy achievable using perturbative calculations is estimated as $(\Lambda_{\mathrm{QCD}}/Q)^{2u}$ with (half-)integer u for an observable with typical scale $Q \gg \Lambda_{\mathrm{QCD}}$. Here, $\Lambda_{\mathrm{QCD}} \sim 300$ MeV is the non-perturbative scale of QCD, indicating that the uncertainty caused by renormalon, which is the limit of perturbative calculations, is associated with a non-perturbative (low-energy) physics. For a system of the electroweak scale physics, $\Lambda_{\mathrm{QCD}}/Q \sim 0.1\%$ would be negligible at present, while for a system of the bottom or charm quarks, $\Lambda_{\mathrm{QCD}}/Q \sim 10\%$ jeopardizes the precision of the prediction significantly. Today, in the era of high-precision experiments on flavor physics, it is required to remove the uncertainty due to renormalons from theoretical predictions.

Historically, cancellation of renormalons made a strong impact in perturbative calcula-

tions for the heavy quarkonium system. Quarkonium is a bound state of quark-antiquark pairs, and it is known that the static QCD potential, which describes the binding energy of quark-antiquark pairs, shows drastic divergent behavior due to renormalons [12]. On the other hand, the potential alone is not an observable, and the quantity combined with the twice of on-shell mass (pole mass), which is the rest energy of the heavy quark-antiquark pair, is observed as the total energy of the quarkonium. In fact, the pole mass is also known to have renormalons, and the perturbative series of the pole mass expressed in terms of a short-distance mass (e.g. $\overline{\rm MS}$ mass) also shows divergent behavior [13, 14]. These divergent behaviors have been shown to mostly cancel out in the combination as the total energy, that is, the perturbative series of a physical observable [15, 16, 17]. Besides heavy quarkonium, the first renormalon in B meson observables (e.g. decay widths) is also known to cancel out by rewriting the pole mass by the $\overline{\rm MS}$ mass [14, 18, 19]. The cancellation of renormalons has radically improved the predictabilities of perturbative QCD expansions. These features have been applied successfully in the accurate determinations of fundamental physical constants, such as the masses of various heavy quarks [20, 21, 22, 23, 24], some of the Cabbibo-Kobayashi-Maskawa matrix elements [25, 26, 27], and the strong coupling constant α_s [28].

In order to make the perturbative calculations more precise, it is necessary to eliminate multiple renormalons beyond the first one, which requires a theoretical framework that systematically incorporates non-perturbative QCD effects. The operator product expansion [29] (OPE) enables to incorporate non-perturbative QCD effects based on low-energy effective field theory (EFT) and it is believed that the uncertainties caused by renormalons cancel out within the framework of OPE. In the OPE, an observable is given by an expansion in the inverse powers of the hard scale Q. This can be interpreted as the result of integrating out the ultraviolet (UV) degrees of freedom, and the coefficient functions of the expansion are called Wilson coefficients. Perturbative effects are pushed into them, hence theoretical prediction of the Wilson coefficient is destabilized by renormalons. On the other hand, each term of the OPE is proportional to an expectation value of a local operator (non-perturbative matrix element) that behaves as an integer power of $\Lambda_{\rm QCD}$, which is believed to absorb the corresponding renormalon of the Wilson coefficients [30]. After the renormalon cancellation, each term in the $1/Q$ expansion of the OPE becomes well-defined and the OPE gains predictability by incorporating non-perturbative effects. It is noteworthy that the validity of the OPEs has recently been confirmed with various observables in several OPEs implementing the first renormalon cancellation by rewriting the pole mass by a short-distance mass; see, for example, [23, 27]. Beyond the cancellation of the first renormalon, all we have to do is to separate the contributions of renormalons from the Wilson coefficients so as to be consistent with the renormalon cancellation in the OPE. One of the purposes of this thesis is a development of the method for separating renormalons from the Wilson coefficients of general observables.

Separating renormalons from the Wilson coefficients

Separating the effect of renormalon from the Wilson coefficients in the OPE of general observables requires a nontrivial procedure. In principle, focusing on the internal gluons in Feynman diagrams, the contributions from renormalons can be removed from the

calculation of a Wilson coefficient by separating the contribution of gluons with infrared (IR) momenta [31, 32]. Such an idea has been applied to several observables under an assumption called the large-β_0 approximation [33, 34, 35]. This is because the perturbative calculation can be written as a one-parameter integral with respect to the gluon momentum. Hence it is difficult to generalize this method to diagrams with more than one internal gluon. Also, the topology of the diagram depends on the details of the observable, which also prevents the generalization of the above method. In this thesis, we depart from the renormalon separation method based on the diagram calculation and construct a new method applicable to general observables.

The new method uses a transformation, called dual transform, which maps a divergent series due to renormalons to a convergent series. The mapped space is called the dual space characterized by the (dual-)momentum scale τ, which is dual to hard scale Q. Thus, no renormalon appears in the dual space. Below we briefly explain how we came to adopt this method.

The dual transformation is developed based on the knowledge of a specific physical quantity, the static QCD potential. It is empirically known that the perturbative series of the static QCD potential, a function of the quark-antiquark distance r, has a renormalon, whereas the potential in the momentum q-space does not show renormalon behavior [16, 17, 36]. Ref. [37] showed that the uncertainties from renormalons behaving as the integer power of the hard scale is suppressed by the Fourier transform, which is shown using analytic continuation. Inverse Fourier transform of the q-space potential reproduces renormalons in the original r-space, where the one-parameter q integral representation can be used to isolate the renormalon contribution. Importantly, even for higher-order perturbative expansions computed from diagrams with complex topology, the renormalon contributions can be systematically separated using the Fourier transform and inverse Fourier transform of the perturbative series. This method was used for precise determination of α_s by comparing a relatively low-scale lattice simulation with the renormalon-subtracted prediction [38, 39]. We have originally developed a method, called FTRS method (Renormalon Subtraction method using Fourier Transform), for separating renormalons from the Wilson coefficients using the Fourier transform as a dual transform for general observables [40, 41, 42]. We have applied the FTRS method to various observables such as the Adler function, the inclusive semileptonic decay width of B meson and masses of B and D mesons. The obtained results have shown a good consistency with theoretical expectations.

In this thesis, the inverse Laplace transform is employed as the dual transform, which also suppresses IR renormalons in the dual space. We call this method DSRS method (Renormalon Subtraction method using Dual Space). The DSRS method is preferable compared to the FTRS method in that the former can construct a more convergent dual-space series. Basic properties of the DSRS method are common to the FTRS method, which enables us to separate renormalons from the Wilson coefficients of general observables in a more sophisticated way than the other methods developed by previous studies [43, 44, 45, 46, 47].

Although the separation of renormalon contributions is generally scheme-dependent, the DSRS method gives the results in the same scheme as the methods of previous studies (principal value (PV) scheme) [43, 44, 45, 46, 47]. A particularly important property, compared with the previous methods, is the ability to simultaneously separate the con-

tributions of multiple renormalons, i.e., non-perturbative effects of different powers in $\Lambda_{\rm QCD}/Q$. In principle, the previous studies can also separate multiple renormalon contributions, but the separation of renormalons corresponding to higher order non-perturbative effects requires multiple steps of calculation to estimate the magnitude of the effect, which complicates the calculation procedure. The only information necessary to separate renormalons in the DSRS method is identification of non-perturbative effects which cancel the renormalons. This is determined by theoretical requirements from the OPE and renormalization group equation (RGE). The separation procedure is simpler than those of the previous studies.

Masses of B and D mesons

Another goal of this thesis is to determine the fundamental constants of particle physics by applying the DSRS method to observables of the heavy quark systems. First, we apply the DSRS method to the masses of the heavy-light mesons such as B and D mesons, which are bound states of a heavy quark and a light anti-quark. Observables of heavy-light mesons are computed in the OPE framework of the low energy EFT called the heavy quark effective theory (HQET) [48, 49, 50, 51, 52, 53]. HQET is an EFT suitable for hadrons containing only one heavy quark and a few light quarks, and the leading order (LO) contribution in the OPE calculation is described by the rest energy of the heavy quark. In addition, non-perturbative effects such as the kinetic energy of the heavy quark appear in the OPE. The non-perturbative parameters of HQET are common among the OPEs of various observables of the different mesons, defined in the infinite mass limit of heavy quarks. However, the on-shell mass (pole mass) of the heavy quark, equivalent to the rest energy, is known to have renormalons. They are canceled with the non-perturbative terms of the OPE of B and D. Using the DSRS method to separate the renormalons renders the non-perturbative parameters of HQET well-defined and enables their accurate determinations. We construct the OPE by subtracting the first two renormalons contained in the quark pole mass using the DSRS method. We use the latest perturbative expansion of the pole-$\overline{\rm MS}$ mass relation [5, 6, 7]. Then we determine the two parameters of HQET with the input $\overline{\rm MS}$ masses, by comparing the OPEs to the experimental values of masses of B and D mesons. This is the first time to determine the kinetic energy parameter μ_π^2 by eliminating renormalons in the PV scheme.

$|V_{cb}|$ determination

The second application is to determine the absolute value of one of the Cabbibo-Kobayashi-Maskawa (CKM) matrix elements, $|V_{cb}|$, by eliminating renormalons. The CKM matrix elements play important roles to explain flavor physics and CP violation in the SM. The value of $|V_{cb}|$ is determined using the experimental results of the semileptonic B decay process $B \to X_c \ell \bar{\nu}$. In fact, there has been a long-standing problem, which is called $|V_{cb}|$ puzzle, that there is a sizable discrepancy between the values of $|V_{cb}|$ determined by the exclusive decays $\bar{B} \to D^{(*)} \ell \bar{\nu}_\ell$ and by the inclusive decays $\bar{B} \to X_c \ell \bar{\nu}_\ell$. According to the

Particle Data Group (PDG) [54], the average value of the former analyses is given by

$$|V_{cb}|_{\text{excl.}} = (39.4 \pm 0.8) \times 10^{-3}, \tag{1.1}$$

while that of the latter is given by

$$|V_{cb}|_{\text{incl.}} = (42.2 \pm 0.8) \times 10^{-3}, \tag{1.2}$$

and the total average value of $|V_{cb}|$ is reported as $|V_{cb}|_{\text{ave.}} = (40.8 \pm 1.4) \times 10^{-3}$. The discrepancy between Eqs. (1.1) and (1.2) ($\sim 2.4\sigma$) is too large to be explained by the new physics possibilities, e.g., the new physics of the $V - A$ type is already ruled out by the experimental restriction to the $Zb\bar{b}$ vertex [55]. Recently, the contribution of new physics to the inclusive semileptonic decay has also been investigated [56]. In any case, before considering such a possibility, the accuracy of each analysis within SM should be tested carefully.

In this thesis, we calculate the OPE of the width of the inclusive semileptonic B decay by subtracting the renormalons from the LO Wilson coefficient using the latest perturbative calculation up to $\mathcal{O}(\alpha_s^3)$ [57]. In this analysis, the first renormalon of the LO Wilson coefficient is canceled out in the perturbative expansion by rewriting the quark pole mass by the $\overline{\text{MS}}$ mass [14, 18, 19]. Since the remaining renormalon is absorbed by one of the HQET parameters μ_π^2 by the DSRS method, the value of μ_π^2 determined from the B and D mesons can be used to calculate the renormalon-subtracted OPE of the decay width. This is then compared with the experimental data to determine $|V_{cb}|$ with the NLO renormalon removed. We compare our results with the results in other previous studies using the latest perturbative expansion [58, 59, 60]. We rewrite the pole mass by the $\overline{\text{MS}}$ mass, while other studies have used different mass schemes. In addition, paying attention to differences in theoretical parameters and input values from experimental data, we examine carefully the value of $|V_{cb}|$ determined from the inclusive decay.

Organization of Ph.D thesis

This thesis is organized as follows. In Chap. 2, the renormalon problem and its solution are briefly reviewed. First we introduce the OPE for a general observable, and the origin of renormalons in the Wilson coefficients is explained within the large-β_0 approximation. Then we discuss the conjecture to subtract renormalons in the framework of the OPE. In Chap. 3, we define the DSRS method and present several analyses in simple cases. First the basic concept of the DSRS method is explained. Secondly the DSRS method is formulated within the large-β_0 approximation and how to go beyond the large-β_0 approximation is discussed. Finally we apply the DSRS method to several examples in order to investigate its predictabilities. In Chap. 4, we apply the DSRS method to the observables of heavy quark systems, the B and D meson masses, and the inclusive semileptonic decay width of the B meson. First, we introduce the HQET to incorporate non-perturbative effects to observables of heavy-light mesons in the OPE framework. Secondly we determine the non-perturbative parameters in HQET by subtracting renormalons. Finally, we determine $|V_{cb}|$ using the $\overline{\text{MS}}$ mass of the bottom quark and subtracting renormalons and compare the results with the determinations in the previous studies. Chap. 5 is devoted to the conclusions and discussion. Details are presented in Appendices. In App. A, we

collect the perturbative coefficients used in our analyses. In App. B, we derive the relation between the Borel transform and dual transform. In App. C, we discuss the inclusion of logarithmic corrections to the renormalons into our method. In App. D, we explain how to resum the UV renormalons in the DSRS method in the large-β_0 approximation. In App. E, we derive the one-parameter integral form of the UV contribution to the quark pole mass in the PV scheme in the large-β_0 approximation. In App. F, we give a review of how the LO renormalon in the inclusive semileptonic B decay width is canceled by rewriting the quark pole mass by the $\overline{\rm MS}$ mass in the large-β_0 approximation. In App. G, we explain the details of the $|V_{cb}|$ determination at $\mathrm{N^3LO}$ level using the mass of the 1S bottomonium state.

Chapter 2

Theoretical framework for high precision QCD calculation

In this chapter, we briefly review the renormalon problem and the conjecture for its solution. In Sec. 2.1, we introduce the operator product expansion to systematically incorporate the non-perturbative QCD effects in theoretical calculations. In Sec. 2.2, the origin of renormalons is explained within the so-called large-β_0 approximation. Also in this section, the Borel transform, a standard method of renormalon analysis, is introduced. In Sec. 2.3, a conjecture to subtract renormalons in the framework of the OPE is discussed. Finally, we emphasize that it is necessary to develop a practical method to subtract renormalons, in order to achieve high precision QCD calculations.

2.1 Operator Product Expansion

In order to make theoretical calculations of physical observables in QCD more precise, non-perturbative corrections as well as perturbative effects must be considered simultaneously. The operator product expansion [29] (OPE) is a theoretical framework that enables factorization of QCD to systematically incorporate non-perturbative effects characterized by the QCD scale $\Lambda_{\rm QCD}$. Let us consider a physical observable $S(Q)$ that is renormalization group (RG) invariant and characterized by a single hard scale Q. The OPE of $S(Q)$ is given by

$$S(Q) = \sum_{i=0}^{\infty} C_i(Q) \frac{\langle \mathcal{O}_i \rangle}{Q^{d_i}}. \tag{2.1}$$

C_i is called the Wilson coefficient, which includes the ultraviolet (UV) contribution calculated by a perturbative calculation. $\mathcal{O}_i$ denotes the operator basis in the low energy effective field theory (EFT). In the case with dimensionless observable, d_i denotes the dimension of the operator $\mathcal{O}_i$. In particular, $\langle \mathcal{O}_i \rangle = \mathcal{O}(\Lambda_{\overline{\rm MS}}^{d_i})$, which implies that the OPE contains the non-perturbative corrections to S. Here $\Lambda_{\overline{\rm MS}} = \mathcal{O}(\Lambda_{\rm QCD})$ is the integration constant in the $\overline{\rm MS}$ scheme defined by

$$\frac{\Lambda_{\overline{\rm MS}}^2}{\mu^2} = \exp\left[-\left\{ \frac{1}{b_0 \alpha_s} + \frac{b_1}{b_0^2} \log\left(b_0 \alpha_s\right) + \int_0^{\alpha_s} dx \left(\frac{1}{\beta(x)} + \frac{1}{b_0 x^2} - \frac{b_1}{b_0^2 x} \right) \right\} \right], \tag{2.2}$$

where b_i's are the coefficients of the QCD beta function $\beta(\alpha_s)$. In this thesis, we take the convention

$$\beta(\alpha_s) = \mu^2 \frac{\partial \alpha_s(\mu^2)}{\partial \mu^2} = -\sum_{i=0}^{\infty} \alpha_s(\mu^2)^{i+2} b_i, \tag{2.3}$$

$$b_0 = \frac{1}{4\pi}\left(11 - \frac{2}{3}n_f\right), \quad b_1 = \frac{1}{(4\pi)^2}\left(102 - \frac{38}{3}n_f\right), \cdots, \tag{2.4}$$

where n_f is the number of light quarks. The latest perturbative expansion is known up to b_4 ($\mathrm{N^4LO}$) [1].

For the observables studied in this thesis, the LO term of the OPE corresponds to the partonic perturbative calculation of S. This term is proportional to $\langle \mathcal{O}_0 \rangle = 1$. The LO Wilson coefficient $C_0(Q)$ is perturbatively given by

$$C_0(Q) = \sum_{n=0}^{\infty} \alpha_s(Q^2)^{n+1} c_n. \tag{2.5}$$

Assuming that $C_0(Q)$ does not have anomalous dimension, the expansion of $C_0(Q)$ in $\alpha_s(\mu^2)$ is described using the QCD beta function, since $C_0(Q)$ is also RG invariant. It is given by

$$C_0(Q) = \sum_{n=0}^{\infty} \alpha_s(\mu^2)^{n+1} c_n(L_Q), \tag{2.6}$$

where $L_Q = \log(\mu^2/Q^2)$. $c_n(L_Q)$ can be determined by comparing the coefficient of $\alpha_s(\mu^2)^{n+1}$ on both sides of the relation

$$\sum_{n=0}^{\infty} \alpha_s(\mu^2)^{n+1} c_n(L_Q) = e^{\hat{H}\log(\mu^2/Q^2)} \sum_{n=0}^{\infty} \alpha_s(\mu^2)^{n+1} c_n. \tag{2.7}$$

We note that $c_n = c_n(L_Q = 0)$. Here the operator $\hat{H}$ is given by

$$\hat{H} = -\beta(\alpha_s(\mu^2)) \frac{\partial}{\partial \alpha_s(\mu^2)}, \tag{2.8}$$

which operates on the $\alpha_s(\mu^2)$ expansion on the right hand side of Eq. (2.7). Then $c_n(L_Q)$ is obtained as the n-th order polynomial of L_Q.

In general, a naive perturbative calculation in QCD gives an asymptotic divergent series due to renormalons [8, 9, 10, 11]. Renormalons in $C_0(Q)$ set a limit of the perturbative prediction, which is equal to or greater than the magnitude of the non-perturbative corrections of the OPE. Therefore, in order to properly incorporate non-perturbative effects in the OPE framework, the renormalon problem must be resolved. In the next section, we analytically examine renormalons within the large-β_0 approximation and then briefly outline how the renormalon problem is recognized beyond that approximation.

2.2 Renormalons in QCD

The large-β_0 approximation

The large-β_0 approximation is an extension of the large-n_f approximation, which is useful to approximately calculate QED observables. In the limit that the number of massless

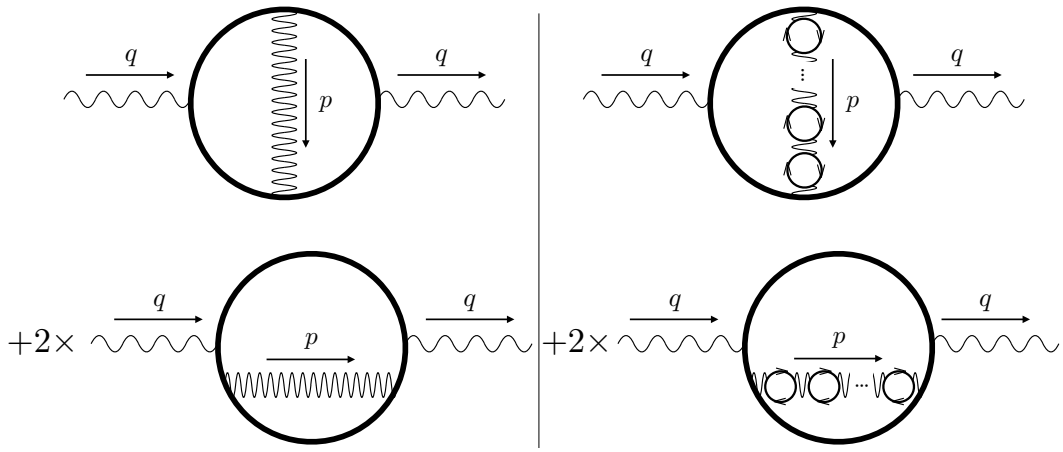

Figure 2.1: Diagrams which contribute to the vacuum polarization of photon in the large-n_f approximation.

fermions n_f is sufficiently large, the N^{n}LO corrections to an QED observable is given as the diagrams in Fig. 2.1 (b), where n fermion vacuum bubbles are inserted into the internal photon of LO diagram given in Fig. 2.1 (a). The contributions from such diagrams are proportional to n_f^n. In the large-β_0 approximation, the N^{n}LO corrections to an QCD observable is given by replacing $n_f \to -3/2(\beta_0 - 11)$ of QED calculation in the large-n_f approximation. Corresponding diagrams are shown in Fig. 2.2 (b), where n one-loop vacuum polarizations are inserted into the internal gluon of LO diagram given in Fig. 2.1 (a), which are proportional to the n-th power of $b_0 = (11-2n_f/3)/(4\pi)$. In the cases where renormalon contributions are large, empirically, the perturbative coefficients computed in the large-β_0 approximation well reproduce the divergent behavior of the real perturbative coefficients.

Origin of renormalons

Renormalons are known as the cause of a factorial divergent behavior of a perturbative expansion as $c_n \sim b_0^n n!$.[1] In the large-β_0 approximation, the origin is understood as follows. In this approximation, the N^{n}LO correction to $C_0(Q)$ is given by the diagrams in Fig. 2.2 (b), where p is a loop momentum transferred by the internal gluon and $-q^2 = Q^2$ denotes a hard external momentum. This contribution is expressed in the following form

$$\alpha_s(\mu^2)^{n+1} c_n^{\beta_0}(L_Q) = \alpha_s(\mu^2)^{n+1} \int_0^\infty dp_E^2 \, F(p_E^2, \mu^2/Q^2, \mu^2/p_E^2) \big(b_0 \, \log(\mu^2 \, e^{-5/3}/p_E^2)\big)^n, \tag{2.9}$$

where $L_Q = \log(\mu^2/Q^2)$, and we use the one-loop $\overline{\rm MS}$ running coupling constant as

$$\alpha_s(\mu^2) = \frac{1}{b_0 \log(\mu^2/\Lambda^2_{\overline{\rm MS}})}, \tag{2.10}$$

[1] There is another source of the rapid growth, behaved as $c_n \sim n!/(4\pi)^n$, which is occured from the proliferation of the number of Feynman diagrams. In this paper, we ignore the divergence due to the proliferation, since it is greatly suppressed compared to that due to renormalons.

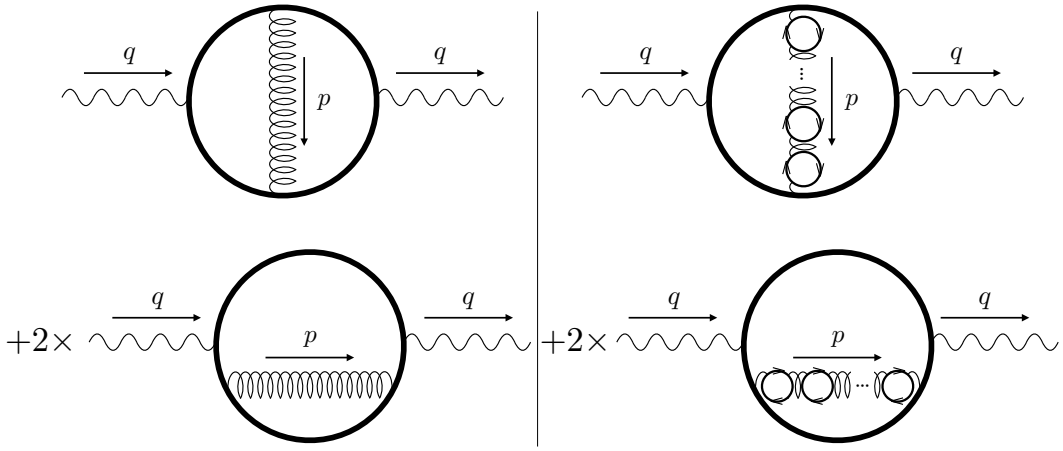

(a) $\mathcal{O}(\alpha_s)$ (b) $\mathcal{O}(\alpha_s^{n+1})$

Figure 2.2: Diagrams which contribute to the vacuum polarization of photon in the large-β_0 approximation.

in this approximation. Here $\Lambda_{\overline{\rm MS}}$ is given by Eq. (2.2) with $b_{i\geq 1} = 0$. p_E^2 is the square of the Euclidean momentum of the internal gluon, after the Wick rotation. F denotes the structure function of the LO loop diagrams. The logarithmic factor comes from each of n vacuum bubbles, and each factor is proportional to b_0.

If the structure function F behaves as $(p_E^2)^{u_{IR}-1}$ ($u_{IR} > 0$) when p_E^2 is sufficiently small (infrared), Eq. (2.9) is IR finite. However, since the logarithmic factor increases in the IR regions, $c_n^{\beta_0}$ for a large n behaves asymptotically as

$$c_n^{\beta_0}(L_Q) \approx n!\big(\mu^2/Q^2\big)^{u_{IR}}\big(b_0/u_{IR}\big)^{n+1} \quad (\text{from IR region}), \tag{2.11}$$

which shows a sign-definite growth since $b_0 > 0$ in QCD. The source of this behavior is called the IR renormalons, which breaks down the naive perturbative expansion and limits the accuracy of prediction. Considering the case with a sufficiently large number of perturbative coefficients c_n's $= \{c_0, c_1, \cdots, c_k\}$, we can see that the following relation

$$|\alpha_s(\mu^2)^k c_{k-1}(L_Q)| \approx |\alpha_s(\mu^2)^{k+1} c_k(L_Q)|, \tag{2.12}$$

gives the limit of the prediction using known coefficients. It implies that the size of the perturbative correction is minimal at $n \approx k$ and that the sum up to this term gives the best prediction achievable using the perturbative expansion. In the large-β_0 approximation, $c_n \to c_n^{\beta_0}$, using the asymptotic behavior Eq. (2.11), we obtain

$$k \approx \frac{u_{IR}}{b_0 \alpha_s(\mu^2)}, \tag{2.13}$$

which gives the size of an inevitable uncertainty for perturbative calculation as

$$|\alpha_s(\mu^2)^{k+1} c_k(L_Q)| \approx \left(\frac{\Lambda_{\overline{\rm MS}}^2}{Q^2}\right)^{u_{IR}}, \tag{2.14}$$

where we use the one-loop running coupling constant Eq. (2.10). This has a non-perturbative form in α_s, which tells us that the renormalons represent a non-perturbative limit of perturbative calculations.

Similarly the ultraviolet behavior of $F(p_E^2)$ as $(p_E^2)^{u_{UV}-1}$ ($u_{UV} < 0$) generates the asymptotic behavior of $c_n^{\beta_0}$ as

$$c_n^{\beta_0} \approx n!\big(\mu^2/Q^2\big)^{u_{UV}}\big(-b_0/|u_{UV}|\big)^{n+1} \quad (\text{from UV region}), \tag{2.15}$$

which shows a sign-alternating growth. It is called the UV renormalon. We note that the UV renormalons in QCD also make the theoretical prediction worse in fixed order calculation. The size of the theoretical uncertainty is estimated as

$$|\alpha_s(\mu^2)^{k+1} c_k(L_Q)| \approx \left(\frac{\Lambda^2_{\overline{\rm MS}} Q^2}{\mu^4}\right)^{|u_{UV}|}, \tag{2.16}$$

with

$$k \approx \frac{|u_{UV}|}{b_0 \alpha_s(\mu^2)}. \tag{2.17}$$

We note that Eq. (2.16) is scale-dependent, which gets smaller when we take μ at higher scale. Moreover, such contributions can be resummed using the Borel resummation introduced in the next section. On the other hand, contributions from the IR renormalons cannot be resummed unambiguously.

Borel transform and renormalons

The standard framework to investigate the renormalons is known as the Borel transform. For the LO Wilson coefficient $C_0(Q)$ given by Eq. (2.6), the Borel transform of C_0 is defined as

$$B_{C_0}(u) = \sum_{n=0}^{\infty} \frac{c_n(L_Q)}{n!}\left(\frac{u}{b_0}\right)^n. \tag{2.18}$$

In the large-β_0 approximation, Eq. (2.18) behaves as

$$B_{C_0}(u) \approx \left(\frac{\mu^2}{Q^2}\right)^u \frac{1}{1-u/u_{IR}}, \tag{2.19}$$

due to IR renormalons Eq. (2.11) and

$$B_{C_0}(u) \approx \left(\frac{\mu^2}{Q^2}\right)^u \frac{1}{1+u/|u_{UV}|}, \tag{2.20}$$

due to UV renormalons Eq. (2.15). We can see that IR/UV renormalons cause the singularities on the positive/negative real axis in the complex u plane (Borel plane) as in Fig. 2.3. By convention, the position of the pole singularity at $u = u_*$ is called the $u = u_*$ renormalon. In the large-β_0 approximation, the singularity from renormalons is a pole. On the other hand, beyond this approximation, IR (UV) renormalons cause branch points, where the branch cut extends along the real axis to the right (left).

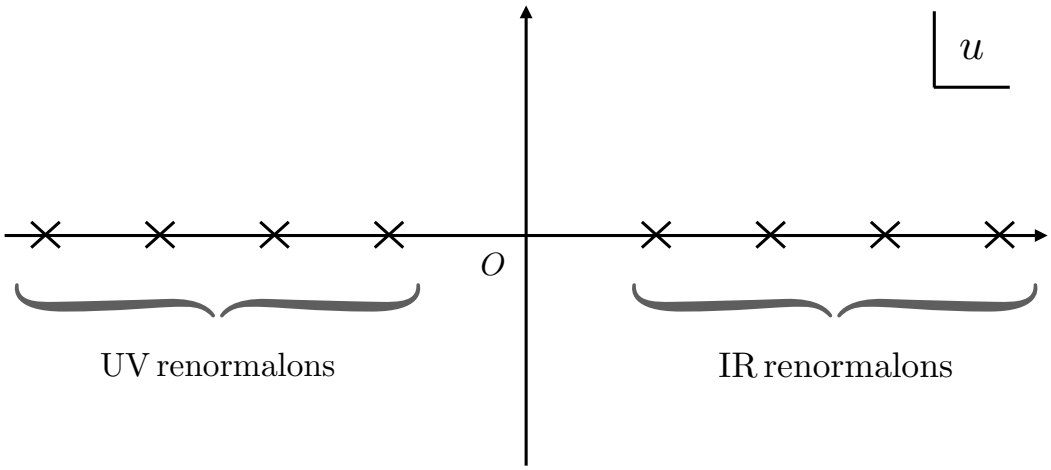

Figure 2.3: The singularities in the complex u plane caused by the IR and UV renormalons in the large-β_0 approximation. In the case beyond the large-β_0 approximation, discontinuities are caused on the real axis.

One of the good properties of the large-β_0 approximation is that it is easy to perform perturbative calculations by Eq. (2.9), regardless of how high the order of the perturbation. The Borel transform is suited to describe the all-order perturbative series in the large-β_0 approximation. A static QCD potential, for example, is calculated in the large-β_0 approximation as

$$V(r) = -\frac{4\pi C_F}{r}\sum_{n=0}^{\infty}\alpha_s(\mu^2)^{n+1}a_n^{(\beta_0)}(L_r), \tag{2.21}$$

where $C_F = 4/3$ and $L_r = \log(\mu^2 r^2)$. The Borel transform of $V(r)$ is given by

$$B_V(u) = \sum_{n=0}^{\infty}\frac{a_n^{(\beta_0)}(L_r)}{n!}(u/b_0)^n = \left(\frac{\mu^2 r^2 e^{5/3}}{4}\right)^u \frac{1}{4\pi^{3/2}}\frac{\Gamma(1/2-u)}{\Gamma(1+u)}, \tag{2.22}$$

which has the information of all-order coefficients. We can see that a static QCD potential contains the IR renormalons at $u = 1/2,\, 3/2,\, 5/2, \cdots$.

Naively, $C_0(Q)$ is reproduced by the Borel resummation given by

$$C_0(Q)\text{“}=\text{”}\frac{1}{b_0}\int_0^{\infty} du\, e^{-\frac{u}{b_0\alpha_s(\mu^2)}} B_{C_0}(u). \tag{2.23}$$

This equality is valid only if there is no IR renormalon in C_0, which results in a singularity on the integration contour of Eq. (2.23), otherwise Eq. (2.23) is ill-defined. If we expand B_{C_0} in u, the integral becomes well-defined but reproduces the factorial behavior of perturbative expansion because

$$\frac{1}{b_0}\int_0^{\infty} du\, e^{-\frac{u}{b_0\alpha_s}}(u/b_0)^n = n!\,\alpha_s^{n+1}. \tag{2.24}$$

The well-defined resummation formula can be given by

$$\left[C_0(Q)\right]_{\pm} = \frac{1}{b_0}\int_{C_{\pm}} du\, e^{-\frac{u}{b_0\alpha_s(\mu^2)}} B_{C_0}(u), \tag{2.25}$$

where $C_\pm(u)$ denotes the integration contour connecting $u = 0$ and $u = +\infty \pm i0$ infinitesimally above/below the positive real axis on which the discontinuities are located. Then Eq. (2.25) is a finite-value (well-deifined) integral but contains an imaginary part due to the contour $C_\pm$. The imaginary part of $\big[C_0\big]_\pm$ is given by

$$\mathrm{Im}\big[C_0(Q)\big]_\pm \equiv \pm i\,\delta C_0(Q), \tag{2.26}$$

where

$$\delta C_0(Q) = \frac{1}{2b_0 i}\int_{C_+-C_-} du\, e^{-\frac{u}{b_0\alpha_s(\mu^2)}} B_{C_0}(u). \tag{2.27}$$

The integration contour can be deformed to surround the singularities due to the IR renormalons. Since the sign of the imaginary part depends on the integration contour in Eq. (2.26), δC_0 is interpreted as a measure of the uncertainty of the perturbation prediction. In the large-β_0 approximation, Eq. (2.19) tells us that

$$\delta C_0(Q) \approx -\frac{1}{2b_0 i}\oint du\, e^{-\frac{u}{b_0\alpha_s(\mu^2)}}\left(\frac{\mu^2}{Q^2}\right)^u \frac{1}{1-u/u_{IR}} \propto \left(\frac{\Lambda^2_{\overline{\rm MS}}}{Q^2}\right)^{u_{IR}}, \tag{2.28}$$

which is an inevitable theoretical uncertainty consistent with Eq. (2.14) estimated from the IR renormalon at $u = u_{IR}$.

On the other hand, the real part of Eq. (2.25) is given by

$$\begin{aligned}\mathrm{Re}\big[C_0(Q)\big]_\pm &= \frac{1}{2b_0}\int_{C_++C_-} du\, e^{-\frac{u}{b_0\alpha_s(\mu^2)}} B_{C_0}(u) \\ &= \frac{1}{2b_0}\int_{0,\mathrm{PV}}^{\infty} du\, e^{-\frac{u}{b_0\alpha_s(\mu^2)}} B_{C_0}(u),\end{aligned} \tag{2.29}$$

which is independent of the choice of the contour. In this thesis, we define the finite prediction of $C_0(Q)$ by Eq. (2.29). This prescription is called PV scheme, which is a standard framework to calculate the renormalon-subtracted prediction in QCD, even beyond the large-β_0 approximation.

We note that the UV renormalons does not cause a problem in the Borel resummation. Since the singularities due to the UV renormalons are located on the negative real axis in the complex u plane (see Fig. 2.3), they does not make Eq. (2.23) ill-defined. Using Eq. (2.20), for example, the Borel resummation integral is evaluated as

$$\frac{1}{b_0}\int_0^\infty du\, e^{-\frac{u}{b_0\alpha_s(\mu^2)}}\left(\frac{\mu^2}{Q^2}\right)^u \frac{1}{1+u/|u_{UV}|} = -\frac{|u_{UV}|}{b_0} e^{\frac{|u_{UV}|}{b_0\alpha_s(Q^2)}}\mathrm{Ei}\Big(\frac{-|u_{UV}|}{b_0\alpha_s(Q^2)}\Big), \tag{2.30}$$

where $\mathrm{Ei}(z) = -\int_{-z}^\infty dt\, e^{-t}/t$.

2.3 Renormalon subtraction based on OPE

Conjecture to subtract renormalons

In the Borel resummation, IR renormalons cause an inevitable imaginary part to the Wilson coefficients. The imaginary part measures the uncertainty of the perturbative calculation of the Wilson coefficient, which has a non-perturbative form as in Eq. (2.28). As

explained in Sec. 2.1, the non-perturbative QCD effects are incorporated in the framework of the OPE as in Eq. (2.1). Such an imaginary part is expected to vanish within the OPE framework as described below.

Let us consider the LO Wilson coefficient $C_0(Q)$ given by Eq. (2.5), and assume that it has an IR renormalon at $u = u_0$, which is the closest to the origin in the Borel u plane among all the IR renormalons. This renormalon causes an imaginary part $\pm i\,\delta C_0(Q)$ including $\log(Q)$ corrections in the case beyond the large-β_0 approximation. Conjecture of the renormalon subtraction in the OPE framework is that the imaginary part due to the renormalon is absorbed by the same size of imaginary part of the non-perturbative correction of the OPE of S. Assuming that the imaginary part due to the renormalon at $u = u_0$ is absorbed by the first non-perturbative correction to S in Eq. (2.1), $\delta C_0(Q)$ is required to have the same Q-dependence as the $1/Q^{d_1}$ term [30]. Then $\delta C_0(Q)$ is determined as follows [11]:

$$\delta C_0(Q)\Big|_{u=u_0} = N_{u_0}\left(\frac{\Lambda^2_{\overline{\rm MS}}}{Q^2}\right)^{u_0}(b_0\alpha_s(Q))^{\gamma_0/b_0}\left(1+\sum_{n=0}^{\infty}s_n\alpha_s(Q)^{n+1}\right),\quad u_0=\frac{d_1}{2}. \tag{2.31}$$

γ_i is the coefficient of the anomalous dimension γ for the leading operator $\mathcal{O}_1$ given by

$$\gamma(\alpha_s) = \sum_{i=0}^{\infty}\alpha_s^{i+1}\gamma_i. \tag{2.32}$$

The perturbative coefficient s_n can be constructed from the RGE parameters b_i, γ_i and the perturbative expansion coefficients of the Wilson coefficient C_1. Apart from the normalization N_{u_0}, which depends on the observable S, in principle all the parameters are determined using the OPE and RGE framework. Eq. (2.31) implies that the Borel transform of C_0, beyond the large-β_0 approximation, has the following singular structure in the vicinity of $u = u_0$.

$$B_{C_0}(u) = \left(\frac{\mu^2}{Q^2}\right)^{u_0}\frac{N'_{u_0}}{(1-u/u_0)^{1+\nu_{u_0}}}\sum_{n=0}^{\infty}s'_n(L_Q)(1-u/u_0)^n + (\text{regular part}), \tag{2.33}$$

where

$$N'_{u_0} = \frac{b_0}{\pi}\frac{\Gamma(1+\nu_{u_0})}{{u_0}^{1+\nu_{u_0}}}N_{u_0}. \tag{2.34}$$

Coefficient s'_n is also determined by the RGE parameters and the perturbative coefficients of the Wilson coefficients. We note that the assumption to cancel imaginary parts in the OPE cannot determine the normalization parameter N'_{u_0} and the full analytic structure of B_{C_0}.

Practical way to subtract renormalons

In the large-β_0 approximation, perturbative calculations can be performed at an arbitrary power of α_s, by considering the bubble-chain diagrams. Then factorial behavior due to renormalons leads to singularities on the real axis in the Borel plane. In realistic cases beyond the large-β_0 approximation, only a limited number of terms can be computed and then the Borel transform cannot be resummed by definition. Assuming the

cancellation of the imaginary parts in the framework of the OPE as in Sec. 2.3, singular structures of the Borel transform can be described using the OPE and RGE as in Eq. (2.33), but a full analytic structure of the Borel transform cannot be determined. Then the renormalon-subtracted Wilson coefficient, which is calculated by Eq. (2.29), only reproduces the original divergent series because the Borel transform is incomplete. Thus, in practical cases, it is necessary to develop a method for approximately calculating Eq. (2.29) from the information of a finite number of perturbative coefficients. In the next chapter, we propose a new method to calculate Eq. (2.29) using the properties of the inverse Laplace transform, which constructs a dual space where perturbative series becomes convergent. Using such a dual-space series, we can compute the renormalon-subtracted Wilson coefficient systematically from a finite number of coefficients.

Chapter 3

Method for renormalon subtraction using dual space

In this chapter, we advocate a method for subtracting IR renormalons from the Wilson coefficient by introducing a dual space. We call this method DSRS method (Renormalon Subtraction method using Dual Space). In Sec. 3.1, the basic concept of the DSRS method is explained. In Sec. 3.2, the DSRS method is formulated within the large-β_0 approximation and how to go beyond the large-β_0 approximation is discussed. In Sec. 3.3, we apply the DSRS method to a static QCD potential computed in the large-β_0 approximation. Towards practical applications in Chap. 4, we investigate the stability of the prediction obtained with a finite number of perturbative coefficients. Moreover, we analyze UV renormalons in the dual space based on a toy model.

3.1 Basic concept of dual space

Using Eq. (2.9), the all-order expansion of $C_0(Q)$ in the large-β_0 approximation is given by

$$\begin{aligned} C_0(Q)\Big|_{\rm LB} &= \sum_{n=0}^{\infty} \alpha_s(Q^2)^{n+1} c_n^{\beta_0} \\ &= \int_0^\infty dp_E^2\, F(p_E^2, Q^2/p_E^2) \sum_{n=0}^{\infty} \alpha_s(Q^2)^{n+1} \big(b_0\, \log(Q^2\, e^{-5/3}/p_E^2)\big)^n \\ &= \int_0^\infty dp_E^2\, F(p_E^2, Q^2/p_E^2)\, \alpha_{\beta_0}(p_E^2), \end{aligned} \tag{3.1}$$

where logarithmic factors are resummed and absorbed into the running coupling constant α_{β_0} given by

$$\alpha_{\beta_0}(q^2) = \frac{\alpha_s(\mu^2)}{1 - b_0 \alpha_s(\mu^2)\, \log(\mu^2\, e^{-5/3}/q^2)} = \frac{1}{b_0 \log\left(q^2/(\Lambda_{\overline{\rm MS}}\, e^{5/6})^2\right)}. \tag{3.2}$$

We can see that Eq. (3.1) is an ill-defined (divergent) integral because of the Landau singularities of the running coupling constant. This is an alternative view of the divergence

of perturbative calculations by renormalons. We can define the well-defined momentum integral by contour deformation to $C_\pm$. It is given by

$$\left[C_0(Q)\right]_\pm = \int_{C_\mp} dp_E^2\, F(p_E^2, Q^2/p_E^2)\, \alpha_{\beta_0}(p_E^2), \tag{3.3}$$

which consists of a finite real part and an uncertain imaginary part depending on the contour $C_\pm$. It is important to note that the integrand of Eq. (3.3) is a convergent series in the $\alpha_s(\mu^2)$ expansion in the momentum p_E space, which enables us to predict the renormalon-subtracted Wilson coefficient from a finite number of coefficients. Beyond the large-β_0 approximation, however, this calculation procedure is difficult to perform. It is because the loop integral in the realistic case contains multiple loop momenta, and it is generally cumbersome to rewrite it in a simple one-parameter integral form such as Eq. (3.3). Moreover, rewriting the loop integral in such a way depends on the details of the observable and it is not a suitable way to address the problem of renormalons that is universal to QCD calculations. In the next section, the concept of a dual space is introduced to calculate the renormalon-subtracted Wilson coefficient from a finite number of perturbative coefficients. We will see that the IR renormalons can be suppressed in the dual space, i.e., the dual-space perturbative series converges.

3.2 Formula for renormalon subtraction

In this section, we formulate the DSRS method. First, we consider the case within the large-β_0 approximation which helps us to understand the mechanism of the DSRS method. After that, generalization to the case beyond the large-β_0 approximation is discussed.

In the large-β_0 approximation

The LO Wilson coefficient $C_0(Q)$ containing IR renormalons is given by

$$C_0(Q) = \sum_{n=0}^{\infty} \alpha_s(\mu^2)^{n+1} c_n(L_Q) = e^{\hat{H}\log(\mu^2/Q^2)} \sum_{n=0}^{\infty} \alpha_s(\mu^2)^{n+1} c_n, \tag{3.4}$$

where the operator $\hat{H}$ is given by Eq. (2.8). The QCD beta function in the large-β_0 approximation is

$$\beta(\alpha_s) = -b_0\, \alpha_s^2, \tag{3.5}$$

which determines the running coupling constant $\alpha_s(\mu^2)$ as in Eq. (2.10). $L_Q = \log(\mu^2/Q^2)$ dependence of $c_n(L_Q)$ is determined as in Eq. (2.7).

A dual space is constructed by a dual transform based on the inverse Laplace transform

$$\int_{v_0-i\infty}^{v_0+i\infty} \frac{dv}{2\pi i}\, e^{v\,w} v^u = \frac{1}{w^{1+u}} \frac{1}{\Gamma(-u)}, \quad v_0 > 0. \tag{3.6}$$

$\tilde{C}_0(\tau)$, the LO Wilson coefficient in the dual space, is defined as

$$\tilde{C}_0(\tau) = \int_{x_0^2-i\infty}^{x_0^2+i\infty} \frac{dx^2}{2\pi i}\, e^{\tau^2 x^2} x^{2au'} C_0(Q = x^{-a}), \quad x_0^2 > 0, \tag{3.7}$$

where we define $x = Q^{-1/a}$ and introduce the parameters (a, u') which are necessary for renormalon subtraction. Substituting $\delta C_0 = (\Lambda^2_{\overline{\rm MS}} x^{2a})^{u_*}$ in place of C_0 on the right hand side of Eq. (3.7), we obtain the $u = u_*$ renormalon in the dual space given by

$$\delta\tilde{C}_0(\tau) = \frac{1}{(\tau^2)^{1+au'}} \frac{1}{\Gamma(-a(u_* + u'))} \left(\frac{\Lambda^2_{\overline{\rm MS}}}{\tau^{2a}}\right)^{u_*}. \tag{3.8}$$

We can see that the right hand side of Eq. (3.8) is zero when $a(u_* + u') = 0, 1, 2, \cdots$, which means that the renormalons in the dual space can be suppressed by the dual transform with a proper choice of the parameters. In particular, it is crucial that multiple renormalons are suppressed simultaneously. We assume that the $u_* = u_0 (> 0)$ renormalon is the one closest to the origin in the Borel plane and the minimal interval between the positions of IR renormalons is δu. Then adjusting the parameters as $(a, u') = (1/\delta u, -u_0)$ makes all the renormalons (at $u = u_0,\ u_0 + \delta u,\ u_0 + 2\delta u, \cdots$) suppressed in the dual space as in Fig. 3.1. Thus, in the dual space, we can construct convergent series $\tilde{C}_0$, whose explicit form in $\alpha_s(\mu^2)$ expansion is given by

$$\tilde{C}_0(\tau) = \frac{1}{(\tau^2)^{1+au'}} \sum_{n=0}^{\infty} \alpha_s(\mu^2)^{n+1} \tilde{c}_n(L_\tau) = \frac{1}{(\tau^2)^{1+au'}} e^{\hat{H}\log(\mu^2/\tau^{2a})} \sum_{n=0}^{\infty} \alpha_s(\mu^2)^{n+1} \tilde{c}_n, \tag{3.9}$$

where $L_\tau = \log(\mu^2\tau^{2a})$. L_τ dependence of $\tilde{c}_n(L_\tau)$ is determined as in Eq. (2.7). $\tilde{c}_n = \tilde{c}_n(L_\tau = 0)$ is determined by comparing the coefficient of $\alpha_s(\mu^2)^{n+1}$ on both sides of the following relation

$$\sum_{n=0}^{\infty} \alpha_s(\mu^2)^{n+1} \tilde{c}_n = \frac{1}{\Gamma(-a(\hat{H} + u'))} \sum_{n=0}^{\infty} \alpha_s(\mu^2)^{n+1} c_n. \tag{3.10}$$

We note that the Borel transform of the dual-space series $B_{\tilde{C}_0}(u) \equiv \sum_{n=0}^{\infty} \frac{\tilde{c}_n(L_\tau)}{n!}(u/b_0)^n$, in the large-$\beta_0$ approximation, is expressed by

$$B_{\tilde{C}_0}(u) = \frac{1}{\Gamma(-a(u + u'))} B_{C_0}(u)\Big|_{L_Q \to L_\tau}, \tag{3.11}$$

where $B_{C_0}(u)$ is given by Eq. (2.18). It implies that the dual transform directly suppresses renormalon poles in the Borel plane.

When we set $\mu = \tau^a$ in Eq. (3.9), the logarithmic dependence is resummed and $\tilde{C}_0(\tau)$ exhibits a good convergence for sufficiently small $\alpha_s(\tau^{2a})$. From a finite number of perturbative coefficients $\{c_0, c_1, \cdots, c_k\}$, we can use the truncated series of Eq. (3.9) given by

$$\tilde{C}_0^{(k)}(\tau) = \frac{1}{(\tau^2)^{1+au'}} \sum_{n=0}^{k} \alpha_s(\tau^{2a})^{n+1} \tilde{c}_n, \tag{3.12}$$

which would be a good approximation of $\tilde{C}_0(\tau)$ for a large k.

From $\tilde{C}_0$, we can reconstruct C_0 using the inverse dual transform, which is defined by

$$C_0(Q) \text{“} = \text{”} x^{-2au'} \int_0^{\infty} d\tau^2\, e^{-\tau^2 x^2} \tilde{C}_0(\tau). \tag{3.13}$$

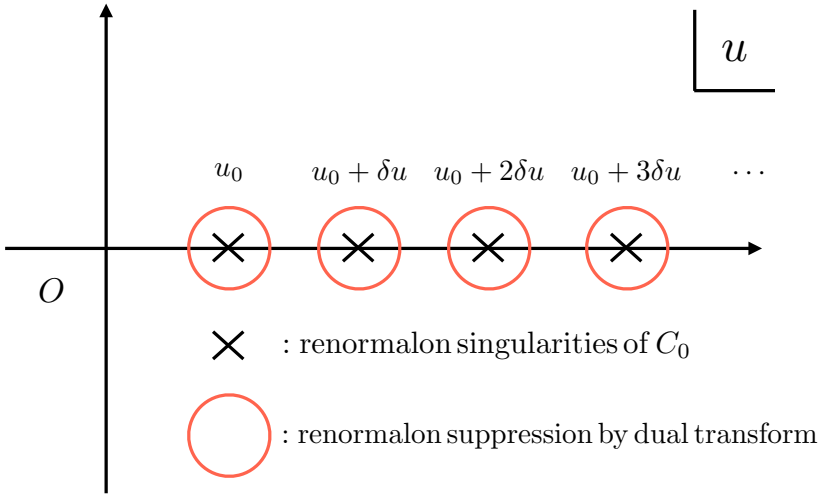

Figure 3.1: Schematic figure explaining the suppression of renormalons in the dual space with parameters set to $(a, u') = (1/\delta u, -u_0)$.

Since the left hand side of Eq. (3.13) contains IR renormalons, the Laplace integral on the right hand side of (3.13) reproduces the renormalons. $\alpha_s(\tau^a)$ in $\tilde{C}(\tau)$ has the Landau pole on the positive real axis in the complex τ plane. Thus the Landau pole of the integrand makes the integral value ill-defined, in other words, it causes the IR renormalons of C_0. Hence, we define the regularized Wilson coefficient such that the integration contour avoids the singularities. It is given by

$$\big[C_0(Q)\big]_\pm = x^{-2au'} \int_{C_\mp} d\tau^2\, e^{-\tau^2 x^2} \tilde{C}_0(\tau), \tag{3.14}$$

where $C_\pm(\tau)$ denotes the integration contour connecting $\tau = 0$ and $\tau = \infty$ avoiding the singularities above/below in the direction of the imaginary axis. We have numerically confirmed that it is possible to choose a contour $C_\pm(\tau)$ such that $|\alpha_s(\tau^a)| < 1$ on the contour. We can utilize the convergence of $\tilde{C}_0(\tau)$ there. Eq. (3.14) contains the imaginary part due to avoiding the Landau singularity, which is regarded as the contributions from IR renormalons. Separating the real and imaginary part of (3.14), we obtain

$$\mathrm{Re}\big[C_0(Q)\big]_\pm \equiv \big[C_0(Q)\big]_{\mathrm{PV}} = x^{-2au'} \int_{0,\mathrm{PV}}^{\infty} d\tau^2\, e^{-\tau^2 x^2} \tilde{C}_0(\tau), \tag{3.15}$$

$$\mathrm{Im}\big[C_0(Q)\big]_\pm \equiv \delta C_0(Q) = \pm\, x^{-2au'} \frac{1}{2i} \int_{C_*} d\tau^2\, e^{-\tau^2 x^2} \tilde{C}_0(\tau), \tag{3.16}$$

where C_* denotes the integration contour shown in Fig. 3.2.

Eq. (3.15) gives the finite value of $C_0(Q)$ by subtracting renormalons at $u = u_0$, $u_0 + \delta u$, $u_0 + 2\delta u$, $\cdots$ with parameters $(a, u') = (1/\delta u, -u_0)$. Eq. (3.16) is the size of the imaginary part due to renormalons, which cancels the same size of imaginary part of OPE corrections as explained in Sec. 2.3. Since $|\tau^2 r^2| \ll 1$ on the contour C_*, Eq. (3.16)

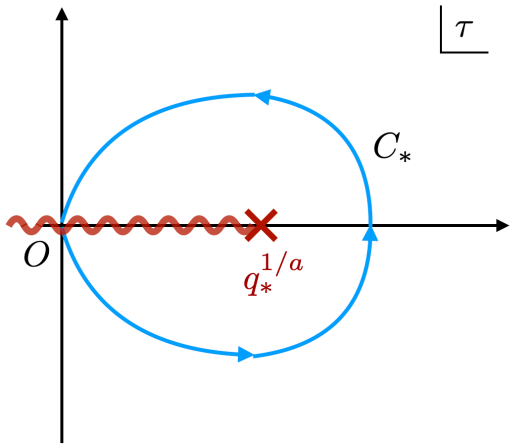

Figure 3.2: Integration contour C_* surrounding the Landau singularities in the complex τ plane. In the N^{k}LL approximation, the branch point of the running coupling constant $\alpha_s(\tau^{2a})$ is at $\tau = q_*^{1/a}$, from which the branch cut represented by the wavy line extends to the left. For the LL approximation, $q_* = \Lambda_{\overline{\rm MS}}$ and there is no discontinuity.

can be expandend in $1/Q$ which is given by

$$\begin{aligned}\delta C_0(Q) &= \pm\, x^{-2au'} \frac{1}{2i} \int_{C_*} d\tau^2 \,(1 - \tau^2 x^2 + \frac{(\tau^2 x^2)^2}{2} + \cdots)\tilde{C}_0(\tau) \\ &= \pm\left(\frac{K_0}{Q^{2u_{*0}}} + \frac{K_1}{(Q^2)^{u_{*0}+\delta u}} + \frac{K_2}{(Q^2)^{u_{*0}+2\delta u}} + \cdots \right), \end{aligned} \tag{3.17}$$

with

$$K_n = \frac{1}{2i} \int_{C_*} \frac{d\tau^2}{\tau^2} (\tau^2)^{n-au'} \sum_{n=0}^{\infty} \alpha_s(\tau^{2a})^{n+1} \tilde{c}_n = \mathcal{O}\big((\Lambda^2_{\overline{\rm MS}})^{u_{*0}+n\delta u}\big). \tag{3.18}$$

The Q-dependence of $\delta C_0(Q)$ is consistent with the renormalons in C_0.

In fact, the regularized form of the Wilson coefficient in our method (Eq. (3.14)) is equivalent to that in the PV scheme using the Borel resummation (Eq. (2.25)) in the large-β_0 approximation. Its proof is given in App. B, which is based on the discussion in Appendix. C of Ref. [41][1]. Other methods for renormalon subtraction [43, 44, 45, 46, 47] are also based on the PV scheme, and then the results of our method can be compared to them directly.

The advantages of our method can be stated as follows. First, our formulation to subtract renormalons works without knowing normalization constants N_{u_*} of the renormalons to be subtracted, following the above calculation procedure. In other methods [43, 44, 45, 46, 47] one needs to estimate the normalization constants N_{u_*} of the corresponding renormalons. Normalization constants of renormalons far from the origin are generally difficult to estimate. Although we certainly need to know large order perturbative series to improve the accuracy of renormalon-subtracted results, the above feature

[1]The FTRS method, which is also our method for renormalon subtraction in Refs. [40, 41, 42], is essentially equivalent to the DSRS method. It is because the Fourier transform used in the FTRS method is closely related to the dual transform (Eq. (3.7)). It implies that the properties for the FTRS method is also valid for the DSRS method.

of our method practically facilitates subtracting multiple renormalons even with a small number of known perturbative coefficients. Secondly, we can give predictions avoiding instability caused by the unphysical singularity around $Q \sim \Lambda_{\overline{\rm MS}}$ of the running coupling constant, in the same way as the previous study of $V_{\rm QCD}(r)$ [33]. Since renormalons and the unphysical singularity are the main sources destabilizing perturbative results at IR regions, the removal of these factors is a marked feature of our method.

Beyond the large-β_0 approximation

We discuss the renormalon subtraction using the dual space beyond the large-β_0 approximation. In the (next-to-)^k leading log (N^{k}LL) approximation, we use the QCD beta function given by $\beta(\alpha_s) = -\sum_{i=0}^{k} \alpha_s^{i+2} b_i$ and the running coupling constant $\alpha_s = \alpha_s\big|_{\rm N^kLL}$ is defined by Eq. (2.2). Then the equivalence of Eq. (3.14) and Eq. (2.25) holds provided that our assumptions are satisfied: (i)Renormalons cancel between the Wilson coefficient and the corresponding operator matrix elements in the OPE; (ii)The QCD beta function beyond 5 loops does not alter the analytic structure of the roots of the beta function which holds up to N^{4}LL; (iii)There are no singularities except those which we suppress by the dual transform Eq. (3.7) (on the positive real axis) in the Borel plane. See App. B for the relevant argument.

One may doubt if the condition (iii) is valid beyond the large-β_0 approximation, since the condition (i) implies that Q-dependence of $\delta C_0(Q)$ deviates from a simple power of $(\Lambda^2_{\overline{\rm MS}}/Q^2)^u$; it contains α_s corrections and the effect of the anomalous dimension, which is given as Eq. (2.31). In principle, such corrections in the dual space are expected to be suppressed by using the extended formula given in App. C, which is based on the discussion in Appendix. B of Ref. [41]. The crucial point is that these corrections have the Q-dependence as $\log^n(Q)Q^{-2u}$, and such effects can be suppressed by combining the dual transform and some linear operations. Therefore the condition (iii) is satisfied beyond the large-β_0 approximation.

In Chap. 4, we apply the DSRS method to observables in the heavy quark systems beyond the large-β_0 approximation. Since the LO renormalon of these observables does not have α_s corrections nor anomalous dimension, we can highly suppress the leading contribution of renormalons by not using the extended formula. Before applications, we test the stability of our method within the large-β_0 approximation in the next section, which helps us to study the systematic uncertainty of our method in the application section.

3.3 Renormalon subtraction with simple cases

In this section, we demonstrate the renormalon subtraction using the DSRS method with the perturbative series obtained in the large-β_0 approximation. Throughout this section, we set $b_0 = b_0|_{n_f=3}$ when indicating specific values. The static QCD potential is a good example. Its perturbative expansion in $\alpha_s(\mu^2)$ is given by Eq. (2.21). The Borel transform of this series is given by Eq. (2.22), which contains the IR renormalons at $u = 1/2,\ 3/2,\ 5/2, \cdots$ in the Borel plane. Naive perturbative expansion (Eq. (2.21))does

not give a convergent series due to divergent behavior from IR renormalons:

$$V \approx -\frac{1}{r}\Big(1.333\,\alpha_s + 2.694\,\alpha_s^2 + 7.693\,\alpha_s^3 + 34.06\,\alpha_s^4 + 196.8\,\alpha_s^5 + 1411\,\alpha_s^6 + \cdots\Big). \quad (3.19)$$

Based on Eq. (2.29), all-order prediction (exact value) of $V(r)$ is calculated by taking the principal value (PV) as

$$\big[V(r)\big]_{\rm PV} = -\frac{4\pi C_F}{r}\frac{1}{b_0}\int_{0,\,\rm PV}^{\infty} du\, e^{-\frac{u}{b_0\alpha_s(\mu^2)}} B_V(u). \quad (3.20)$$

We can also express $\big[V(r)\big]_{\rm PV}$ in terms of the PV of the Fourier integral:

$$\big[V(r)\big]_{\rm PV} = -\frac{2C_F}{\pi r}\int_{0,\,\rm PV}^{\infty} dq\,\frac{\sin(qr)}{q}\alpha_{\beta_0}(q^2). \quad (3.21)$$

Using Eq. (3.20) or Eq. (3.21), we obtain a reference value at $r = r_0 = \frac{1}{10\Lambda_{\overline{\rm MS}}} (\sim (3\ {\rm GeV})^{-1})$,

$$\big[V(r = r_0)\big]_{\rm PV} = \Lambda_{\overline{\rm MS}} \times (-6.27485\cdots). \quad (3.22)$$

The separated imaginary part $\delta V(r)$ is also calculated as

$$\delta V(r) = \mp\frac{C_F}{i\pi r}\int_{C_*} dq\,\frac{\sin(qr)}{q}\alpha_V(q^2) = \pm\Big(K_0^V + K_1^V r^2 + \mathcal{O}(\Lambda_{\overline{\rm MS}}^5 r^4)\Big). \quad (3.23)$$

We note that K_m^V, the normalization of the imaginary part, is independent of r. It is analytically evaluated as

$$K_m^V = -\frac{C_F}{\pi i}\int_{C_*} dq\,\frac{(-q^2)^m}{(2m+1)!}\alpha_V(q^2) = (-1)^{m+1}\frac{C_F}{b_0}\frac{\big(\Lambda_{\overline{\rm MS}}\, e^{5/6}\big)^{2m+1}}{(2m+1)!}. \quad (3.24)$$

Here we construct the dual-space series using the DSRS method. In this analysis, we attempt to eliminate renormalons in two different schemes. First, we subtract renormalons from $V(r)$ by scheme (A): we set $(a, u') = (1, -1/2)$ to suppress the renormalons at $u = 1/2,\ 3/2,\ 5/2, \cdots$ in the dual space. Using Eqs. (3.7) and (3.10), the dual-space potential $\tilde{V}_{\rm A}(\tau)$ is calculated as

$$\begin{aligned}
\tilde{V}_{\rm A}(\tau) &= \int_{x_0^2-i\infty}^{x_0^2+i\infty}\frac{dx^2}{2\pi i}\, e^{\tau^2 x^2} x^{2\times 1\times(-1/2)}(xV(r=x)) \\
&= -4\pi C_F\int_{x_0^2-i\infty}^{x_0^2+i\infty}\frac{dx^2}{2\pi i}\, e^{\tau^2 x^2} x^{-1} e^{\hat{H}\log(\mu^2 x^2)}\sum_{n=0}^{\infty}\alpha_s(\mu^2)^{n+1} a_n^{(\beta_0)} \\
&= -\frac{4\pi C_F}{\tau}\sum_{n=0}^{\infty}\alpha_s(\mu^2)^{n+1}\tilde{a}_n^{(\rm A)}(L_\tau), \qquad (3.25)
\end{aligned}$$

where $L_\tau = \log(\mu^2/\tau^2)$, and $\tilde{a}_n^{(\rm A)}(L_\tau)$ is read from the following Borel transform

$$B_{\tilde{V}_{\rm A}}(u) = \sum_{n=0}^{\infty}\frac{\tilde{a}_n^{(\rm A)}(L_\tau)}{n!}(u/b_0)^n = \frac{B_V(u)}{\Gamma(1/2-u)}\bigg|_{L_Q\to L_\tau} = \left(\frac{\mu^2 e^{5/3}}{4\tau^2}\right)^u \frac{1}{4\pi^{3/2}}\frac{1}{\Gamma(1+u)}. \quad (3.26)$$

It can be seen that there is no renormalon in Eq. (3.26), i.e., a perturbative expansion of $\tilde{V}_A$ is convergent:

$$\tilde{V}_{\rm A} \approx -\frac{1}{\tau}\Big(0.752\,\alpha_s + 0.462\,\alpha_s^2 - 0.351\,\alpha_s^3 - 0.331\,\alpha_s^4 + 0.624\,\alpha_s^5 + 0.0102\alpha_s^6 + \cdots\Big). \quad (3.27)$$

Using the inverse dual transform, we obtain the renormalon-subtracted prediction of V given by

$$\begin{aligned}\big[V(r)\big]_{\rm PV} &= \int_{0,\rm PV}^{\infty} d\tau^2\, e^{-\tau^2 x^2}\tilde{V}_{\rm A}(\tau) \\ &= -4\pi C_F \int_{0,\rm PV}^{\infty} \frac{d\tau^2}{\tau}\, e^{-\tau^2 r^2} \sum_{n=0}^{\infty} \alpha_s(\mu^2)^{n+1}\tilde{a}_n^{(\rm A)}(L_\tau). \end{aligned} \quad (3.28)$$

Since $V(r)$ is RG-invariant, Eq. (3.28) should be independent of the scale setting of μ. We assume a practical case with a finite number of perturbative coefficients up to $n = k$. Then $\tilde{V}_A$ is replaced by $\tilde{V}_A^{(k)}$ based on Eq. (3.12). When we set $\mu = s\tau$ before integration as

$$\big[V(r)\big]_{\rm PV} = -4\pi C_F \int_{0,\rm PV}^{\infty} \frac{d\tau^2}{\tau}\, e^{-\tau^2 r^2} \sum_{n=0}^{k} \alpha_s(s^2\tau^2)^{n+1}\tilde{a}_n^{(\rm A)}(L_\tau = \log(s^2)), \quad (3.29)$$

the integral value would exhibit more stable behavior with respect to changes in s for a larger k due to the RG invariance and convergence of $\tilde{V}_A$.

Fig. 3.3 shows a scale-dependence of $\big[V(r)\big]_{\rm PV}$ in the case with a finite number of perturbative coefficients. Here we set a physical scale r as $r = r_0$ ($\alpha_s(1/r_0^2) \approx 0.3032$). The vertical axis is normalized by $\Lambda_{\overline{\rm MS}}$. The horizontal axis is displayed on a linear (logarithmic) scale in the left (right) panel. The colored solid lines are calculated by using $\tilde{V}_A^{(k)}$ for $k = 0$, 2, 4, 6, 8, 10. The dashed line represents the PV value of $V(r = r_0)$ (Eq. (3.22)). We can see that the stable region extends around $s = \mathcal{O}(1)$ as k increases, and the prediction in its vicinity approaches the value of $\big[V(r_0)\big]_{\rm PV}$. Furthermore, it seems that the length of the stable region extends exponentially.

The reason of stability for a large k is understood as follows. When we set $\mu = s\tau$ and truncate the series at $n = k(\gg 1)$ in Eq. (3.28), the s-dependence of this integral for large s is approximately controlled by

$$I_k(s;r) = \int_{0,\rm PV}^{\infty} \frac{d\tau^2}{\tau} e^{-\tau^2 r^2} \alpha_s(s^2\tau^2)^{k+1}\tilde{a}_0^{(A)}\big[b_0\log(s^2)\big]^k, \quad (3.30)$$

where the logarithmic factor appears from the RG equation. Since the integrand of Eq. (3.30) becomes large at around $\tau = \Lambda_{\overline{\rm MS}}/s$, using the LL running coupling constant Eq. (2.10), we approximate I_k by evaluating the residue at $\tau = \Lambda_{\overline{\rm MS}}/s$, which is given by

$$I_k(s;r) \approx \frac{\tilde{a}_0^{(A)}}{b_0}\frac{e^{-\hat{r}^2/s^2}}{s}\big[\log(s)\big]^k(1 + \mathcal{O}(1/s)), \quad (3.31)$$

where $\hat{r} = \Lambda_{\overline{\rm MS}}\, r$. Thus the stationary point of $I_k(s,r)$ when s is large is estimated by

$$k \approx \log(s)\Big(1 - \frac{\hat{r}^2}{s^2}\Big) \approx \log(s). \quad (3.32)$$

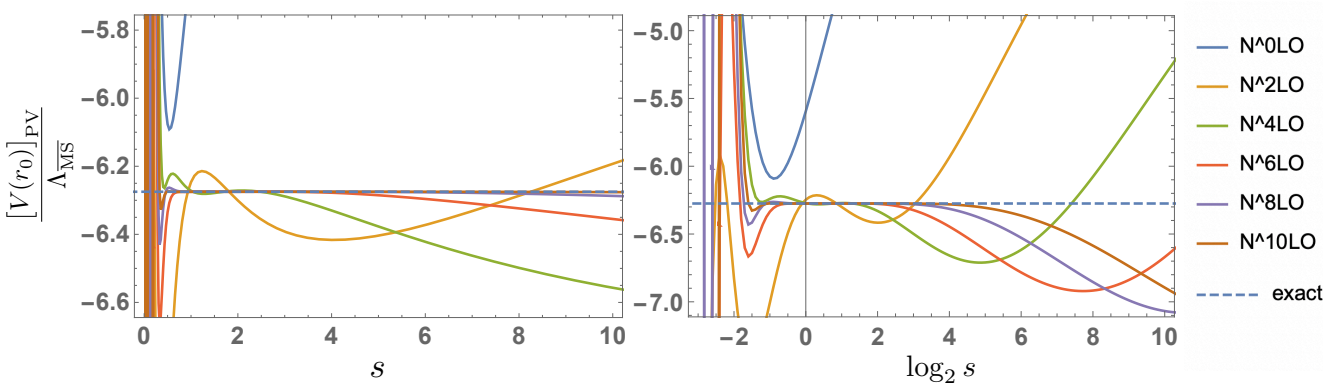

Figure 3.3: Scale dependence of $\left[V(r_0)\right]_{\rm PV}$ in scheme (A). The colored solid lines show the predictions of $\left[V(r_0)\right]_{\rm PV}$ when we truncate $\tilde{V}_A$ at α_s^{k+1} for $k = 0, 2, 4, 6, 8, 10$. The dashed line represents the exact value given by Eq. (3.22). In the left panel, the stable region expands around $s = \mathcal{O}(1)$ as k increases. In the right panel, we can see that the length of a such region is almost proportional to e^k for truncation order k.

This means that the stationary point moves away exponentially with increasing k (in the left panel in Fig. 3.3). In other words, the position of the right-most stationary point is shifted by a constant on the logarithmic scale (see the right panel of Fig. 3.3). On the other hand, since the dual-space series is a convergent series when we set $\mu = \tau$, it is natural to assume that the prediction should approach the true value at $s = \mathcal{O}(1)$. In practice, for sufficiently large k, it is possible to find a stable region extending around $s = \mathcal{O}(1)$ and evaluate the approximated value by systematic uncertainty from the changes in s.

Following a similar procedure, we can also calculate the imaginary part $\delta V(r)$ using the DSRS method. It is given by

$$\delta V(r) = \pm\frac{1}{2i}\int_{C_*} d\tau^2\, e^{-\tau^2 x^2}\tilde{V}_{\rm A}(\tau) = \pm\left(K_0^{V,{\rm A}} + K_1^{V,{\rm A}} r^2 + \mathcal{O}(\Lambda_{\overline{\rm MS}}^5 r^4)\right), \tag{3.33}$$

$$K_m^{V,{\rm A}} = -\frac{4\pi C_F}{i}\int_{C_*} d\tau\, \frac{(-\tau^2)^m}{m!}\sum_{n=0}^{\infty}\alpha_s(\mu^2)^{n+1}\tilde{a}_n^{({\rm A})}(L_\tau). \tag{3.34}$$

When we set $\mu = s\tau$, Eq. (3.34) is analytically calculated as

$$\begin{aligned} K_m^{V,{\rm A}} &= (-1)^{m+1}\frac{4\pi^2 C_F}{b_0}\frac{\Lambda_{\overline{\rm MS}}^{2m+1}}{m!\, s^{2m+1}} B_{\tilde{V}_{\rm A}}(u = m + 1/2)\Big|_{\mu = s\tau} \\ &= (-1)^{m+1}\frac{C_F}{b_0}\frac{(\Lambda_{\overline{\rm MS}}\, e^{5/6})^{2m+1}}{(2m+1)!}, \end{aligned} \tag{3.35}$$

where we use the Borel transform $B_{\tilde{V}_{\rm A}}$ given by eq. (3.26). Eq. (3.35) is equal to Eq. (3.24). If we set $\mu = s\tau$ and truncate the series at α_s^{k+1} in Eq. (3.34), we obtain s-dependent coefficient $K_n^{V,{\rm A}}(s,k)$, which converges to Eq. (3.35) in the limit $k \to \infty$. For a sufficiently large k, we can also predict the imaginary part by investigating the stable s-behavior as done for $\left[V(r)\right]_{\rm PV}$.

Secondly, we subtract renormalons from $V(r)$ in another scheme (B): we set $(a, u') = (2, -1/2)$ to suppress the renormalons at $u = 1/2, 1, 3/2, \cdots$ in the dual space. There is no renormalon at $u = 1, 2, 3, \cdots$ originally, but we examine if we can correctly compute $\big[V(r)\big]_{\rm PV}$ in such a case. The dual-space series is defined by

$$\begin{aligned}\tilde{V}_{\rm B}(\tau) &= \int_{x_0^2-i\infty}^{x_0^2+i\infty} \frac{dx^2}{2\pi i}\, e^{\tau^2 x^2} x^{2\times 2\times(-1/2)} (x^2 V(r=x^2)) \\ &= -4\pi C_F \int_{x_0^2-i\infty}^{x_0^2+i\infty} \frac{dx^2}{2\pi i}\, e^{\tau^2 x^2} x^{-2} e^{\hat{H}\log(\mu^2 x^2)} \sum_{n=0}^{\infty} \alpha_s(\mu^2)^{n+1} a_n^{(\beta_0)} \\ &= -4\pi C_F \sum_{n=0}^{\infty} \alpha_s(\mu^2)^{n+1} \tilde{a}_n^{(\rm B)}(L_\tau), \end{aligned} \tag{3.36}$$

where $L_\tau = \log(\mu^2/\tau^4)$, and $\tilde{a}_n^{(\rm B)}(L_\tau)$ can be read from the following Borel transform,

$$B_{\tilde{V}_{\rm B}}(u) = \sum_{n=0}^{\infty} \frac{\tilde{a}_n^{(\rm B)}(L_\tau)}{n!}(u/b_0)^n = \frac{B_V(u)}{\Gamma(1-2u)}\bigg|_{L_Q \to L_\tau} = \left(\frac{\mu^2 e^{5/3}}{\tau^4}\right)^u \frac{1}{4\pi^2}\frac{\sin(\pi u)}{u}. \tag{3.37}$$

We note that the mass dimension of x is $-1/2$ and that of τ is $1/2$. $\tilde{V}_{\rm B}$ is also convergent series:

$$\tilde{V}_{\rm B} \approx -\frac{1}{\tau}\Big(1.33\,\alpha_s + 1.59\,\alpha_s^2 - 0.350\,\alpha_s^3 - 5.79\,\alpha_s^4 - 9.69\,\alpha_s^5 + 5.75\alpha_s^6 + \cdots\Big). \tag{3.38}$$

Then $\big[V(r)\big]_{\rm PV}$ is calculated by the inverse dual transform of $\tilde{V}_{\rm B}(\tau)$, which is given by

$$\begin{aligned}\big[V(r)\big]_{\rm PV} &= \int_{0,{\rm PV}}^{\infty} d\tau^2\, e^{-\tau^2 x^2} \tilde{V}_{\rm B}(\tau) \\ &= -4\pi C_F \int_{0,{\rm PV}}^{\infty} d\tau^2\, e^{-\tau^2 r} \sum_{n=0}^{\infty} \alpha_s(\mu^2)^{n+1} \tilde{a}_n^{(\rm B)}(L_\tau). \end{aligned} \tag{3.39}$$

Fig. 3.4 shows the scale-dependence of $\big[V(r)\big]_{\rm PV}$ when we set $\mu = s\tau^2$ in the case with a finite number of coefficients. Here we also set the physical scale r as $r = r_0$. The setups of axes and lines are the same as in Fig. 3.3. We can also see that there is a flat region around $s = \mathcal{O}(1)$ and its length extends exponentially as k increases. It is because, from the similar consideration to Eq. (3.30), the right-most stationary point is estimated to be at $s \approx e^k$ for a truncation order k. Thus, the scheme (B) can also predict the all-order result from a finite number of coefficients.

We comment on the calculation of the imaginary part, which is given by

$$\delta V(r) = \pm\frac{1}{2i}\int_{C_*} d\tau^2\, e^{-\tau^2 x^2} \tilde{V}_{\rm B}(\tau) = \pm\Big(\kappa_0^{V,{\rm B}} + \kappa_1^{V,{\rm B}} r + \mathcal{O}(\Lambda_{\overline{\rm MS}}^3 r^2)\Big), \tag{3.40}$$

$$\kappa_\ell^{V,{\rm B}} = -\frac{4\pi C_F}{2i}\int_{C_*} d\tau^2\, \frac{(-\tau^2)^\ell}{\ell!} \sum_{n=0}^{\infty} \alpha_s(\mu^2)^{n+1} \tilde{a}_n^{(\rm B)}(L_\tau). \tag{3.41}$$

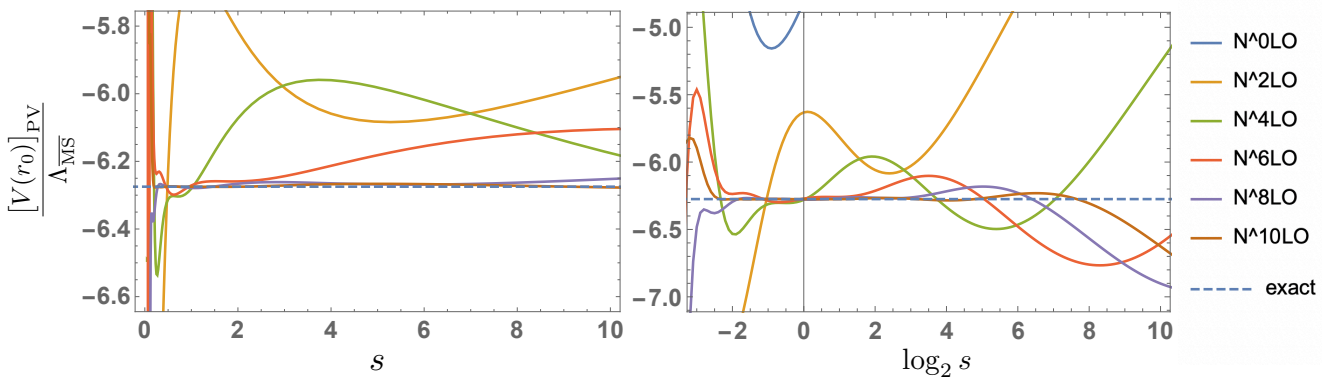

Figure 3.4: Scale dependence of $\left[V(r_0)\right]_{\rm PV}$ in scheme (B). The colored solid lines show the predictions of $\left[V(r_0)\right]_{\rm PV}$ when we truncate $\tilde{V}_B$ at α_s^{k+1} for $k = 0,\ 2,\ 4,\ 6,\ 8,\ 10$. The dashed line represents the exact value given by Eq. (3.22). Also in this scheme, we can see that the stable region extends exponentially with k increased.

Although at first glance, Eq. (3.40) appears to have an imaginary part that is inconsistent with the renormalon of $V(r)$, in fact the normalization of such contributions is zero in the limit of $k \to \infty$. When we set $\mu = s\tau^2$, Eq. (3.41) is analytically calculated as

$$\begin{aligned}\kappa_\ell^{V,\rm B} &= (-1)^{\ell+1}\frac{4\pi^2 C_F}{b_0}\frac{\Lambda_{\overline{\rm MS}}^{\ell+1}}{2\,\ell!\,s^{\ell+1}}B_{\tilde{V}_{\rm B}}\left(u=\frac{\ell+1}{2}\right)\Big|_{\mu=s\tau^2} \\ &= \begin{cases} (-1)^{m+1}\dfrac{C_F}{b_0}\dfrac{(\Lambda_{\overline{\rm MS}}\,e^{5/6})^{2m+1}}{(2m+1)!} & \text{for} \quad \ell = 2m\,(=0,\,2,\,4,\cdots) \\ 0 & \text{for} \quad \ell = 2m+1\,(=1,\,3,\,5,\cdots) \end{cases}, \end{aligned} \tag{3.42}$$

where we use the Borel transform given by eq. (3.37). We can see that $\kappa_{2m}^{V,\rm B} = K_m^V$ given by Eq. (3.24), and the others are zero.

Before concluding this chapter, we examine the effects of the UV renormalons in the dual-space series. We consider a toy model containing the IR and UV renormalons at $u = -1, 1, 2, 3, \cdots$, which is given by

$$W(Q) = \sum_{n=0}^{\infty}\alpha_s(\mu^2)^{n+1}w_n(L_Q), \tag{3.43}$$

and the Borel transform is given by

$$B_W(u) = \sum_{n=0}^{\infty}\frac{w_n(L_Q)}{n!}\left(\frac{u}{b_0}\right)^n = \left(\frac{\mu^2}{Q^2}\right)^u\frac{\Gamma(1-u)}{1+u}. \tag{3.44}$$

Using Eq. (3.7) with the parameter $(a, u') = (1, -1)$, the dual-space series with the IR renormalons suppressed is constructed as

$$\begin{aligned}\tilde{W}(\tau) &= \int_{x_0^2-i\infty}^{x_0^2+i\infty}\frac{dx^2}{2\pi i}\,e^{\tau^2x^2}x^{-2}W(Q=x^{-1}) \\ &= \sum_{n=0}^{\infty}\alpha_s(\mu^2)^{n+1}\tilde{w}_n(L_\tau), \end{aligned} \tag{3.45}$$

where $L_\tau = \log(\mu^2/\tau^2)$, and $\tilde{w}_n$'s are read from the Borel transform $B_{\tilde{W}}$. It is given by

$$B_{\tilde{W}}(u) = \sum_{n=0}^{\infty} \frac{\tilde{w}_n(L_\tau)}{n!}\left(\frac{u}{b_0}\right)^n = \frac{B_W(u)}{\Gamma(1-u)}\bigg|_{L_Q\to L_\tau} = \left(\frac{\mu^2}{\tau^2}\right)^u \frac{1}{1+u}, \tag{3.46}$$

where there is no renormalon except the UV renormalon at $u=-1$. Eq. (3.15) gives

$$\begin{aligned}\big[W(Q)\big]_{\rm PV} &= x^2 \int_{0,\rm PV}^{\infty} d\tau^2 e^{-\tau^2 x^2}\tilde{W}(\tau) \\ &= \frac{1}{Q^2}\int_{0,\rm PV}^{\infty} d\tau^2 e^{-\tau^2/Q^2}\sum_{n=0}^{\infty}\alpha_s(\mu^2)^{n+1}\tilde{w}_n(L_\tau),\end{aligned} \tag{3.47}$$

which is equivalent to the result using the Borel resummation in the case with an all-order perturbative series. However, when truncating $\tilde{W}$ at a finite order, the UV renormalon limits the computational accuracy, creating uncertainty of $\mathcal{O}(\Lambda^2_{\overline{\rm MS}}\tau^2/\mu^4)$ for $\tilde{W}$ according to Eq. (2.16).

On the other hand, the UV renormalons in the dual space can be resummed in the large-β_0 approximation. This property is natural because the DSRS method gives equivalent result using the Borel resummation which can resum UV renormalons. According to the resummation formula in App. D,

$$\big[W(Q)\big]_{\rm PV} = \frac{1}{Q^2}\int_{0,\rm PV}^{\infty}\frac{d\tau^2}{(1+\tau^2/Q^2)}\sum_{n=0}^{\infty}\alpha_s(\mu^2)^{n+1}\tilde{w}'_n(L_\tau), \tag{3.48}$$

where $\tilde{w}'_n$'s are read from

$$B_{\tilde{W}'}(u) = \sum_{n=0}^{\infty}\frac{\tilde{w}'_n(L_\tau)}{n!}\left(\frac{u}{b_0}\right)^n = \frac{B_W(u)}{\Gamma(1-u)\Gamma(1+u)}\bigg|_{L_Q\to L_\tau} = \left(\frac{\mu^2}{\tau^2}\right)^u\frac{1}{\Gamma(2+u)}. \tag{3.49}$$

Tab. 3.1 compares w_n, $\tilde{w}_n$ and $\tilde{w}'_n$, which indicates that the resummation of the $u=-1$ renormalon, in addition to the suppression of the IR renormalons, gives a convergent series in the dual space.

In Fig. 3.5, the scale-dependences of $\big[W(Q=Q_0)\big]_{\rm PV}$ calculated by Eqs. (3.47) and (3.48), respectively, are compared. Here $Q_0 = 10\Lambda_{\overline{\rm MS}}$ and we truncate $\tilde{W}$ at $n=k$ and set $\mu = s\tau$. The horizontal axis is displayed on a logarithmic scale in both panels. The colored lines represent the results with $k=0$, 2, 4, 6, 8, 10, and the dashed line is drawn to show the exact value given by

$$\big[W(Q=Q_0)\big]_{\rm PV} = \frac{1}{b_0}\int_{0,\rm PV}^{\infty} du\, e^{-\frac{u}{b_0\alpha_s(\mu^2)}}B_W(u)\bigg|_{Q=Q_0} = 0.316248\cdots. \tag{3.50}$$

In the left figure, as k increases, the flat region extends in the direction where $s \gg 1$, while the unstable region widens around $s=\mathcal{O}(1)$. This is a manifestation of the effects of the UV renormalon. For large s (at high energy scale), the contribution from the UV renormalon is strongly suppressed, so the flat region extends exponentially to the right direction, as in the analysis with the static potential. Nevertheless, perturbative

Table 3.1: Comparison of the dual-space coefficient $\tilde{w}_n$ and $\tilde{w}'_n$ with the original one w_n. Owing to the dual transform, the divergent behavior of $\tilde{w}_n$'s from IR renormalons is suppressed while the $u = -1$ UV renormalon remains. On the contrary, $\tilde{w}'_n$'s exhibit a good convergence.

n	w_n	$\tilde{w}_n$	$\tilde{w}'_n$	n	w_n	$\tilde{w}_n$	$\tilde{w}'_n$
0	1	1	1	11	-5.08×10^5	-1.02×10^6	-2.63
1	-0.303	-0.716	-0.303	12	1.31×10^7	8.72×10^6	11.7
2	1.45	1.03	-0.239	13	-4.06×10^7	-8.12×10^7	-16.7
3	-1.11	-2.20	0.421	14	1.22×10^9	8.14×10^8	-0.130
4	9.38	6.31	-0.155	15	-4.37×10^9	-8.75×10^9	54.9
.....	...	...	...	...	...	...	...

expansion of a sufficiently high order is required to predict the true value. For small s (at low energy scale), Eq. (3.47) approaches its true value from a small number of perturbative coefficients, but as k increases, the factorial behavior of the UV renormalon emerges and stability is lost. Thus, if the UV renormalons remain in the dual space, the region stable to changes in s is narrowed. On the other hand, in the right figure, the scale dependence is stable around $s = \mathcal{O}(1)$, owing to the resummation of the UV renormalon.

From a practical point of view, two points should be mentioned. First, the resummation method is effective only for the case in the large-β_0 approximation. The method given in App. D could in principle be extended beyond the large-β_0 approximation by reference to App. C. However, unlike IR renormalons, it is not theoretically clear what $\log(Q)$ correction UV renormalons have in general [11]. Thus the parameters to resum the exact structure of UV renormalons cannot be chosen properly. Secondly, if the UV renormalons are sufficiently far from the origin in the Borel plane, the effect is negligible for relatively low-order perturbative calculations. For example, the UV renormalons of the pole-$\overline{\rm MS}$ mass relation, discussed in the next section, start from $u = -1$, and we will see later that this effect is almost negligible at the N^{3}LO level, which is the state-of-the-art perturbation order. For these reasons, we basically do not resum the UV renormalons in the analyses in Chap. 4.

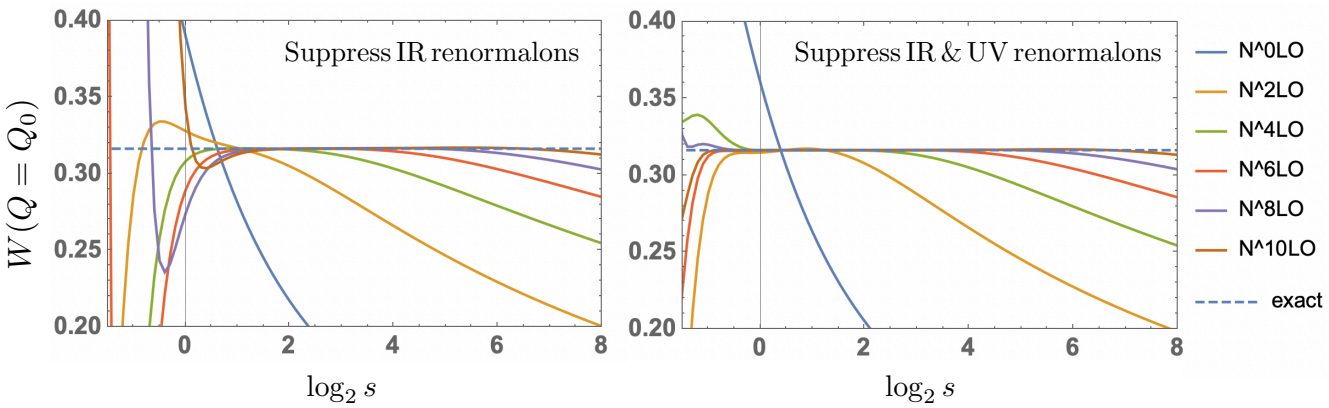

Figure 3.5: The left/right panel shows the scale dependence of $\left[W(Q_0)\right]_{\rm PV}$ with/without the UV renormalon at $u = -1$ in the dual space. The colored solid lines show the predictions of $\left[W(Q_0)\right]_{\rm PV}$ when we truncate $\tilde{W}$ at α_s^{k+1} for $k = 0,\ 2,\ 4,\ 6,\ 8,\ 10$. The dashed line represents the exact value given by Eq. (3.50). The UV renormalon causes the instability of scale dependence around $s = \mathcal{O}(1)$.

Chapter 4

Renormalon subtraction in heavy quark systems

In this chapter, the DSRS method is applied to several observables of heavy quark systems. In Sec. 4.1, we introduce the heavy quark effective theory (HQET) to incorporate non-perturbative effects to observables of heavy-light mesons such as B and D mesons in the OPE framework. As specific examples, the OPEs of the masses of B and D mesons and that of the inclusive semileptonic decay width of B meson are presented. In Sec. 4.2, the DSRS method is applied to the quark pole mass to eliminate (or suppress) the renormalons of $\mathcal{O}(\Lambda_{\overline{\rm MS}})$ and $\mathcal{O}(\Lambda^2_{\overline{\rm MS}})$ orders from the OPEs of B and D meson masses. Then we determine the non-perturbative parameters in HQET after subtraction of IR renormalons. In Sec. 4.3, we determine $|V_{cb}|$, one of the CKM matrix elements, from the inclusive semileptonic decay width of B meson. In this determination, we use the HQET parameters determined in Sec. 4.2. This is the first time to determine $|V_{cb}|$ with the NLO IR renormalon suppressed in the PV scheme using the $\overline{\rm MS}$ mass scheme.

4.1 OPE for Heavy Quark Systems

4.1.1 Heavy Quark Effective Theory

B meson is a bound state of the bottom quark and the single light quark (up or down quark). Because the mass of bottom quark is much larger than that of light quark (m_u, $m_d \ll m_b$), from the light quark's point of view, the heavy bottom quark appears to be almost at rest. Therefore the dynamics can be viewed as the non-relativistic motion of bottom quark due to the transfer momentum of order $\mathcal{O}(\Lambda_{\rm QCD})$ carried by the light quark in the B-meson center-of-mass system.

The heavy quark effective theory (HQET) [48, 49, 50, 51, 52, 53] describes the physics of hadrons called heavy-light mesons which consist of a single heavy quark and a few light quarks, i.e., B meson, D meson, etc. Let us consider that single heavy quark h in heavy-light meson X that moves with the same velocity v as the meson X, that is $p^\mu_X = m_X v^\mu$. In this system, h is almost on shell. Thus the momentum of h can be written by

$$p^\mu_h = m_h v^\mu + k^\mu, \tag{4.1}$$

where $v^2 = 1$ and we assume that the residual momentum $k \sim \Lambda_{\overline{\rm MS}}$ (off-shellness of h) is much smaller than m_h, the mass of the heavy quark h. Since the heavy quark h is almost at rest, it is natural to describe HQET in terms of the pole mass (on-shell mass) of the heavy quark. The pole mass is defined as the pole of the propagator, which is consistent with the concept of the static energy of the particle. The HQET Lagrangian is constructed by treating the heavy quark mass m_h as the pole mass. If m_h is shifted by $\delta m_h = \mathcal{O}(\Lambda_{\overline{\rm MS}})$, the residual momentum k in Eq. (4.1) absorbs it as $k^\mu \to k^\mu + \delta m_h v^\mu$. That is, the quark mass definition by pole mass has $\mathcal{O}(\Lambda_{\overline{\rm MS}})$ ambiguity.

The field operator $h(x)$, which denotes the massive quark in QCD, is decomposed into two pieces as follows

$$h(x) = e^{-im_h v\cdot x}\big(h_v(x) + H_v(x)\big), \tag{4.2}$$

$$h_v(x) = e^{im_h v\cdot x}\frac{1+\not{v}}{2}h(x), \quad H_v(x) = e^{im_h v\cdot x}\frac{1-\not{v}}{2}h(x) \tag{4.3}$$

We note that h_v and H_v satisfy $\not{v}\, h_v = h_v$ and $\not{v}\, H_v = -H_v$. In the rest frame of the hadron $v^\mu = (1, \vec{0})$, h_v and H_v correspond to upper and lower component of Dirac spinor respectively. In other words, h_v (H_v) denotes the heavy quark (anti-quark) field.

We can see that using h_v and H_v, the QCD Lagrangian containing h is expressed by

$$\begin{aligned}\mathcal{L}_h &= \bar{h}(i\not{D} - m_h)h \\ &= \bar{h}_v(iv\cdot D)h_v - \bar{H}_v(iv\cdot D + 2m_h)H_v + \bar{h}_v(i\not{D}_\perp)H_v + \bar{H}_v(i\not{D}_\perp)h_v,\end{aligned} \tag{4.4}$$

where D^μ is the covariant derivative and $D^\mu_\perp = D^\mu - v^\mu(v\cdot D)$ is orthogonal to v, i.e., $v \cdot D_\perp = 0$. It can be seen that h_v does not have a mass term while H_v acquires a mass $2m_h$. The remaining terms in the Lagrangian describe interactions between h_v and H_v. In the sense of EFT, h_v/H_v is identified as the light/heavy degree of freedom.

At the tree level, the HQET Lagrangian is obtained after integrating out H_v using equation of motion for H_v (or in the formulation of path-integral), which is given by

$$\begin{aligned}\mathcal{L}^{\rm tree}_{\rm HQET} &= \bar{h}_v(iv\cdot D)h_v + \bar{h}_v(i\not{D}_\perp)(iv\cdot D + 2m_h)^{-1}(i\not{D}_\perp)h_v \\ &= \bar{h}_v(iv\cdot D)h_v + \bar{h}_v\frac{(i\not{D}_\perp)(i\not{D}_\perp)}{2m_h}h_v + \mathcal{O}(1/m_h^2) \\ &= \bar{h}_v(iv\cdot D)h_v + \frac{\bar{h}_v(i\not{D}_\perp)^2 h_v}{2m_h} + \bar{h}_v\frac{\frac{g_s}{2}\sigma_{\mu\nu}G^{\mu\nu}}{2m_h}h_v + \mathcal{O}(1/m_h^2),\end{aligned} \tag{4.5}$$

where $G^{\mu\nu}$ is the field strength tensor and we use

$$\gamma_\mu\gamma_\nu = \frac{1}{2}\{\gamma_\mu, \gamma_\nu\} + \frac{1}{2}[\gamma_\mu, \gamma_\nu] = g_{\mu\nu} - i\sigma_{\mu\nu}. \tag{4.6}$$

The leading term in Eq. (4.5) is the Lagrangian for a static heavy quark with velocity v. The physical interpretation of the second and third terms are as follows. The second term represents the kinetic energy of the heavy quark, which breaks the flavor symmetry. The third term is the energy from the chromo-magnetic interaction, which breaks both flavor

and spin symmetries. In order to incorporate radiative corrections, matching of QCD and HQET is necessary. The schematic form of $\mathcal{L}_{\rm HQET}$ is given by

$$\mathcal{L}_{\rm HQET} = \bar{h}_v(iv\cdot D)h_v + \frac{\bar{h}_v(i\not{D}_\perp)^2 h_v}{2m_h} + C_{cm}(m_h)\,\bar{h}_v\frac{\frac{g_s}{2}\sigma_{\mu\nu}G^{\mu\nu}}{2m_h}h_v + \mathcal{O}(1/m_h^2). \tag{4.7}$$

Up to this order, only the chromomagnetic operator is renormalized, and its Wilson coefficient is given by $C_{cm} = 1 + \mathcal{O}(\alpha_s)$, which is calculated up to $\mathcal{O}(\alpha_s^3)$ ($\mathrm{N^3LO}$ level) [61]. The Wilson coefficient of the kinetic term is exactly one reflecting the fact that the kinetic energy is not renormalized. That is ensured by the reparameterization invariance [62, 63], which is related to the Lorentz invariance of QCD.

The OPE of the heavy light meson X is given by $1/m_h$ expansion using the expectation values of the operators appearing in the HQET Lagrangian. The normalization of the state defining the expectation value is given by

$$\langle X(v',k')|X(v,k)\rangle = 2v^0\delta_{v_0v_0'}(2\pi)^3\delta^{(3)}(\boldsymbol{k}-\boldsymbol{k}'), \tag{4.8}$$

where $|X(v)\rangle = |X(v,k=0)\rangle$ denotes the ground state of X in the infinite mass limit. The advantage of using this state is that the matrix elements defined by this state do not depend on the flavor of heavy quark. The matrix element of $\bar{h}_v(iv\cdot D)h_v$ is $\mathcal{O}(1/m_h)$ due to the equation of motion. So the leading non-perturbative matrix elements from Eq. (4.7) are given by

$$\mu_\pi^2 = -\langle X(v)|\bar{h}_v(iD_\perp)^2 h_v|X(v)\rangle, \tag{4.9}$$

which is the kinetic energy of the heavy quark, and

$$\mu_G^2 = -\langle X(v)|\bar{h}_v\frac{g_s}{2}\sigma_{\mu\nu}G^{\mu\nu}h_v|X(v)\rangle, \tag{4.10}$$

which is the energy of chromomagnetic interaction. μ_π^2 and μ_G^2 are defined to be independent of the mass of the heavy quark. To paraphrase, these matrix elements are common between B meson and D meson, Λ_b baryon and between Λ_c baryon, and so on. Furthermore, these parameters can describe the non-perturbative effects of various observables, i.e., their values are common among different observables. We call this property the universality of the HQET parameters.

4.1.2 Renormalons of quark pole mass

We mentioned in the previous section that the definition of pole mass has an uncertainty of $\mathcal{O}(\Lambda_{\overline{\rm MS}})$. This implies that the pole mass has the IR renormalons starting from $u = 1/2$ when calculated by perturbative expansion. Since the pole mass is calculated by the quark self-energy, the internal IR gluons in loop diagrams induce factorial divergent behavior of perturbative series. Perturbative calculation of the pole mass is provided by introducing a short-distance mass. The $\overline{\rm MS}$ mass $m_h^{\overline{\rm MS}}$ is one example. The quark propagator $S(p)$ in the on-shell scheme is defined by

$$S(p) = \frac{-iZ_2^{\rm OS}}{\not{p} - m_{h,0} + \Sigma(p,m_h)} \to \frac{-i}{\not{p}-m_h} \quad \text{as } p^2 \to m_h^2, \tag{4.11}$$

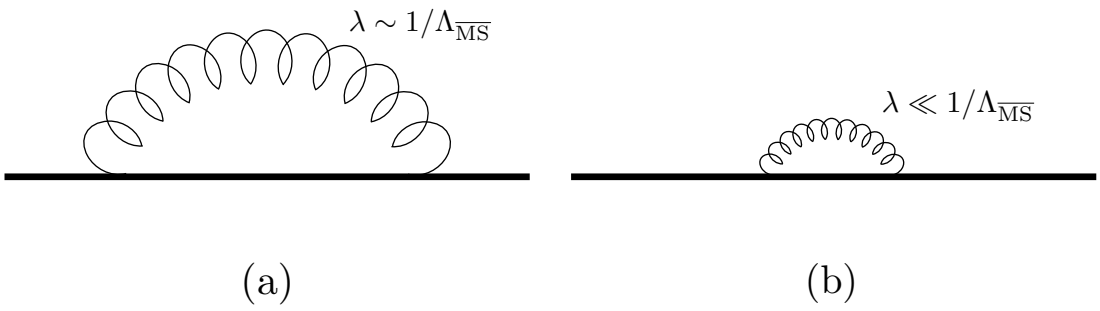

Figure 4.1: Schematic figure representing the difference between the renormalization of the quark self-energy in the on-shell scheme and the $\overline{\rm MS}$ scheme. (a) In the on-shell scheme, gluons involving the quark self energy is both IR and UV, of which the wavelength λ reaches the length $\sim 1/\Lambda_{\overline{\rm MS}}$. (b) In the $\overline{\rm MS}$ scheme, only UV gluons contribute to the quark self-energy because it removes only the UV divergence.

where $m_{h,0}$ is the bare mass of h related to m_h as

$$m_{h,0} = Z_m^{\rm OS} m_h. \tag{4.12}$$

By definition, the quark pole mass m_h contains the one-particle-irreducible self-energy $\Sigma(p)$, which has the contributions from both IR and UV gluons. We can also define $S(p)$ in the $\overline{\rm MS}$ scheme and obtain

$$m_{h,0} = Z_m^{\overline{\rm MS}} m_h^{\overline{\rm MS}}. \tag{4.13}$$

Then the perturbative relation of the pole mass and the $\overline{\rm MS}$ mass is expressed by

$$m_h = \frac{Z_m^{\overline{\rm MS}}}{Z_m^{\rm OS}} m_h^{\overline{\rm MS}} = m_h^{\overline{\rm MS}} \left(1 + \sum_{n=0}^{\infty} \alpha_s^{n+1} d_n \right). \tag{4.14}$$

The coefficients d_n's are calculated up to $\mathcal{O}(\alpha_s^4)$ [64, 65, 66, 68, 69, 5, 6, 7]. The internal massive quark effects for $\mathcal{O}(\alpha_s^2)$ and $\mathcal{O}(\alpha_s^3)$ corrections are contained, while those for $\mathcal{O}(\alpha_s^4)$ has not been calculated. Their explicit values are given in App. A. Since the $\overline{\rm MS}$ mass is defined in the $\overline{\rm MS}$ scheme which removes only the UV divergence of the self-energy, Eq. (4.14) strongly reflects the IR contribution of the self-energy and exhibits factorial divergence behavior [13, 14]. Such IR renormalons in the pole mass should be absorbed by the non-perturbative effects of the OPE based on HQET. In the following sections, we describe how renormalons are removed in this thesis through the OPEs of specific observables.

4.1.3 Masses of B and D mesons

From this section, we consider the heavy-light meson $H\,(= B,\, D)$ composed by a single heavy quark $h\,(= b,\, c)$ and a single light quark $(= u$ or $d)$. The OPE of its mass M_H based on HQET is given in $1/m_h$ expansion, given by

$$M_H^{(s)} = m_h + \bar{\Lambda} + \frac{\mu_\pi^2}{2m_h} + A(s) C_{cm}(m_h) \frac{\mu_G^2(m_h)}{2m_h} + \mathcal{O}\left(\frac{\Lambda_{\overline{\rm MS}}^3}{m_h^2} \right), \tag{4.15}$$

where $s\,(=0,\,1)$ denotes the spin of H. The leading contribution to M_H is the heavy quark mass m_h. As mentioned in the previous section, the quark mass definition by the pole mass has theoretical uncertainties starting from $\mathcal{O}(\Lambda_{\overline{\rm MS}})$, so the non-perturbative corrections also start from $\mathcal{O}(\Lambda_{\overline{\rm MS}})$ to cancel them. The first non-perturbative correction $\bar{\Lambda} = \mathcal{O}(\Lambda_{\overline{\rm MS}})$ is the contribution from the light degrees of freedom of H, which can be written by the matrix element of light sector of QCD Lagrangian. $\bar{\Lambda}$ is independent of the heavy quark mass in the sense that

$$\bar{\Lambda} = \lim_{m_h\to\infty}\Big[M_H - m_h\Big]. \tag{4.16}$$

μ_π^2 and μ_G^2 are given by Eqs (4.9) and (4.10) respectively. The Wilson coefficient C_{cm} is the same one as in Eq. (4.7). Since the chromomagnetic interaction breaks the spin symmetry in the HQET Lagrangian, μ_G^2 term is proportional to a spin-dependent coefficient $A(s)$; $A(s) = -1$ for $s = 0$ (pseudo-scalar meson H^*) and $A(s) = 1/3$ for $s = 1$ (vector meson H). Up to this order, we can separate the spin-dependent part by a simple combination of $M_H^{(s)}$. A clever choice is to express it by the hyperfine-splitting of the H mesons as

$$C_{cm}(m_h)\mu_G^2(m_h) = \frac{3}{4}\big(M_{H^*}^2 - M_H^2\big) + \mathcal{O}\bigg(\frac{\Lambda_{\overline{\rm MS}}^3}{m_h}\bigg), \tag{4.17}$$

in which the pole mass of h is hidden into the NLO correction. Since the experimentally measurable quantity does not contain renormalons, μ_G^2 is irrelevant to the $\mathcal{O}(\Lambda_{\overline{\rm MS}}^2)$ renormalon (at $u = 1$) of m_h. In Ref. [60], the value of $\mu_G^2(\overline{m}_b)$ using C_{cm} at N^{3}LO level [61] is determined as

$$\mu_G^2(\overline{m}_b) = 0.284 \pm 0.014\ \text{GeV}^2, \tag{4.18}$$

in which the uncertainty is comparable to $\mathcal{O}(\Lambda_{\overline{\rm MS}}^3/\overline{m}_c)$ reflecting the fact that C_{cm} contains the $u = 1/2$ renormalon.

On the other hand, the spin-independent part is given by the linear combination of M_H and M_{H^*} as

$$\big[M_H\big]_{\text{spin ave.}} = \frac{M_H + 3M_{H^*}}{4} = m_h + \bar{\Lambda} + \frac{\mu_\pi^2}{2m_h} + \mathcal{O}\bigg(\frac{\Lambda_{\overline{\rm MS}}^3}{m_h^2}\bigg). \tag{4.19}$$

In this thesis, we assume that m_h contains the IR renormalons at $u = 1/2$ and $u = 1$ at least and the imaginary part from them are absorbed into $\bar{\Lambda}$ and μ_π^2, respectively. We separate the imaginary part from m_h using the DSRS method without the extended formula in App. C since $\bar{\Lambda}$ and μ_π^2 does not have α_s corrections and anomalous dimension.[1] We denote the renormalon-subtracted pole mass by $\big[m_h\big]_{\rm PV}$ and call it the PV mass of h. It is defined by

$$\big[m_h\big]_\pm = \big[m_h\big]_{\rm PV} \pm iN_{1/2}\Lambda_{\overline{\rm MS}} + \pm iN_1\frac{\Lambda_{\overline{\rm MS}}^2}{\big[m_h\big]_{\rm PV}} + \mathcal{O}\bigg(\frac{\Lambda_{\overline{\rm MS}}^3}{\big[m_h\big]_{\rm PV}^2}\bigg), \tag{4.20}$$

[1] In later section, we will see that this treatment causes small uncertainty due to the inverse power of m_h in the OPE based on HQET. Although it can be resolved by using the extended formula in App. C, we neglect its contribution in our analysis to avoid complications in the calculations.

where $\left[m_h\right]_\pm$ is the regularized pole mass using the DSRS method. The way to calculate $\left[m_h\right]_{\rm PV}$ using the DSRS method is discussed in Sec. 4.2. $N_{1/2}$ and N_1 are the normalization coefficients of the imaginary part due to renormalons. These do not have to be calculated explicitly because the non-perturbative matrix elements absorb the imaginary part as follows. The renormalon-subtracted OPE is expressed by

$$\left[M_H\right]_{\text{spin ave.}} = \left[m_h\right]_{\rm PV} + \left[\bar{\Lambda}\right]_{\rm PV} + \frac{\left[\mu_\pi^2\right]_{\rm PV}}{2\left[m_h\right]_{\rm PV}} + \mathcal{O}\left(\frac{\Lambda_{\overline{\rm MS}}^3}{m_h^2}\right). \tag{4.21}$$

$\left[\bar{\Lambda}\right]_{\rm PV}$ and $\left[\mu_\pi^2\right]_{\rm PV}$ are defined by

$$\left[\bar{\Lambda}\right]_{\rm PV} = \bar{\Lambda} \pm iN_{1/2}\Lambda_{\overline{\rm MS}}, \tag{4.22}$$

and

$$\left[\mu_\pi^2\right]_{\rm PV} = \mu_\pi^2 \pm iN_1\Lambda_{\overline{\rm MS}}^2. \tag{4.23}$$

The matrix elements $\bar{\Lambda}$ and μ_π^2 can be determined by comparing the experimental values of M_H's and theoretical calculations in Eq. (4.21). It is important to note that Eqs. (4.21) and (4.17) are common between $H = B$ and D ($h = b$ and c) since the matrix elements are defined to be independent of the mass of the heavy quark. In order to subtract renormalons of m_b and m_c, we have to keep $n_f = 3$ for the matrix elements to be common, i.e., we assume that up, down and strange quarks are massless and charm and bottom quarks are massive (m_c, $m_b \gg \Lambda_{\rm QCD}$). Otherwise, for example, if we take $n_f = 4$ for the OPE of M_B and $n_f = 3$ for that of M_D, the matrix elements cannot be treated as common between them because the Lagrangian of the light sector is different.

In particular for the $u = 1/2$ renormalon, this feature is demonstrated in the large-β_0 approximation with the finite charm quark mass included in loops, as follows. The bottom quark pole mass in this approximation is given by the loop momentum integration,

$$\frac{m_{b,\rm pole} - \overline{m}_b}{\overline{m}_b} = \int d^4k\, F_{kin}(k, \overline{m}_b)\, \frac{1}{k^2}\, \frac{\alpha_s^{(4)}(\mu^2)}{1 - \alpha_s^{(4)}(\mu^2)\Pi(k^2, \overline{m}_c)}, \tag{4.24}$$

where $F_{kin}(k, \overline{m}_b)$ is a kinematic function and $\alpha_s^{(n_f)}$ represents the strong coupling constant of the n_f-flavor theory. We have rewritten $\alpha_s^{(5)}$ by $\alpha_s^{(4)}$, which absorbs the effect of the bottom quark loops. $\Pi(k^2, \overline{m}_c)$ is the one-loop vacuum polarization which includes the massive charm quark loop,

$$\Pi(k^2, \overline{m}_c) = \Pi_{\rm light}(k^2) + \Pi_c(k^2, \overline{m}_c), \tag{4.25}$$

where $\Pi_{\rm light}$ represents the contribution from the light degrees of freedom (gluons and massless quarks) while Π_c represents the charm quark contribution. In the IR region $k^2 \simeq 0$, they are given by

$$\Pi_{\rm light}(k^2) = b_0^{(3)} \left[\log\left(-\frac{\mu^2}{k^2}\right) + \frac{5}{3}\right], \tag{4.26}$$

$$\Pi_c(k^2, \overline{m}_c) = -\frac{1}{6\pi}\log\left(\frac{\mu^2}{\overline{m}_c^2}\right) + \mathcal{O}\left(\frac{k^2}{\overline{m}_c^2}\right), \tag{4.27}$$

with $b_0^{(n_l)} = (11 - 2n_l/3)/(4\pi)$. Π_c does not have $\log(k^2)$ behavior in the IR region [84], since the charm quark mass works as an IR regulator in the fermion loop integration. As a result the charm quark contributions do not give renormalons.

We can absorb the $\log(\mu^2/\overline{m}_c^2)$ term in Eq. (4.27) if we use the coupling constant of the 3-flavor theory,

$$\frac{\alpha_s^{(4)}(\mu^2)}{1 - \alpha_s^{(4)}(\mu^2)\Pi(k^2, \overline{m}_c)} = \frac{\alpha_s^{(3)}(\mu^2)}{1 - \alpha_s^{(3)}(\mu^2)\Pi_{\text{light}}(k^2) + \mathcal{O}(k^2/\overline{m}_c^2)}, \tag{4.28}$$

due to the one loop threshold correction in the $\overline{\text{MS}}$ scheme

$$\frac{1}{\alpha_s^{(4)}(\mu^2)} = \frac{1}{\alpha_s^{(3)}(\mu^2)} - \frac{1}{6\pi}\log(\mu^2/\overline{m}_c^2). \tag{4.29}$$

After this rewriting, one can clearly see that the renormalon we encounter coincides with the one in the $n_f = 3$ theory:

$$\frac{m_{b,\text{pole}} - \overline{m}_b}{\overline{m}_b} \approx K \sum_{n=0}^{\infty} (2b_0)^n n! [\alpha_s^{(3)}(\overline{m}_b^2)]^{n+1}\,. \tag{4.30}$$

In fact, it was pointed out that one should use $\alpha_s^{(3)}$ rather than $\alpha_s^{(4)}$ as the expansion parameter [70].

We now show that, in order for the DSRS method to work with our parameter choice $(a, u') = (2, -1/2)$, it is necessary to express the perturbative series in the 3-flavor coupling constant. In fact, renormalons remain in the dual space when we use the 4-flavor coupling constant. With the 4-flavor coupling constant, from Eqs. (4.26) and (4.27), the Borel transform close to the first IR renormalon is given by

$$B^{\text{4-flavor}}(u) = \sum_{n=0}^{\infty} \frac{d_n}{n!}\left(\frac{u}{b_0^{(4)}}\right)^n \approx \left(\frac{\mu^2 e^{5/3}}{\overline{m}_b^2}\right)^{\frac{b_0^{(3)}}{b_0^{(4)}}u} \left(\frac{\mu^2}{\overline{m}_c^2}\right)^{\frac{u}{6\pi b_0^{(4)}}} \frac{1}{1 - 2\frac{b_0^{(3)}}{b_0^{(4)}}u} \tag{4.31}$$

The singularity is located at $u = b_0^{(4)}/(2b_0^{(3)})$. Then the Borel transform of the dual-space perturbative series is given by

$$\tilde{B}^{\text{4-flavor}}(u) \approx \left(\frac{\mu^2 e^{5/3}}{\tau^{2a}}\right)^{\frac{b_0^{(3)}}{b_0^{(4)}}u} \left(\frac{\mu^2}{\overline{m}_c^2}\right)^{\frac{u}{6\pi b_0^{(4)}}} \frac{1}{1 - 2\frac{b_0^{(3)}}{b_0^{(4)}}u} \times \frac{1}{\Gamma\Big(-a\big(\frac{b_0^{(3)}}{b_0^{(4)}}u + u'\big)\Big)}. \tag{4.32}$$

The singularity at $u = b_0^{(4)}/[2b_0^{(3)}]$ cannot be eliminated in the dual space with the parameter set $(a, u') = (2, -1/2)$, which is chosen to eliminate the $u = 1/2$ renormalon.[2] Using the 3-flavor coupling constant instead, the Borel transform has the $u = 1/2$ renormalon,

$$B^{\text{3-flavor}}(u) \approx \left(\frac{\mu^2 e^{5/3}}{\overline{m}_b^2}\right)^u \frac{1}{1 - 2u}. \tag{4.33}$$

[2]One can eliminate the renormalons by setting the parameters to $(a, u') = (2, -b_0^{(3)}/(2b_0^{(4)}))$.

Hence, we can properly eliminate the $u = 1/2$ renormalon in the dual space with $(a, u') = (2, -1/2)$:

$$\tilde{B}^{\text{3-flavor}}(u) \approx \left(\frac{\mu^2 e^{5/3}}{\overline{m}_b^2}\right)^u \frac{1}{1-2u} \frac{1}{\Gamma\left(-a\left(u+u'\right)\right)}$$
$$\approx \mathcal{O}\left(\left(u-\frac{1}{2}\right)^0\right). \tag{4.34}$$

This indicates that the $n_f = 3$ theory correctly describes the renormalon structure better than the $n_f = 4$ theory. Physically, internal massive quarks in loops does not contaminate the IR structure. That is, it can be understood that internal charm quarks with non-zero (finite) masses do not contribute to the renormalon divergence of the bottom quark pole masses, i.e., all the charm quark mass effects in $n_f = 4$ theory are the decoupling effects.

4.1.4 Inclusive semileptonic decay of B meson

In the case of inclusive decays $\bar{B} \to X_c \ell \bar{\nu}_\ell$, the theoretical approach by the OPE is effective, taking advantage of the fact that the decay width is proportional to the imaginary part of the forward scattering amplitude $\langle B|\mathcal{M}|B\rangle$. For example, the total decay width of inclusive B decay Γ is given by the following OPE form:

$$\Gamma = \frac{G_F^2 |V_{cb}|^2}{192\pi^3} A_{\text{EW}} m_b^5 \left[C^\Gamma_{\bar{Q}Q}(m_b, \rho) + C^\Gamma_{\text{kin}} \frac{\mu_\pi^2}{m_b^2} + C^\Gamma_{\text{cm}} \frac{\mu_G^2}{m_b^2} + \mathcal{O}\left(\frac{\Lambda^3_{\text{QCD}}}{m_b^3}\right)\right], \tag{4.35}$$

with $\rho = m_c/m_b$. Here, $G_F \approx 1.166 \times 10^{-5}\,\text{GeV}^{-2}$ is the Fermi constant and $A_{EW} \approx 1.014$ is electroweak correction to this decay width. The uncertainties of these values are negligible. m_b is the pole mass of the bottom quark. $C^\Gamma_{\bar{Q}Q}$, C^Γ_{kin} and C^Γ_{cm} are Wilson coefficients which are calculated perturbatively. μ_π^2 and μ_G^2 are given by Eqs. (4.9) and (4.10). Up to $\mathcal{O}(1/m_b^2)$, $C^\Gamma_{\text{kin}} = -\frac{1}{2} C^\Gamma_{\bar{Q}Q}$ due to the reparameterization invariance [62, 63]. At present, $C^\Gamma_{\bar{Q}Q}$ and C^Γ_{cm} are calculated up to $\mathcal{O}(\alpha_s^3)$ [71, 72, 73, 74, 75, 76, 77, 57] and $\mathcal{O}(\alpha_s)$ [78, 79, 80, 81], respectively. We note that $\mathcal{O}(\Lambda_{\overline{\text{MS}}})$ non-perturbative term like $\bar{\Lambda}$ is prohibited in this OPE because HQET Lagrangian does not contain the dimension-four operator whose form is $\bar{b}\,\mathcal{O}\,b$. In this system, the typical energy scale is much larger than $\Lambda_{\overline{\text{MS}}}$ since the weak decay process $b \to uW \to u\ell\overline{\nu}$ has the large momentum transfer. Hence, it is reasonable that low energy gluons which cause an $\mathcal{O}(\Lambda_{\overline{\text{MS}}})$ mass shift cannot appear between the b quark operator insertions and $\mathcal{O}(\Lambda_{\overline{\text{MS}}})$ contributions are absent. In fact, the expression of the OPE in terms of the pole mass of the bottom quark behaves badly due to the renormalons, which make perturbative expansion grow rapidly. In order to avoid this bad convergence of perturbative calculation, the mass of the bottom quark should be changed from the pole mass to the short-distance mass. Short-distance mass is the quark mass defined only by the UV object from which IR gluons decouple. After change of the mass scheme using a perturbative relation between the pole mass and the short-distance mass, the perturbative expansion in terms of the short-distance mass exhibits better convergence due to the cancellation of $u = 1/2$ renormalon, and the remaining renormalon starts at $u = 1$.

The most popular short-distance mass is the $\overline{\rm MS}$ mass discussed in Sec. 4.1.2. We can prove that the $u = 1/2$ renormalon is subtracted in the large-β_0 approximation after rewriting the pole masses m_b and m_c by the $\overline{\rm MS}$ masses $\overline{m}_b$ and $\overline{m}_c$ in Γ, respectively (See App. F). However, the $\overline{\rm MS}$ mass scheme is not favored for rewriting the OPE of the B meson observables, because it is known that the perturbative expansions in terms of the $\overline{\rm MS}$ mass show bad convergence even after $u = 1/2$ renormalon is subtracted. Such bad behavior is caused by the fact that the $\overline{\rm MS}$ mass (≈ 4.18 GeV) without infrared-ness is far from the pole mass (≈ 4.8 GeV). In particular, there is another reason regarding the inclusive B decay width Γ; Γ is proportional to m_b^5, which enhances difference between the pole mass and the $\overline{\rm MS}$ mass. Since this behavior is not the evidence of renormalons, the prediction in terms of the $\overline{\rm MS}$ mass also should eventually converge to the exact value using the DSRS method to subtract higher order renormalons.

Conventionally, favorable choice of short-distance mass is the kinetic mass, which is defined by the relation between the heavy-light meson mass and the corresponding quark mass [82, 83, 27]. Heavy-light meson is a bound state of one heavy quark and one light quark, which is an IR sensitive object. Kinetic mass is defined by introducing factorization scale μ_f, which enables us to subtract $u = 1/2$ and $u = 1$ renormalons of quark pole mass simultaneously. In exchange for eliminating the renormalons, the kinetic quark mass and non-perturbative parameters have factorization scale dependence. Using the latest perturbative calculation of $C^{\Gamma}_{\bar{Q}Q}$ and kinetic-pole mass relation up to $\mathcal{O}(\alpha_s^3)$, the value of $|V_{cb}|$ is extracted as

$$|V_{cb}| = \sqrt{\frac{\mathcal{B}(B \to X_c \ell \bar{\nu})}{(10.66 \pm 0.15)\%}} \times 0.04216(51) \quad (\text{NNNLO, decay width}), \tag{4.36}$$

in which $\mathcal{B}(B \to X_c \ell \bar{\nu})$ is the semileptonic branching ratio and the NNNLO calculations of the total decay width Γ and the NNLO calculation of the lepton energy moments $d\Gamma/dq^2$ are used [58], and

$$\begin{aligned} |V_{cb}| &= \sqrt{\frac{\mathcal{B}(B \to X_c \ell \bar{\nu})}{(10.48 \pm 0.13)\%}} \times 0.04169(59) \\ &= \sqrt{\frac{\mathcal{B}(B \to X_c \ell \bar{\nu})}{(10.63 \pm 0.19)\%}} \times 0.04199(65) \quad (\text{NNNLO, lepton energy moments}), \end{aligned} \tag{4.37}$$

in which NNNLO calculations of both Γ and $d\Gamma/dq^2$ are used [59]. The uncertainty besides each value is the combined value of the systematic, statistical and experimental uncertainties. We note that Ref. [59] calls for caution in choosing experimental value of $\mathcal{B}(B \to X_c \ell \bar{\nu})$. This will be discussed in detail in Sec. 4.3.2.

The 1S mass is another short-distance mass, which is defined by a half of (perturbatively calculated) mass of the heavy quarkonium, which is a bound state of a heavy quark and an anti-heavy quark pair [25, 26]. Since the heavy quarkonium is a sufficiently UV object with a small radius, contributions from long-wavelength gluons are decoupled naturally. We determined $|V_{cb}|$ using the NNNLO perturbative expansion of pole-1S mass relation from the energy levels of two different bottomonium states $\Upsilon(1S)$ and $\eta_b(1S)$ [60].

The results are given by

$$|V_{cb}| = 0.0421\,(7)_{\rm sys} \quad (\text{from}\,\Upsilon(1\text{S})\,\text{mass}), \tag{4.38}$$

and

$$|V_{cb}| = 0.0429\,(7)_{\rm sys} \quad (\text{from}\,\eta_b(1\text{S})\,\text{mass}), \tag{4.39}$$

where the systematic uncertainties are combined. Since there is a large difference of the central values between Eqs. (4.38) and (4.39), we gave the combined result by

$$|V_{cb}| = 0.0425\,(7)_{\rm sys}\,(8)_{\rm spin} = 0.0425(11) \tag{4.40}$$

in Ref. [60] with a large systematic uncertainty from the difference of the spin dependence of the 1S bottomonium states.

In this thesis, we discuss the possibilities of using the $\overline{\rm MS}$ mass as the short-distance mass and subtracting $u = 1$ renormalon by the DSRS method to determine $|V_{cb}|$ precisely. In the analysis, we use the extended formula beyond the simple one defined in Chap. 3. We will see that the prediction accuracy with the $\overline{\rm MS}$ mass is improved by using that formula and the determined value of $|V_{cb}|$ is consistent and competitive with the results using the other mass schemes.

4.2 Application I: Masses of B and D mesons

In this section, we determine the PV masses of the bottom and charm quarks by subtracting renormalons using the DSRS method. The relation between the pole mass and $\overline{\rm MS}$ mass is used for this purpose. We first analyze the large-β_0 approximation case, which allows us to predict how the result of the DSRS method converges to the exact value as the truncation order of the dual-space series increases. Secondly, we determine the PV masses from the actual N^{3}LO or the estimated N^{4}LO perturbative expansion. Finally, using the result of the PV masses and the experimental values of B meson and D meson masses, the HQET parameters $\bar{\Lambda}$ and μ_π^2 are determined with renormalon subtraction.

4.2.1 PV mass determination from $\overline{\rm MS}$ mass

In the large-β_0 approximation

First, we investigate the pole-$\overline{\rm MS}$ mass relation in the large-β_0 approximation. Perturbative relation between the pole mass m_h and the $\overline{\rm MS}$ mass $\overline{m}_h$ of the heavy quark is given by

$$m_h = \overline{m}_h\big(1 + \delta_g(\overline{m}_h) + \delta_G(\overline{m}_h)\big), \tag{4.41}$$

where $\overline{m}_h = m_h^{\overline{\rm MS}}(m_h^{\overline{\rm MS}})$ is RG invariant. The perturbative expansion of δ_g[13, 84] is given by

$$\delta_g(\overline{m}_h) = \frac{C_F}{2\pi b_0^2}\sum_{n=0}^{\infty}\alpha_s(\mu^2)^{n+1}\frac{(-1)^n}{n+1}g_{n+1}(L_{\overline{m}}), \tag{4.42}$$

where $L_{\overline{m}} = \log(\mu^2/\overline{m}_h^2)$, and the coefficients g_n's are read from

$$g(u) = \sum_{n=0}^{\infty} g_n(L_{\overline{m}})\left(\frac{u}{b_0}\right)^n = \left(\frac{\mu^2}{\overline{m}_h^2}\right)^u \frac{3-2u}{6}\frac{\Gamma(4-2u)}{\Gamma(1+u)\Gamma(2-u)\Gamma(3-u)}. \tag{4.43}$$

Since Eq. (4.42) is a convergent series, the all-order contribution can be resummed in the following integral form [35]

$$\delta_g(\overline{m}_h) = -\frac{C_F}{2\pi b_0^2}\int_0^{-a} du\,\frac{g(u)-g(0)}{u}; \quad a = b_0\alpha_s(\mu^2). \tag{4.44}$$

On the other hand, the perturbative expansion of δ_G [13, 84] is given by

$$\delta_G(\overline{m}_h) = \frac{C_F}{2\pi b_0^2}\sum_{n=0}^{\infty}\alpha_s(\mu^2)^{n+1}G_{n+1}(L_{\overline{m}})\,n!, \tag{4.45}$$

where coefficients G_n's are read from

$$G(u) = \sum_{n=0}^{\infty}G_n(L_{\overline{m}})\left(\frac{u}{b_0}\right)^n = \left(\frac{\mu^2 e^{5/3}}{\overline{m}_h^2}\right)^u (1-u)\frac{\Gamma(1+u)\Gamma(1-2u)}{\Gamma(3-u)}. \tag{4.46}$$

Eq. (4.45) is apparently divergent due to factorial behavior. The Borel transform of δ_G is given by

$$B_{\delta_G}(u) = \frac{C_F}{2\pi b_0}\frac{G(u)-G(0)}{u}, \tag{4.47}$$

which contains the IR renormalons at $u = 1/2,\, 3/2,\, 2,\, 5/2, \cdots$ and the UV renormalons at $u = -1,\, -2,\, -3, \cdots$. These IR renormalons cause the imaginary parts of m_h, which has the form of

$$\mathcal{O}(\Lambda_{\overline{\rm MS}} \times (\Lambda_{\overline{\rm MS}}/\overline{m}_h)^{2u}) \quad \text{for} \quad u = 1/2,\, 3/2,\, 2,\, 5/2, \cdots . \tag{4.48}$$

We can see that in the large-β_0 approximation for the quark pole mass, the renormalon at $u = 1$ is absent, which implies that the μ_π^2 in Eq. (4.19) might not contain an imaginary part. The PV mass of the heavy quark h is defined by

$$\big[m_h\big]_{\rm PV} = \overline{m}_h\big(1 + \delta_g(\overline{m}_h) + \big[\delta_G(\overline{m}_h)\big]_{\rm PV}\big), \tag{4.49}$$

where $\big[\delta_G(\overline{m}_h)\big]_{\rm PV}$ is calculated by the principal value of the Borel resummation

$$\big[\delta_G(\overline{m}_h)\big]_{\rm PV} = \frac{1}{b_0}\int_{0,{\rm PV}}^{\infty} du\, e^{-\frac{u}{b_0\alpha_s(\mu^2)}} B_{\delta_G}(u). \tag{4.50}$$

According to Ref. [35], $\big[\delta_G(\overline{m}_h)\big]_{\rm PV}$ can be also calculated by the following one-parameter momentum integral form

$$\begin{aligned}\big[\delta_G(\overline{m}_h)\big]_{\rm PV} &= \frac{C_F}{4\pi b_0}\int_{0,{\rm PV}}^{e^{5/3}} d\tau\,\frac{\tau + (2-\tau)\sqrt{1+4/\tau}}{2}\,\frac{1}{\log(\tau\,\overline{m}_h^2/\Lambda_{\overline{\rm MS}}'^2)} \\ &+ \frac{C_F}{4\pi b_0}\int_{e^{5/3}}^{\infty} d\tau\left(\frac{\tau + (2-\tau)\sqrt{1+4/\tau}}{2} - \frac{3}{\tau}\right)\frac{1}{\log(\tau\,\overline{m}_h^2/\Lambda_{\overline{\rm MS}}'^2)},\end{aligned} \tag{4.51}$$

where $\Lambda'_{\overline{\rm MS}} = \Lambda_{\overline{\rm MS}}\, e^{5/6}$. Derivation of Eq. (4.51) is given in App. E. Using Eq. (4.44) and Eqs. (4.50) or (4.51), the reference values of $\big[m_b\big]_{\rm PV}$ and $\big[m_c\big]_{\rm PV}$ are obtained. For the bottom quark reference point $\overline{m}_b = 4.18$ GeV $(\Lambda_{\overline{\rm MS}}/0.3$ GeV),

$$\big[m_b\big]_{\rm PV} = 17.13 \times \Lambda_{\overline{\rm MS}} = 5.138\ {\rm GeV}\left(\frac{\Lambda_{\overline{\rm MS}}}{0.3\ {\rm GeV}}\right), \tag{4.52}$$

Table 4.1: Comparison of the dual-space coefficient $\tilde{d}_n^{(\beta_0)}$ with the one in the original space $d_n^{\beta_0}$. Owing to the dual transform, the divergent behavior of the dual-space coefficients from $u = 1/2, 3/2, ...$ IR renormalons is greatly suppressed while the effects of the UV renormalons remain.

n	$d_n^{(\beta_0)}$	$\tilde{d}_n^{(\beta_0)}$	n	$d_n^{(\beta_0)}$	$\tilde{d}_n^{(\beta_0)}$
0	0.4244	0.4244	12	3.490×10^{10}	-1.747×10^5
1	1.424	1.074	13	6.498×10^{11}	3.712×10^6
2	3.836	0.339	14	1.303×10^{13}	-3.337×10^7
3	17.13	-3.574	15	2.800×10^{14}	3.398×10^8
4	97.59	-9.651	16	6.417×10^{15}	-4.059×10^9
...	...	...	...	...	...

and for the charm quark reference point $\overline{m}_c = 1.27$ GeV $(\Lambda_{\overline{\rm MS}}/0.3$ GeV),

$$\big[m_c\big]_{\rm PV} = 5.169 \times \Lambda_{\overline{\rm MS}} = 1.551 \text{ GeV} \left(\frac{\Lambda_{\overline{\rm MS}}}{0.3 \text{ GeV}}\right). \tag{4.53}$$

We set $n_f = 3$ to evaluate them, and the values of the $\overline{\rm MS}$ masses correspond to the central values of the PDG values [54].

We consider the dual space series to suppress the IR renormalons at $u = 1/2,\ 3/2,\ 2,\ 5/2,\ \cdots$, by choosing the parameters $(a, u') = (2, -1/2)$. This scheme is the same as the scheme (B) in Sec. 3.3. Eq. (4.41) is written as

$$\frac{m_h - \overline{m}_h}{\overline{m}_h} = \delta(\overline{m}_h) = \sum_{n=0}^{\infty} \alpha_s(\mu^2)^{n+1} d_n^{(\beta_0)}(L_{\overline{m}}), \tag{4.54}$$

with

$$d_n^{(\beta_0)}(L_{\overline{m}}) = \frac{C_F}{2\pi b_0^2}\Big[G_{n+1}(L_{\overline{m}})\, n! + \frac{(-1)^n}{n+1} g_{n+1}(L_{\overline{m}})\Big]. \tag{4.55}$$

The dual-space series of δ is given by

$$\begin{aligned}\tilde{\delta}(\tau) &= \int_{x_0^2 - i\infty}^{x_0^2 + i\infty} \frac{dx^2}{2\pi i}\, e^{\tau^2 x^2} x^{2\times 2\times(-1/2)} \delta(\overline{m} = 1/x^2) \\ &= \sum_{n=0}^{\infty} \alpha_s(\mu^2)^{n+1} \tilde{d}_n^{(\beta_0)}(L_\tau),\end{aligned} \tag{4.56}$$

where $L_\tau = \log(\mu^2/\tau^4)$, and $\tilde{d}_n^{(\beta_0)}$'s can be read from

$$\sum_{n=0}^{\infty} \alpha_s(\mu^2)^{n+1} \tilde{d}_n^{(\beta_0)} = \frac{1}{\Gamma(1 - 2\hat{H})} \sum_{n=0}^{\infty} \alpha_s(\mu^2)^{n+1} d_n^{(\beta_0)}. \tag{4.57}$$

We note that, in the dual space, the UV renormalons at $u = -1,\ -2,\ \cdots$ remain, while the IR renormalons are all suppressed. Tab. 4.1 compares $d_n^{(\beta_0)}$ with $\tilde{d}_n^{(\beta_0)}$. Due to the

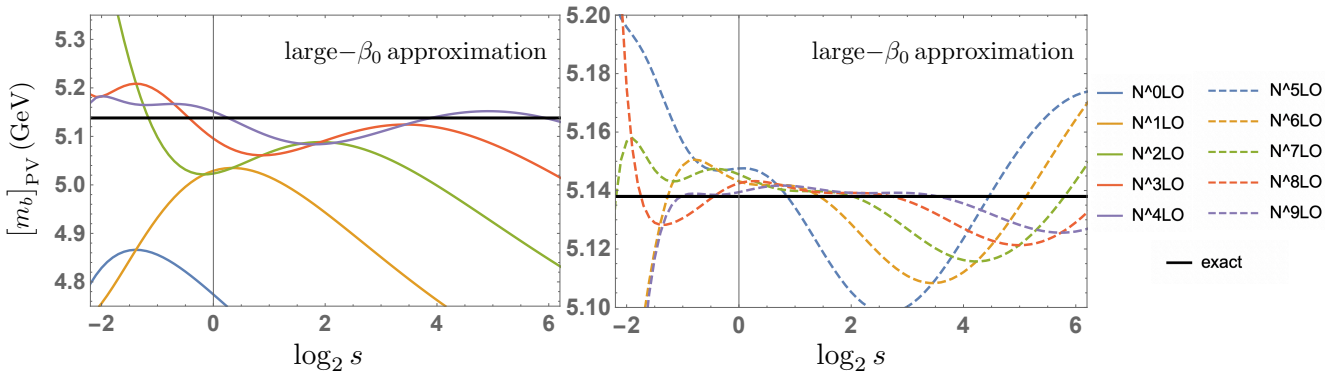

Figure 4.2: Scale dependence of $\left[m_b\right]_{\rm PV}$. We set $n_f = 3$ and use inputs that $\overline{m}_b = 4.18$ GeV and $\Lambda_{\overline{\rm MS}} = 0.3$ GeV. The colored lines show the predictions of $\left[m_b\right]_{\rm PV}$ when we truncate $\tilde{\delta}$ at α_s^{k+1} for $k = 0,\, 1,\, 2, \cdots, 9$. The black solid line represents the exact value given by Eq. (4.52).

suppression of the IR renormalons at $u = 1/2, 3/2, \cdots$ in the dual space, the growth of $\tilde{d}_n^{(\beta_0)}$ is milder than that of the original one at lower orders. We can confirm that as n increases, the UV renormalon at $u = -1$ causes the sign-alternating divergent behavior of $\tilde{d}_n^{(\beta_0)}$. By the inverse dual transform, the renormalon-subtracted pole mass, PV mass, is calculated as

$$\left[m_h\right]_{\rm PV} = \overline{m}_h\Big(1 + \left[\delta(\overline{m}_h)\right]_{\rm PV}\Big), \tag{4.58}$$

where

$$\begin{aligned}\left[\delta(\overline{m}_h)\right]_{\rm PV} &= x^{-2}\int_{0,{\rm PV}} d\tau^2\, e^{-\tau^2 x^2}\tilde{\delta}(\tau) \\ &= \frac{1}{\overline{m}_h}\int_{0,{\rm PV}} d\tau^2\, e^{-\tau^2/\overline{m}_h}\sum_{n=0}^{\infty}\alpha_s(\mu^2)^{n+1}\tilde{d}_n^{(\beta_0)}(L_\tau).\end{aligned} \tag{4.59}$$

The results of the DSRS method (Eq. (4.58)) are compared with the exact values of the PV masses (Eqs. (4.52) and (4.53)). Fig. 4.2 shows the scale dependence of $\left[m_b\right]_{\rm PV}$ when we set $\mu = s\tau^2$ and truncate $\tilde{\delta}$ at α_s^{k+1} for $k = 0, 1, 2, \cdots, 9$. The horizontal axis is displayed on the logarithmic scale. In the right panel, the scale dependence at higher orders is slightly unstable around $s = \mathcal{O}(1)$. The analysis of the toy model in Sec. 3.3 shows that it is due to the UV renormalons, but the magnitude of the instability is small enough to reflect the fact that the UV renormalons start from $u = -1$. The left figure shows that the predicted value at N^{3}LO or N^{4}LO level is close enough to the exact value around $s = 10$.

Similarly, Fig. 4.3 shows the scale dependence of $\left[m_c\right]_{\rm PV}$, where the setups of the analysis is the same as Fig. 4.2. Compared with the case for $\left[m_b\right]_{\rm PV}$, we can see that $\left[m_c\right]_{\rm PV}$ converges more slowly to the exact value with increasing perturbation order. In particular, in the left panel, the value in the flat region of the N^{3}LO result around $s = \mathcal{O}(1)$ deviates from the exact value by about 5 %. Nevertheless, as k grows, the prediction converses to the exact value around $s = \mathcal{O}(1)$ and the flat region extends gradually.

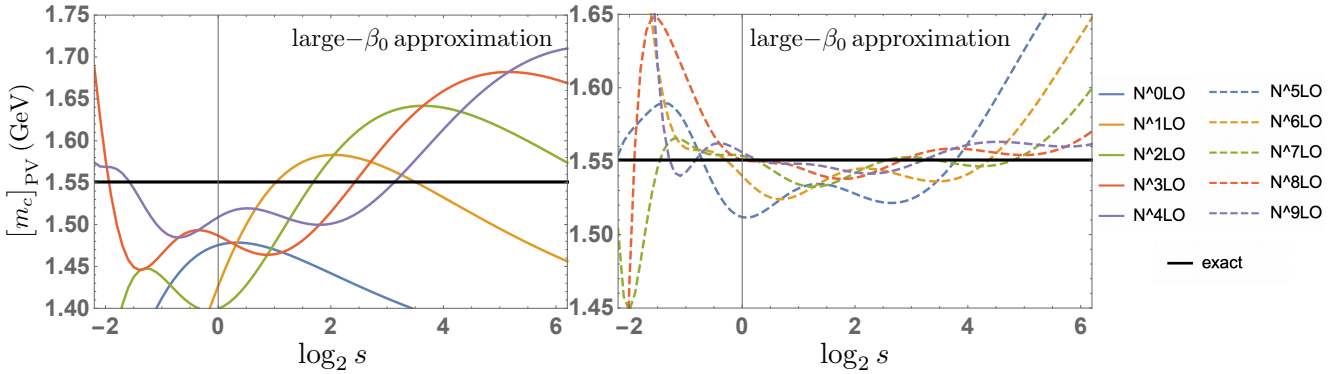

Figure 4.3: Scale dependence of $\left[m_c\right]_{\rm PV}$. We set $n_f = 3$ and use inputs that $\overline{m}_c = 1.27$ GeV and $\Lambda_{\overline{\rm MS}} = 0.3$ GeV. The colored lines show the predictions of $\left[m_c\right]_{\rm PV}$ when we truncate $\tilde{\delta}$ at α_s^{k+1} for $k = 0, 1, 2, \cdots, 9$. The black solid line represents the exact value given by Eq. (4.53).

Actual perturbation theory

Now let us determine the PV masses from the $\overline{\rm MS}$ masses using the DSRS method with the state-of-the-art perturbative coefficients. Since the coefficient in the large-β_0 approximation $d_n^{(\beta_0)}$ reproduces well the divergent behavior of the realistic d_n, the convergence after the renormalon subtraction using the DSRS method should be similar for both cases. The d_n's contain corrections from the internal massive quark, of which the explicit values are given in App. A. We note that in the expansion using the 3-flavor coupling, the d_n's for both m_b and m_c are quite similar to the coefficients with massive corrections turned off. In order to evaluate the PV masses, we use the input values

$$\overline{m}_b = 4.18^{+0.03}_{-0.02}\ \text{GeV}, \tag{4.60}$$

$$\overline{m}_c = 1.27 \pm 0.02\ \text{GeV}, \tag{4.61}$$

$$\alpha_s^{(5)}(M_Z) = 0.1179 \pm 0.0009, \tag{4.62}$$

from the Particle Data Group (PDG) [54].

To repeat, we consider the case that the quark pole mass has the IR renomalons at $u = 1$, although the large-β_0 approximation suggests its absence. Lorentz invariance prohibits the exsistence of this remormalon in the large-β_0 approximation [85], but there is no reason why it should not be absent beyond this approximation. In Ref. [45], however, the leading renormalon-subtracted series has tendency to exhibit the $u = -1$ (UV) renormalon behavior rather than the $u = 1$ one. Therefore, although the existence of $u = 1$ renormalon cannot be denied, its effect is expected to be sufficiently small.

The reader may notice that the DSRS method separates the $u = 1$ renormalon of the form $\Lambda^2_{\overline{\rm MS}}/\overline{m}_b$, according to Eq. (4.48) with $u = 1$, which is different from the definition of the $u = 1$ renormalon (Eq. (4.20)). This can cause the uncertainty to the calculation of $\left[m_h\right]_{\rm PV}$, which is negligible in our analysis for the following reasons. The desired form

of the imaginary part by the $u = 1$ renormalon $\Lambda^2_{\overline{\rm MS}}/\big[m_h\big]_{\rm PV}$, is written as

$$\frac{\Lambda^2_{\overline{\rm MS}}}{\big[m_h\big]_{\rm PV}} = \frac{\Lambda^2_{\overline{\rm MS}}}{\overline{m}_h}\frac{\overline{m}_h}{\big[m_h\big]_{\rm PV}} = \frac{\Lambda^2_{\overline{\rm MS}}}{\overline{m}_h}\Big(1 - \alpha_s(\overline{m}_h^2)d_0 + \mathcal{O}\Big(\alpha_s(\overline{m}_h^2)^2\Big)\Big). \tag{4.63}$$

Here we expand $\big[m_h\big]_{\rm PV}$ in $\alpha_s(\overline{m}_h^2)$ using the pole-$\overline{\rm MS}$ mass relation. The dual transform defined by Eq. (4.56) suppresses the contribution of the form

$$(\text{const.}) \times \Lambda_{\overline{\rm MS}}\left(\frac{\Lambda_{\overline{\rm MS}}}{\overline{m}_h}\right)^{2u}, \tag{4.64}$$

for $u = 1/2,\, 1,\, \cdots$, which indicates that $\mathcal{O}(\Lambda^2_{\overline{\rm MS}}/\overline{m}_h\alpha_s(\overline{m}_h^2))$ uncertainty remains as an unsuppressed renormalon in the calculation of $\big[m_h\big]_{\rm PV}$. The typical size of the uncertainty is estimated as

$$\frac{\Lambda^2_{\overline{\rm MS}}}{\overline{m}_b}\alpha_s(\overline{m}_b^2)d_0 \approx \frac{0.3^2\ \text{GeV}^2}{4.18\ \text{GeV}} \times 0.21 \times \frac{4}{3\pi} \approx \mathcal{O}(1\ \text{MeV}), \tag{4.65}$$

for the bottom quark and

$$\frac{\Lambda^2_{\overline{\rm MS}}}{\overline{m}_c}\alpha_s(\overline{m}_c^2)d_0 \approx \frac{0.3^2\ \text{GeV}^2}{1.27\ \text{GeV}} \times 0.39 \times \frac{4}{3\pi} \approx \mathcal{O}(10\ \text{MeV}), \tag{4.66}$$

for the charm quark. In addition, we can expect for the constant coefficient of the $u = 1$ renormalon to be small according to the above discussion. Actually, the estimated uncertainty size above is sufficiently smaller than the other systematic uncertainties in our determination.

We explicitly show the dual-space series for the d_n's, which is defined by Eqs. (4.54)−(4.59), with $d_n^{(\beta_0)}$ and $\tilde{d}_n^{(\beta_0)}$ replaced by d_n and $\tilde{d}_n$, respectively. We use the N^{4}LO beta function which contains $\{b_0,\, b_1,\, \cdots,\, b_4\}$. The dual-space series $\tilde{\delta}$ is given by

$$\tilde{\delta}(\tau) \approx e^{\hat{H}\log(\mu^2/\tau^4)}\Big[0.4244\,\alpha_s + 0.6865\,\alpha_s^2 + 0.6872\,\alpha_s^3 - 2.656\,\alpha_s^4\Big], \tag{4.67}$$

for the bottom quark and

$$\tilde{\delta}(\tau) \approx e^{\hat{H}\log(\mu^2/\tau^4)}\Big[0.4244\,\alpha_s + 0.6928\,\alpha_s^2 + 0.6906\,\alpha_s^3 - 2.747\,\alpha_s^4\Big], \tag{4.68}$$

for the charm quark. Here $\alpha_s = \alpha_s(\mu^2)$. We can see that convergence of the series is improved in the dual space compared with the original one (see App. A), and its behavior is similar to the large-β_0 approximated one in Tab. 4.1. It implies that we may estimate the N^{4}LO PV masses with good accuracy by using $d_4^{(\beta_0)}$ and N^{4}LO β function, although d_4 has not been computed yet. However, if we naively use $d_4^{(\beta_0)} \approx 97.59$ in place of the realistic d_4, the N^{4}LO coefficient in the dual space is obtained as $\tilde{d}_4 \approx -29$, which is too large for $\tilde{\delta}$ to be a convergent series. It is because the normalization of $u = 1/2$ renormalon is deviated from the large-β_0 approximated one by the effect of $b_1,\, b_2, \cdots$. The lack of such information cannot cancel out the factors from the lower terms propagated by the

DSRS method. By following the procedure in Appendix. A of Ref. [86], we estimate the normalization of the $u = 1/2$ renormalon to mimic the realistic renormalon behavior of d_4. The estimated value $d_4^{\rm est}$ is given by

$$d_4^{\rm est} \approx 111.3 \pm 7.72, \tag{4.69}$$

and the dual-space one is

$$\tilde{d}_4^{\rm est} \approx -15.25 \pm 7.72. \tag{4.70}$$

for the bottom quark and

$$\tilde{d}_4^{\rm est} \approx -15.54 \pm 7.72. \tag{4.71}$$

for the charm quark. The uncertainty comes from the determination of the normalization constant of the $u = 1/2$ renormalon. In our N^{4}LO estimation, we use the above values which is better-behaved than the naive estimation $\tilde{d}_4 \approx -29$. This indicates that the remnant value of the coefficient, after the renormalon suppression in the dual space, is important for the evaluation of the PV mass.

Fig. 4.4 shows the scale dependence of $\left[m_b\right]_{\rm PV}$ when we set $\mu = s\tau^2$ and truncate $\tilde{\delta}$ at α_s^{k+1} after expanding the exponential factor $e^{\hat{H}\log(\mu^2/\tau^4)}$ in Eq. (4.67). The colored lines represent the results for $k = 0$, 1, 2, 3, 4 when the inputs are set to the central value of the PDG values. The result for $k = 4$ is estimated by using $d_4^{\rm est}$ and the uncertainty from the normalization is displayed by dotted and dot-dashed lines. In comparison to Fig. 4.2, the rough shapes of the scale-dependence for both are similar. Furthermore, Fig. 4.4 appears to converge to a certain value more quickly near $s = \mathcal{O}(1)$. Since at the stationary point around $\log_2 s = 3$, the N^{3}LO line is close to the exact value in the large-β_0 approximation in Fig. 4.2, we give the determined value by the green line and band as in Fig 4.4. The band width is estimated by the scale variation from $s_0/2$ to $2s_0$ around the stationary point $s = s_0 \approx 7.408$. It should be careful to evaluate $\left[m_b\right]_{\rm PV}$ using higher order expansion. The analysis with the large-β_0 approximation suggests that the right-most stationary point used in the N^{3}LO determination goes much farther in the calculation at higher orders, giving a prediction value that deviates from the true value. This is because the value at the right-most stationary point is estimated to be $\tilde{d}_0(k/e)^k$ according to Eqs. (3.31) and (3.32), which diverges to $+\infty$ as $k \to +\infty$. At higher orders, one should estimate the value of $\left[m_b\right]_{\rm PV}$ at the stable region expected to appear around $s = \mathcal{O}(1)$ as in the right panel of Fig. 4.2.

The determined value of $\left[m_b\right]_{\rm PV}$ is given by

$$\begin{aligned}\left[m_b\right]_{\rm PV} &= 4.822\,(10)_{\rm PT}\,(1)_{{\rm sub}\,u=1}\,(33)_{\overline{m}_b}\,(0)_{\overline{m}_c}\,(8)_{\alpha_s}\ {\rm GeV} \\ &= 4.822\,(10)_{\rm th}\,(34)_{\rm input}\ {\rm GeV} = 4.822\,(36)\ {\rm GeV},\end{aligned} \tag{4.72}$$

where the central value is given by the value of the N^{3}LO line at $s = s_0 \approx 7.408$. The first bracket in the first line denotes the uncertainty from the scale dependence discussed above. The second one is estimated by the sub-leading effect of the $u = 1$ renormalon considered in Eq. (4.65). The third, fourth and fifth ones represent the uncertainties from the input PDG values of $\overline{m}_b$, $\overline{m}_c$ and $\alpha_s(M_Z)$, respectively. In the second line, the uncertainties are combined. It can be seen that the theoretical uncertainty is sufficiently small compared to the input uncertainties, which is the evidence that the leading contribution from the IR renormalons are subtracted from the calculation of the PV mass.

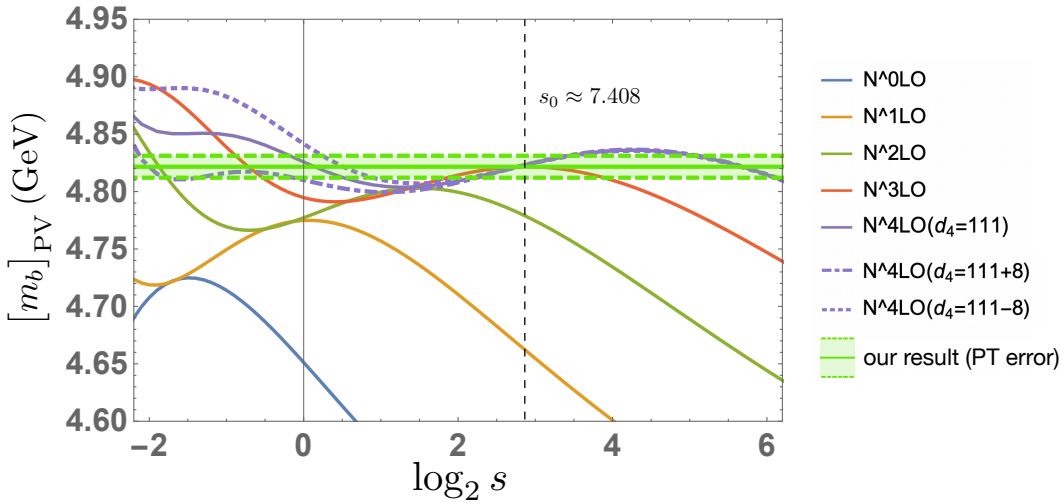

Figure 4.4: Determination of $[m_b]_{\rm PV}$ from the actual perturbative expansion using the DSRS method. The colored lines represent the scale dependence of N^{k}LO results for $k = 0, 1, 2, 3, 4$. We use inputs $\overline{m}_b = 4.18$ GeV, $\overline{m}_c = 1.27$ GeV and $\alpha_s(M_Z) = 0.1179$. $d_4^{\rm est}$ is used to estimate the N^{4}LO result. The green line and shaded area exhibit the determined value using the N^{3}LO result by comparing with the study using the large-β_0 approximation as in Fig. 4.2.

Fig. 4.2 also tells us that in the case with the N^{4}LO perturbative expansion, the rightmost stationary point in the left panel gives a well approximated value of $[m_b]_{\rm PV}$, and the steepness around the hilltop is milder than that of the N^{3}LO calculation. We estimate the N^{4}LO value of $[m_b]_{\rm PV}$ using $d_4^{\rm est}$ and b_4, by investigating the scale variation of purple solid line in Fig. 4.4, which is given by

$$[m_b]_{\rm PV}^{\rm N^4LO\,est.} = 4.836\,(7)_{\rm PT}\,(0)_{d_4}\ \text{GeV}, \tag{4.73}$$

where the central value is given by the value of the N^{4}LO solid line at $s = s_0^{(4)} \approx 19.22$. The first bracket denotes the uncertainty from the scale variation from $s_0^{(4)}/2$ to $2s_0^{(4)}$ around the stationary point $s = s_0^{(4)}$. The second one comes from the uncertainty of $d_4^{\rm est}$. Hence, the next order of the perturbation is expected to determine the bottom quark PV mass more precisely. It is owing to the subtraction of the IR renormalons using the DSRS method.

In order to decrease the other systematic uncertainties, $\overline{m}_b$ should be determined with high precision. Eq. (4.72) is the most conservative result using the PDG value. By using more accurate recent determinations, the uncertainty size from $\overline{m}_b$ would be reduced. For example, the Flavor Lattice Averaging Group (FLAG) [87] recently reports the values of $\overline{m}_b$ as

$$\overline{m}_b = 4.171(20)\ \text{GeV} \quad \text{from} \quad N_f = (2+1)\,\text{lattice}, \tag{4.74}$$

and

$$\overline{m}_b = 4.203(11)\ \text{GeV} \quad \text{from} \quad N_f = (2+1+1)\,\text{lattice}, \tag{4.75}$$

where N_f denotes the number of active quarks in the lattice simulations [3]. These values

[3]There is inconsistency between the results of the lattice simulation for $N_f = 2+1$ and $N_f = 2+1+1$.

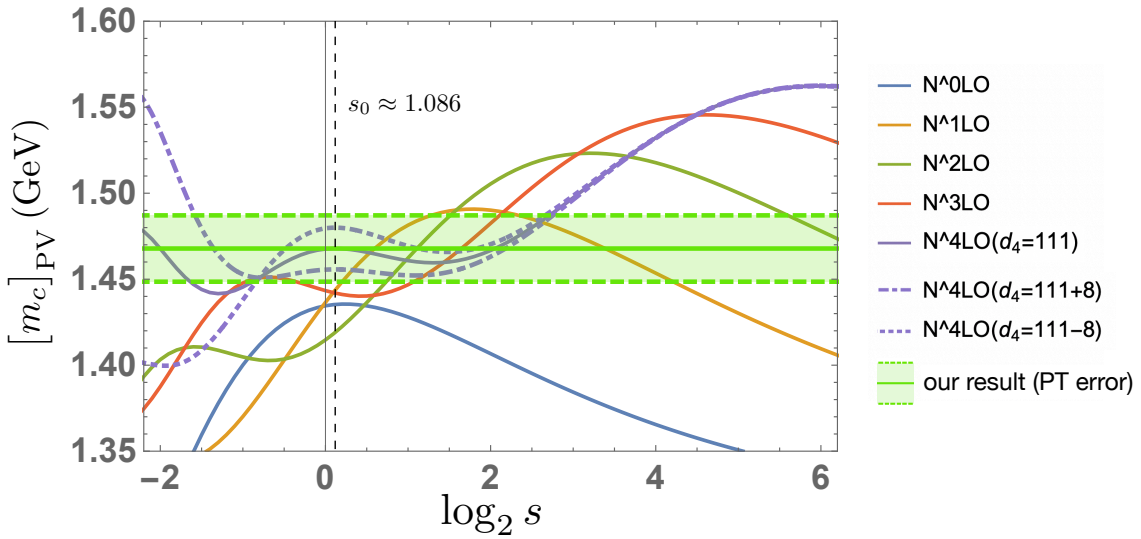

Figure 4.5: Determination of $[m_c]_{\rm PV}$ from the actual perturbative expansion using the DSRS method. The colored lines represent the scale dependence of N^{k}LO results for $k = 0, 1, 2, 3, 4$. Inputs for calculations are same as Fig. 4.4. The green line and shaded area exhibit the determined value using the estimated N^{4}LO result by comparing with the study using the large-β_0 approximation as in Fig. 4.3.

give the determined values

$$[m_b]_{\rm PV} = 4.812\,(22)_{\overline{m}_b}\ \text{GeV} \quad (\text{N}^3\text{LO},\ N_f = (2+1)), \tag{4.76}$$

and

$$[m_b]_{\rm PV} = 4.847\,(12)_{\overline{m}_b}\ \text{GeV} \quad (\text{N}^3\text{LO},\ N_f = (2+1+1)), \tag{4.77}$$

respectively. The other uncertainties of the FLAG inputs results, as in Eq. (4.72), are almost the same.

Similarly Fig. 4.5 shows the scale dependence of $[m_c]_{\rm PV}$ when we set $\mu = s\tau^2$ and truncate $\tilde{\delta}$ at α_s^{k+1}. The setups and inputs of the analysis are the same as Fig. 4.4. The large-β_0 approximation as in Fig. 4.3 implies that at the present, the number of the perturbative coefficients is insufficient to determine $[m_c]_{\rm PV}$ precisely, unlike the bottom quark case. In other words, if we investigate the flat region around $s = \mathcal{O}(1)$ and estimate the scale dependence at current status of the perturbation, the value of $[m_c]_{\rm PV}$ would be over- or under-estimated. It is because the physical scale of the charm quark system (~ 1.5 GeV) enables a perturbation but is low to explain the exact value of observables from a small number of perturbative coefficients. In this thesis, we use the estimated N^{4}LO result to give a determined value of $[m_c]_{\rm PV}$. It is because a lack of the remaining N^{4}LO correction would be smaller than the unknown higher order corrections.

The determined value of $[m_c]_{\rm PV}$ is given by

It is difficult to quantify whether the differences are due to the treatment of the heavy bottom quark, the definition of fermion fields in active flavor quarks, or other effects, and no such analysis has been performed to date. As for the charm quark mass results described below, it is not possible to objectively determine which of the two results is correct. In our determination, the FLAG values are considered as only a reference.

$$\begin{aligned}\left[m_c\right]_{\rm PV} &= 1.468\,(19)_{\rm PT}\,(12)_{d_4}\,(10)_{{\rm sub}\,u=1}\,(0)_{\overline{m}_b}\,(24)_{\overline{m}_c}\,(4)_{\alpha_s}\ {\rm GeV}\\ &= 1.468\,(25)_{\rm th}\,(25)_{\rm input}\ {\rm GeV} = 1.468\,(35)\ {\rm GeV},\end{aligned} \tag{4.78}$$

where the central value is given by the value of the N^{4}LO solid line at $s = s_0 \approx 1.086$. The first bracket in the first line denotes the uncertainty from the scale variation from $s_0/2$ to $2s_0$ around the stationary point $s = s_0$. The second one comes from the uncertainty of $d_4^{\rm est}$. The third one is estimated by the sub-leading effect of the $u = 1$ renormalon considered in Eq. (4.66). The fourth, fifth and sixth ones represent the uncertainties from the input PDG values of $\overline{m}_b$, $\overline{m}_c$ and $\alpha_s(M_Z)$, respectively. In the second line, the uncertainties are combined. It can be seen that the theoretical uncertainty and the input uncertainty are comparable. The theoretical uncertainty can be reduced only by calculating the true N^{4}LO perturbative correction. The input uncertainty also can be reduced by using the recent determinations of $\overline{m}_c$. For example, FLAG [87] reports the value of $\overline{m}_c$ as

$$\overline{m}_c = 1.275(5)\ {\rm GeV} \quad {\rm from} \quad N_f = (2+1)\,{\rm lattice}, \tag{4.79}$$

and

$$\overline{m}_c = 1.278(13)\ {\rm GeV} \quad {\rm from} \quad N_f = (2+1+1)\,{\rm lattice}, \tag{4.80}$$

which give the determined values

$$\left[m_c\right]_{\rm PV} = 1.474\,(6)_{\overline{m}_c}\ {\rm GeV} \quad ({\rm N^3LO},\ N_f = (2+1)), \tag{4.81}$$

and

$$\left[m_c\right]_{\rm PV} = 1.478\,(16)_{\overline{m}_c}\ {\rm GeV} \quad ({\rm N^3LO},\ N_f = (2+1+1)), \tag{4.82}$$

respectively. The other uncertainties of the FLAG inputs results, as in Eq. (4.78), are almost the same.

4.2.2 Determination of HQET parameters

In this section, we determine the HQET parameters $\bar{\Lambda}$ and μ_π^2 based on the renormalon-subtracted OPE in the PV scheme given by

$$\left[M_B\right]_{\rm spin\,ave.} = \frac{M_B + 3M_{B^*}}{4} = \left[m_b\right]_{\rm PV} + \left[\bar{\Lambda}\right]_{\rm PV} + \frac{\left[\mu_\pi^2\right]_{\rm PV}}{2\left[m_b\right]_{\rm PV}} + \mathcal{O}(1/m_b^2), \tag{4.83}$$

and

$$\left[M_D\right]_{\rm spin\,ave.} = \frac{M_D + 3M_{D^*}}{4} = \left[m_c\right]_{\rm PV} + \left[\bar{\Lambda}\right]_{\rm PV} + \frac{\left[\mu_\pi^2\right]_{\rm PV}}{2\left[m_c\right]_{\rm PV}} + \mathcal{O}(1/m_c^2). \tag{4.84}$$

We use the PDG values of the meson masses [54] given by

$$M_B = \frac{5.27965 + 5.27934}{2}\ {\rm GeV},\ M_{B^*} = 5.32470\ {\rm GeV}. \tag{4.85}$$

and

$$M_D = \frac{1.86484 + 1.86966}{2}\ \text{GeV},\ M_{D^*} = 2.00685\ \text{GeV}, \tag{4.86}$$

where the PDG uncertainties are negligible in this analysis. Using the results Eqs. (4.72) and (4.78) in Sec. 4.2.1, we obtain

$$\begin{aligned}\left[\bar{\Lambda}\right]_{\rm PV} &= 0.486\,(16)_{\rm PT}\,(5)_{d_4}\,(5)_{{\rm sub}\,u=1}\,(6)_{1/m_h^2}\,(48)_{\overline{m}_b}\,(11)_{\overline{m}_c}\,(9)_{\alpha_s}\ \text{GeV}\\ &= 0.486\,(19)_{\rm th}\,(50)_{\rm input}\ \text{GeV} = 0.486\,(54)\ \text{GeV},\end{aligned} \tag{4.87}$$

and

$$\begin{aligned}\left[\mu_\pi^2\right]_{\rm PV} &= 0.05\,(9)_{\rm PT}\,(5)_{d_4}\,(4)_{{\rm sub}\,u=1}\,(5)_{1/m_h^2}\,(14)_{\overline{m}_b}\,(11)_{\overline{m}_c}\,(1)_{\alpha_s}\ \text{GeV}^2\\ &= 0.05\,(12)_{\rm th}\,(18)_{\rm input}\ \text{GeV}^2 = 0.05\,(22)\ \text{GeV}^2.\end{aligned} \tag{4.88}$$

In the first line of Eqs. (4.87) and (4.88), the uncertainties are given in the same notation as in Eqs. (4.72) and (4.78), except for the fourth one which denotes the uncertainty estimated from the ignored non-perturbative corrections of $\mathcal{O}(1/m_h^2)$ order. For $\bar{\Lambda}$, the theoretical uncertainty is sufficiently small compared to $\mathcal{O}(\Lambda_{\overline{\rm MS}}) \sim 300$ MeV, reflecting the subtraction of the $u = 1/2$ renormalon. $\overline{m}_b$ uncertainty accounts for most of the size of the input uncertainties, but as discussed in section 4.2.1, that can be improved by using a more accurate value of $\overline{m}_b$. For μ_π^2, however, even the theoretical uncertainty has a magnitude of $\mathcal{O}(\Lambda^2_{\overline{\rm MS}})$, seemingly as if the $u = 1$ renormalon remains in our calculation. We believe that a small number of the known perturbative coefficients result in a large perturbative uncertainty of $\left[m_c\right]_{\rm PV}$, which is reflected in μ_π^2. Thanks to removing renormalons, the perturbative uncertainty will be reduced if higher-order perturbative corrections are incorporated, and the theoretical uncertainty should eventually be reduced to an accuracy of ~ 0.04 GeV^2 due to the effect of the unsuppressed $u = 1$ renormalon. Therefore, the HQET parameters can be determined with even higher accuracy with sufficiently small uncertainties in the near future.

Finally, let us compare our results for $\bar{\Lambda}$ and μ_π^2 with other determinations in the PV schemes. Ref. [23] obtained

$$\left[\bar{\Lambda}\right]_{\rm PV} = 0.435(31)\ \text{GeV}\,, \quad \left[\mu_\pi^2\right]_{\rm PV} = 0.05(22)\ \text{GeV}^2\,. \tag{4.89}$$

In this fit, only the $\mathcal{O}(\Lambda_{\rm QCD})$ renormalon is subtracted, while the $\mathcal{O}(1/m_h)$ corrections are included. They estimate that the uncertainty of μ_π^2 originates from the $\mathcal{O}(\Lambda^2_{\rm QCD})$ renormalon. However, our analysis indicates that it is rather due to the lack of known perturbative coefficients, since the size of the $\mathcal{O}(\Lambda^2_{\rm QCD})$ renormalon is small. (This is estimated by the comparison between the predictions with and without the $\mathcal{O}(\Lambda^2_{\rm QCD})$ renormalon subtraction.) Ref. [45] obtained

$$\left[\bar{\Lambda}\right]_{\rm PV} = 477(\mu)^{-8}_{+17}(Z_m)^{+11}_{-12}(\alpha_s)^{-8}_{+9}(\mathcal{O}(1/m_h))^{+46}_{-46}\ \text{MeV}\,, \tag{4.90}$$

in which only the $\mathcal{O}(\Lambda_{\rm QCD})$ renormalon is subtracted and the $\mathcal{O}(1/m_h)$ corrections are ignored (including the μ_π^2 term). Both of these determinations use the PV scheme and are consistent with our determination within the assigned uncertainties.

4.3 Application II: Inclusive semileptonic B decay

In this section, we determine $|V_{cb}|$ by subtracting renormalons using the DSRS method. We first explain how renormalons cancel using the DSRS method in Sec. 4.3.1. To separate the renormalon part of the decay width, we develop a practical version of the extended dual-transform formula. In Sec. 4.3.2, $|V_{cb}|$ is determined by renormalon subtraction. Using the extended dual-transform formula, we suppress the $u = 1$ renormalon of the LO Wilson coefficient in the $\overline{\rm MS}$ mass scheme, which is studied for the first time.

4.3.1 Renormalon cancellation using the DSRS method

In this section, we discuss how the renormalons $u = 1/2$ and $u = 1$ are subtracted using the DSRS method. Again, the total decay width of $B \to X_c \ell \bar{\nu}$ is given by

$$\Gamma = \frac{G_F^2 |V_{cb}|^2}{192\pi^3} A_{ew} m_b^5 \left[C^\Gamma_{\bar{Q}Q}(m_b, \rho)\Big(1 - \frac{\mu_\pi^2}{2m_b^2}\Big) + C^\Gamma_{cm}(m_b, \rho)\frac{\mu_G^2(m_b)}{m_b^2} + \mathcal{O}\Big(\frac{\Lambda^3_{\overline{\rm MS}}}{m_b^3}\Big)\right], \quad (4.91)$$

with $\rho = m_c/m_b$. Wilson coefficients $C^\Gamma_{\bar{Q}Q}$ and C^Γ_{cm} are given in App. A. First, we rewrite Γ in terms of the $\overline{\rm MS}$ masses $\overline{m}_b$ and $\overline{m}_c$ to cancel the $u = 1/2$ renormalon. In rewriting, to achieve the cancellation of renormalons, we change the number of flavor of the running coupling constant to $n_f = 3$ using the flavor threshold relation given by Eq. (A.23). Then the OPE after the cancellation of the $u = 1/2$ renormalons can be expressed by

$$\Gamma = \frac{G_F^2 |V_{cb}|^2}{192\pi^3} A_{ew} \overline{m}_b^5 \left[\bar{C}^\Gamma_{\bar{Q}Q}\Big(1 - \frac{\mu_\pi^2}{2m_b^2}\Big) + \bar{C}^\Gamma_{cm}\frac{\mu_G^2}{m_b^2} + \mathcal{O}\Big(\frac{\Lambda^3_{\overline{\rm MS}}}{m_b^3}\Big)\right], \quad (4.92)$$

in which we keep the mass scheme of the non-perturbative corrections to be the pole mass scheme. $\bar{C}^\Gamma_{\bar{Q}Q} = \bar{C}^\Gamma_{\bar{Q}Q}(\overline{m}_b, \bar{\rho})$ with $\bar{\rho} = \overline{m}_c/\overline{m}_b$ is defined by

$$\begin{aligned} \bar{C}^\Gamma_{\bar{Q}Q} &= (m_b(\overline{m}_b)/\overline{m}_b)^5 C^\Gamma_{\bar{Q}Q}(m_b = m_b(\overline{m}_b), \rho = \rho(\bar{\rho})) \\ &= X_0(\bar{\rho})\Big(1 + \sum_{n=0}^{\infty} \alpha_s(\overline{m}_b^2)^{n+1} \bar{x}_n\Big), \end{aligned} \quad (4.93)$$

where X_0 is given in App. A. $\bar{x}_n$ is obtained by expanding m_h and ρ in terms of $\alpha_s(\overline{m}_b^2)$ using the pole-$\overline{\rm MS}$ mass relation as

$$m_h(\overline{m}_h) = \overline{m}_h\big(1 + \delta(\overline{m}_h)\big), \quad (4.94)$$

and

$$\rho(\bar{\rho}) = \frac{\overline{m}_c\big(1 + \delta(\overline{m}_c)\big)}{\overline{m}_b\big(1 + \delta(\overline{m}_b)\big)} = \bar{\rho}\Big(1 + \sum_{n=0}^{\infty} \alpha_s(\overline{m}_b)^{n+1} R_n(\overline{m}_b, \bar{\rho})\Big), \quad (4.95)$$

where R_n is constructed from the coefficients of the pole-$\overline{\rm MS}$ mass relation and the QCD beta function[4] .

[4]We note that $\rho(\bar{\rho})$ in terms of $\alpha_s(\overline{m}_b)$ has the $u = 1/2$ renormalon of the form

$$\bar{\rho}\Big(\frac{\Lambda_{\overline{\rm MS}}}{\overline{m}_c} - \frac{\Lambda_{\overline{\rm MS}}}{\overline{m}_b}\Big), \quad (4.96)$$

which is non-trivially canceled against ρ-dependence of the coefficients of $C^\Gamma_{\bar{Q}Q}$ in Eq. (4.93) (see App. F).

The LO renormalon of $\bar{C}^{\Gamma}_{\bar{Q}Q}$ is at $u = 1$, but the m_b dependence of the uncertainty from the $u = 1$ renormalon deviates from the simple power form as follows. In the OPE given by Eq. (4.92), the cancellation of the $u = 1$ renormalon requires that the imaginary part of $\left[\bar{C}^{\Gamma}_{\bar{Q}Q}\right]_{\pm}$ defined by

$$\left[\bar{C}^{\Gamma}_{\bar{Q}Q}\right]_{\pm} = \left[\bar{C}^{\Gamma}_{\bar{Q}Q}\right]_{\rm PV} \pm i\,\delta\bar{C}^{\Gamma}_{\bar{Q}Q}, \tag{4.97}$$

to satisfy the condition

$$0 = {\rm Im}\left[\bar{C}^{\Gamma}_{\bar{Q}Q}\Big(1 - \frac{\mu_\pi^2}{2m_b^2}\Big)\right]_{\mathcal{O}(1/m_b^2)} = \delta\bar{C}^{\Gamma}_{\bar{Q}Q}|_{u=1} - \left[\bar{C}^{\Gamma}_{\bar{Q}Q}\right]_{\rm PV}\frac{{\rm Im}\,\mu_\pi^2}{2\left[m_b\right]^2_{\rm PV}}, \tag{4.98}$$

that is

$$\frac{\delta\bar{C}^{\Gamma}_{\bar{Q}Q}|_{u=1}}{\left[\bar{C}^{\Gamma}_{\bar{Q}Q}\right]_{\rm PV}} = N_1\frac{\Lambda^2_{\overline{\rm MS}}}{2\left[m_b\right]^2_{\rm PV}}, \tag{4.99}$$

where we assume the renormalon cancelation in the OPE of M_H given by Eq. (4.23), i.e., the universality of the HQET parameters in the infinite mass limit. The simple DSRS method defined in Chap. 3 can only subtract the renormalons of the simple power form of hard scale. We have to suppress renormalons including the corrections from $\left[\bar{C}^{\Gamma}_{\bar{Q}Q}\right]_{\rm PV}$ factor in the dual space. In this analysis, we use the extended formula of the dual transform in a more practical way than that in App. C[5].

Let us define a new function

$$\Xi(\overline{m}_b) = \log\left[\bar{C}^{\Gamma}_{\bar{Q}Q}/X_0(\bar{\rho})\right] = \log\left[1 + \sum_{n=0}^{\infty}\alpha_s(\overline{m}_b^2)^{n+1}\bar{x}_n\right] \tag{4.100}$$

$$= \sum_{n=0}^{\infty}\alpha_s(\overline{m}_b^2)^{n+1}\xi_n, \tag{4.101}$$

where we use $\log(1+x) = \sum_{n=1}^{\infty}(-1)^{n+1}x^n/n$ to construct ξ_n. When we replace $\bar{C}^{\Gamma}_{\bar{Q}Q}$ in Eq. (4.100) to Eq. (4.97), the imaginary part of Ξ can be written as

$$\begin{aligned}\delta\Xi = {\rm Im}\log\left[\left[\bar{C}^{\Gamma}_{\bar{Q}Q}\right]_{\rm PV} \pm i\delta\bar{C}^{\Gamma}_{\bar{Q}Q}\right] &= \pm\frac{\delta\bar{C}^{\Gamma}_{\bar{Q}Q}}{\left[\bar{C}^{\Gamma}_{\bar{Q}Q}\right]_{\rm PV}} + \mathcal{O}\left(\frac{\Lambda^3_{\overline{\rm MS}}}{\left[m_b\right]^3_{\rm PV}}\right)\\ &= \pm N_1\frac{\Lambda^2_{\overline{\rm MS}}}{2\left[m_b\right]^2_{\rm PV}} + \mathcal{O}\left(\frac{\Lambda^3_{\overline{\rm MS}}}{\left[m_b\right]^3_{\rm PV}}\right),\end{aligned} \tag{4.102}$$

where we assume that $\left|\left[\bar{C}^{\Gamma}_{\bar{Q}Q}\right]_{\rm PV}\right| \gg \left|\delta\bar{C}^{\Gamma}_{\bar{Q}Q}\right|$ and the LO renormalon of the Wilson coefficient is given by Eq. (4.99). Hence, Ξ has the $u = 1$ renormalon in the form of simple power, which can be eliminated by the DSRS method defined in Chap. 3. In this thesis,

[5]It is difficult to naively apply the extended formula in App. C to this case. It is because the $\log(Q)$ correction in Eq. (C.3) is assumed to be obtained from α_s expansion, while $\left[\bar{C}^{\Gamma}_{\bar{Q}Q}\right]_{\rm PV}$ is resummed after renormalon subtraction. If we expand $\left[\bar{C}^{\Gamma}_{\bar{Q}Q}\right]_{\rm PV}$ in α_s, logarithmic corrections would exhibit a renormalon divergence, which is out of scope of this extended formula.

we separate the $u=1$ renormalon from Ξ, and calculate $\left[\bar{C}^{\Gamma}_{\bar{Q}Q}\right]_{\rm PV}$ from the exponentiation of Ξ as follows.

The dual transform of Ξ is defined by

$$\begin{aligned}\tilde{\Xi}(\tau) &= \int_{x_0^2-i\infty}^{x_0^2+i\infty}\frac{dx^2}{2\pi i}\,e^{\tau^2x^2}x^{2\times1\times(-1)}\Xi(\overline{m}_b=1/x)\\ &= e^{\hat{H}\log(\mu^2/\tau^2)}\sum_{n=0}^{\infty}\alpha_s(\mu^2)^{n+1}\tilde{\xi}_n,\end{aligned}\tag{4.103}$$

in which we set parameters $(a,u')=(1,-1)$ to suppress the $u=1$ renormalon in the dual space. $\tilde{\xi}_n$'s can be read from

$$\sum_{n=0}^{\infty}\alpha_s(\mu^2)^{n+1}\tilde{\xi}_n=\frac{1}{\Gamma(1-\hat{H})}\sum_{n=0}^{\infty}\alpha_s(\mu^2)^{n+1}\xi_n.\tag{4.104}$$

It is noteworthy that we can only suppress renormalons of the form

$$(\text{const.})\times\left(\frac{\Lambda_{\overline{\rm MS}}}{\overline{m}_b}\right)^{2u},\tag{4.105}$$

for $u=1,\,2,\,3,\cdots$ in this method. It indicates that $\mathcal{O}(\alpha_s(\overline{m}_b^2)\Lambda^2_{\overline{\rm MS}}/\overline{m}_b^2)$ uncertainty remains in the calculation of Ξ. From the consideration in Sec. 4.2.1, its contribution to Ξ is about 0.02%, which will be used to estimate a systematic uncertainty for the determination of $|V_{cb}|$ in the next section.

The inverse dual transform gives $\left[\Xi\right]_{\pm}$ by

$$\begin{aligned}\left[\Xi(\overline{m}_b)\right]_{\pm} &= \left[\Xi(\overline{m}_b)\right]_{\rm PV}\pm i\,\delta\Xi(\overline{m}_b)\\ &= x^2\int_{C_{\mp}}d\tau^2\,e^{-\tau^2x^2}\tilde{\Xi}(\tau)\\ &= \frac{1}{\overline{m}_b^2}\int_{C_{\mp}}d\tau^2\,e^{-\tau^2/\overline{m}_b^2}e^{\hat{H}\log(\mu^2/\tau^2)}\sum_{n=0}^{\infty}\alpha_s(\mu^2)^{n+1}\tilde{\xi}_n,\end{aligned}\tag{4.106}$$

which can be calculated numerically. In this analysis, we identify the renormalon-subtracted part of $\bar{C}^{\Gamma}_{\bar{Q}Q}$ as

$$\begin{aligned}\left[\bar{C}^{\Gamma}_{\bar{Q}Q}\right]_{\rm PV} &= X_0(\bar{\rho})\,\mathrm{Re}\,\exp\Big(\left[\Xi(\overline{m}_b)\right]_{\pm}\Big)\\ &= X_0(\bar{\rho})\,\exp\Big(\left[\Xi(\overline{m}_b)\right]_{\rm PV}\Big)\left[1+\mathcal{O}\left(\frac{\Lambda^3_{\overline{\rm MS}}}{\left[m_b\right]^3_{\rm PV}}\right)\right],\end{aligned}\tag{4.107}$$

and the renormalon part as

$$\begin{aligned}\delta\bar{C}^{\Gamma}_{\bar{Q}Q} &= X_0(\bar{\rho})\,\mathrm{Im}\,\exp\Big(\left[\Xi(\overline{m}_b)\right]_{\pm}\Big)\\ &= X_0(\bar{\rho})\,\exp\Big(\left[\Xi(\overline{m}_b)\right]_{\rm PV}\Big)\left[N_1\frac{\Lambda^2_{\overline{\rm MS}}}{2\left[m_b\right]^2_{\rm PV}}+\mathcal{O}\left(\frac{\Lambda^3_{\overline{\rm MS}}}{\left[m_b\right]^3_{\rm PV}}\right)\right].\end{aligned}\tag{4.108}$$

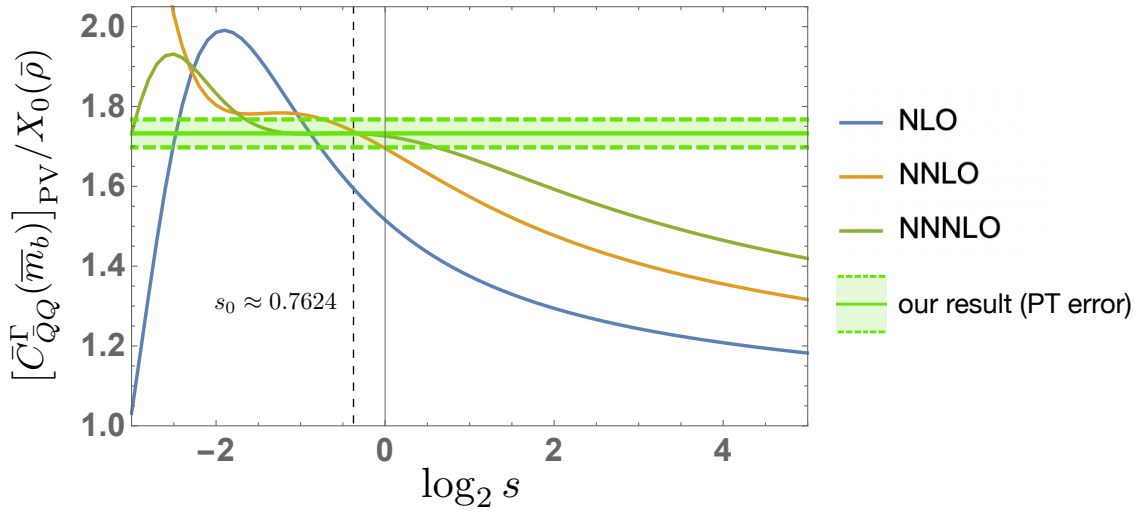

Figure 4.6: Calculation of $\left[\bar{C}^{\Gamma}_{\bar{Q}Q}\right]_{\rm PV}$ using the DSRS method. We use theoretical inputs $\overline{m}_b = 4.18$ GeV, $\overline{m}_c = 1.27$ GeV and $\alpha_s(M_Z) = 0.1179$ from the PDG. The vertical line is normalized by $X_0(\bar{\rho})$. The colored lines represent the scale dependence of $\mathrm{N^kLO}$ results for $k = 1, 2, 3$. The green line and shaded area exhibit the determined value using the $\mathrm{N^3LO}$ result and perturbative uncertainty estimated by the scale dependence by varying μ within $[s_0\tau/2, 2s_0\tau]$ with $s_0 \approx 0.7624$.

Here, we use the formulas $e^{ix} = \cos(x) + i\sin(x)$, $\cos(x) = 1 + \mathcal{O}(x^2)$ and $\sin(x) = x + \mathcal{O}(x^3)$, and assume the renormalon behavior Eq. (4.102). Combining these equations, we find

$$\delta\bar{C}^{\Gamma}_{\bar{Q}Q} = \left[\bar{C}^{\Gamma}_{\bar{Q}Q}\right]_{\rm PV}\left[N_1\frac{\Lambda^2_{\overline{\rm MS}}}{2\left[m_b\right]^2_{\rm PV}} + \mathcal{O}\left(\frac{\Lambda^3_{\overline{\rm MS}}}{\left[m_b\right]^3_{\rm PV}}\right)\right], \tag{4.109}$$

of which m_b dependence is consistent with Eq. (4.99) up to $\mathcal{O}(1/m_b^2)$. Therefore, from the Wilson coefficient defined by Eq. (4.107), the renormalon is correctly subtracted.

Here, we compare the coefficients of the series $\bar{x}_n$, ξ_n and $\tilde{\xi}_n$ using the latest perturbative expansion of $C^{\Gamma}_{\bar{Q}Q}$ up to $\mathcal{O}(\alpha_s^3)$. We obtain

$$\bar{x}_0 \approx 1.593,\ \bar{x}_1 \approx 3.579,\ \bar{x}_2 \approx 8.894, \tag{4.110}$$

$$\xi_0 \approx 1.593,\ \xi_1 \approx 2.311,\ \xi_2 \approx 4.540, \tag{4.111}$$

and

$$\tilde{\xi}_0 \approx 1.593,\ \tilde{\xi}_1 \approx 1.653,\ \tilde{\xi}_2 \approx 1.185, \tag{4.112}$$

when we use the PDG masses $\overline{m}_b = 4.18$ GeV and $\overline{m}_c = 1.27$ GeV as inputs. Due to the fifth power of m_b contained in Γ, $\bar{x}_n$ shows a slow convergence even after renormalon cancellation. On the other hand, ξ_n behaves better than $\bar{x}_n$ because a logarithmic transform partially cancels the large coefficient of $\bar{x}_n$. Thus, $\tilde{\xi}_n$, the coefficients in the dual space from the well-behaved series, also shows a much better convergence.

We compute $\left[\bar{C}^{\Gamma}_{\bar{Q}Q}\right]_{\rm PV}$ and investigate the scale dependence at NNNLO ($\mathcal{O}(\alpha_s^3)$)) level. Fig. 4.6 shows the scale dependence of Eq. (4.107) when we set $\mu = s\tau$ and truncate $\tilde{\Xi}$

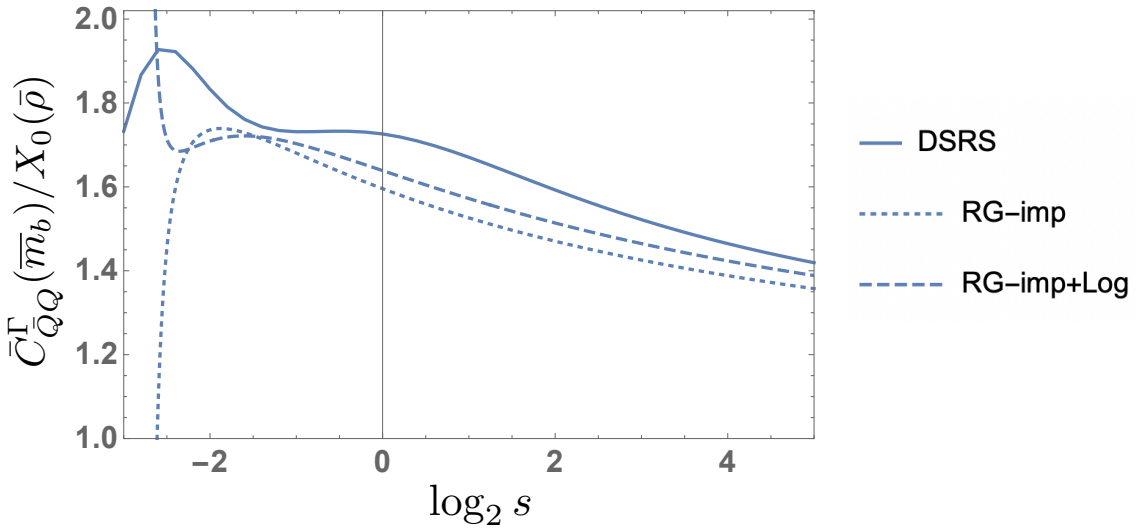

Figure 4.7: Calculation of $\left[\bar{C}^{\Gamma}_{\bar{Q}Q}\right]$ using three different methods. The vertical axis is normalized by $X_0(\bar{\rho})$. The solid, dotted and dashed lines represent the result by the DSRS method, by the RG-improvement and by combining the RG-improvement and Ξ, respectively.

at α_s^{k+1} after expanding $e^{\hat{H}\log(\mu^2/\tau^2)}$ in Eq. (4.103). The colored lines represent the results for $k = 0$, 1, 2 when the inputs $\overline{m}_b$, $\overline{m}_c$ and α_s are set to the PDG central values. Around $s = \mathcal{O}(1)$, we can see the flat region in the NNNLO result. In this analysis, we find the minimal sensitivity scale $s = s_0$ such that the difference between $\left[\bar{C}^{\Gamma}_{\bar{Q}Q}\right]_{\rm PV}$ at $s = 2s_0$ and $s = s_0/2$ is minimized, and give the prediction. At the NNNLO level, we obtain $s_0 \approx 0.7624$. The central result and the perturbative uncertainty of prediction is given by the value at $s = s_0$ and the difference between the values at $s = s_0$ and $s = s_0/2$, respectively. The resulting prediction is given by

$$\left[\bar{C}^{\Gamma}_{\bar{Q}Q}(\overline{m}_b)\right]_{\rm PV}\Big|_{\rm NNNLO} = X_0(\bar{\rho}) \times \left(1.733\,(35)_{\rm PT}\right), \tag{4.113}$$

where the perturbative uncertainty is displayed by the green line and shaded area in Fig. 4.6.

Let us compare the result with the cases based on the conventional perturbative expansion given by Eqs. (4.93) and (4.101). Fig. 4.7 shows the scale dependence of the $\mathcal{O}(\alpha_s^3)$ calculation results for the three different methods. The solid line represents the results by the DSRS method, which is given by

$$\left[\bar{C}^{\Gamma}_{\bar{Q}Q}(\overline{m}_b)\right]_{\rm PV} = X_0(\bar{\rho})\,{\rm Re}\,\exp\left(\int_{C_\mp}\frac{d\tau^2}{\overline{m}_b^2}\,e^{-\tau^2/\overline{m}_b^2}e^{\hat{H}\log(\mu^2/\tau^2)}\sum_{n=0}^{2}\alpha_s(\mu^2)^{n+1}\tilde{\xi}_n\right), \tag{4.114}$$

with $\mu = s\tau$ and we truncate the series at α_s^3 before integration. The dotted line represents the results by the RG-improvement, given by

$$\bar{C}^{\Gamma}_{\bar{Q}Q}(\overline{m}_b)\Big|_{\rm RG-imp} = X_0(\bar{\rho})\left[1 + e^{\hat{H}\log(\mu^2/\overline{m}_b^2)}\sum_{n=0}^{\infty}\alpha_s(\mu^2)^{n+1}\bar{x}_n\right], \tag{4.115}$$

with $\mu = s\overline{m}_b$ and we truncate at α_s^3. The dashed line represents the exponentiation of the result by the RG-improvement of Ξ, given by

$$\begin{aligned}\bar{C}^{\Gamma}_{\bar{Q}Q}(\overline{m}_b)\Big|_{\mathrm{RG-imp+Log}} &= X_0(\bar{\rho})\,\exp\left[\Xi(\overline{m}_b)\right] \\ &= X_0(\bar{\rho})\,\exp\left[e^{\hat{H}\log(\mu^2/\overline{m}_b^2)}\sum_{n=0}^{\infty}\alpha_s(\mu^2)^{n+1}\xi_n\right], \end{aligned} \tag{4.116}$$

with $\mu = s\overline{m}_b$ and we truncate the series at α_s^3 before exponentiation. We can find stationary points in the dotted and dashed lines where s is small, but we can see that the value of $\bar{C}^{\Gamma}_{\bar{Q}Q}$ changes abruptly when the scale is varied around the stationary point. This is because of the unphysical singularity of α_s near $\mu \sim \Lambda_{\overline{\mathrm{MS}}}$. On the other hand, the solid line shows milder scale dependence around the stationary point rather than the others, owing to the removal of the unphysical singularity by the DSRS method. Furthermore, it is observed that the values at the stationary point for all the methods are similar. We expect the good convergence of Eq. (4.114) to continue at higher orders thanks to the subtraction of renormalons.

4.3.2 $|V_{cb}|$ determination

In this section, we determine $|V_{cb}|$ using the result in the previous section. We use the renormalon-subtracted OPE of Γ given by

$$\Gamma = \frac{G_F^2|V_{cb}|^2}{192\pi^3}A_{ew}\bar{m}_b^5\left[\left[\bar{C}^{\Gamma}_{\bar{Q}Q}\right]_{\mathrm{PV}}\left(1-\frac{\left[\mu_\pi^2\right]_{\mathrm{PV}}}{2\left[m_b\right]^2_{\mathrm{PV}}}\right)+\bar{C}^{\Gamma}_{cm}\frac{\mu_G^2}{\left[m_b\right]^2_{\mathrm{PV}}}\right], \tag{4.117}$$

where we neglect the $\mathcal{O}(\Lambda^3_{\overline{\mathrm{MS}}}/m_b^3)$ OPE corrections and the unsuppressed $u=1$ renormalon effect of $\mathcal{O}(\alpha_s(\overline{m}_b)\Lambda^2_{\overline{\mathrm{MS}}}/m_b^2)$. We use $\left[m_b\right]_{\mathrm{PV}}$, $\left[\bar{C}^{\Gamma}_{\bar{Q}Q}\right]_{\mathrm{PV}}$, $\bar{C}^{\Gamma}_{cm}$, $\left[\mu_\pi^2\right]_{\mathrm{PV}}$ and μ_G^2 given by Eqs. (4.72), (4.113), (A.21), (4.88), and (4.18), respectively. The NLO correction to $\bar{C}^{\Gamma}_{cm}$ of $\mathcal{O}(\alpha_s)$ given by Eq. (A.22) is used to estimate the systematic uncertainty. The experimental value of Γ is obtained as follows. In this analysis, we neglect the iso-spin breaking and assume that the semileptonic decay width of B_0 and that of $B^\pm$ is the same. Then we can obtain the semileptonic decay width Γ by

$$\Gamma = \mathcal{B}/\tau_B, \tag{4.118}$$

where $\mathcal{B} = \mathcal{B}(B \to X_c\ell\bar{\nu})$ represents the semileptonic branching ratio obtained for the admixture of $B^0/B^\pm$. τ_B is the lifetime of B meson given by

$$\tau_B = \frac{\tau_{B^\pm}+\tau_{B^0}}{2}+\frac{1}{2}(f^{+-}-f^{00})(\tau_{B^\pm}-\tau_{B^0}), \tag{4.119}$$

as clearly explained in Sec. III A of ref. [88]. Here f^{+-} and f^{00} are the fractions of the B^+B^- production and the $B^0\bar{B}^0$ production from the $\Upsilon(4S)$ decay, respectively. We give the value τ_B by

$$\begin{aligned}\tau_B &= \frac{(1.519\pm0.004)+(1.638\pm0.004)}{2}\times10^{-12}\,\mathrm{sec} \\ &= (1.579\pm0.004)\times10^{-12}\,\mathrm{sec}, \end{aligned} \tag{4.120}$$

neglecting the second term in Eq. (4.119) since it is smaller than the uncertainty of $\tau_{B^\pm}$ or τ_{B^0}. See ref. [89] for the ratio f^{+-}/f^{00}. We should note the value of the branching ratio $\mathcal{B}$. In our default analysis, we use the value $\mathcal{B}$ given by

$$\mathcal{B} = (10.63 \pm 0.19)\%, \tag{4.121}$$

which is the average of the Belle measurement [90] and BaBar measurement [91]. Each value is obtained with a lepton energy cut, and by extrapolating to the full phase space limit. This value is similar to the PDG value given by $\mathcal{B} = (10.65 \pm 0.16)\%$ [54] which is used for the determination in Ref. [60]. It is also close to the value used in Ref. [58].

In fact, however, as already pointed out in Ref. [59], the central value of $\mathcal{B}$ moves significantly when we use a relatively recent BaBar result $\mathcal{B} = (10.15 \pm 0.26)\%$ [92], which is estimated by subtracting background effects from the full semileptonic decay as $\mathcal{B} = \mathcal{B}(B \to X\ell\bar{\nu}) - \mathcal{B}(B \to X_u\ell\bar{\nu})$. Ref. [59] used the average value of Refs. [90, 91, 93] and the BaBar result [92], which is given by

$$\mathcal{B} = (10.48 \pm 0.13)\%. \tag{4.122}$$

Since $|V_{cb}| \propto \mathcal{B}^{1/2}$, the determined value of $|V_{cb}|$ becomes small by using Eq. (4.122) instead of Eq. (4.121). We use Eq. (4.122) to discuss sensitivity of the determination of $|V_{cb}|$ to the experimental inputs.

First we show the result of $|V_{cb}|$ using the PDG values of $\overline{m}_b$, $\overline{m}_c$ and α_s as inputs to compute the OPE of Γ. We use the branching ratio $\mathcal{B}$ given by Eq. (4.121) as the input value. The result is given by

$$\begin{aligned} |V_{cb}| &= 0.04147\,(43)_{\rm PT}\,(^{+61}_{-89})_{\overline{m}_b}\,(43)_{\overline{m}_c}\,(23)_{\alpha_s}\,(38)_{\mathcal{B}}\,(5)_{\tau_B}\,(10)_{\mu_\pi^2}\,(5)_{\mu_G^2}\,(1)_{1/m_b^3}\,(1)_{\rm sub\,u=1} \\ &= 0.04147\,(^{+98}_{-117}) \quad (\text{from PDG inputs}), \end{aligned} \tag{4.123}$$

where the brackets in the first line denote the systematic uncertainties. The first uncertainty comes from the perturbative uncertainty estimated by Eq. (4.113). The second, third and fourth uncertainties are caused by the uncertainties of the PDG inputs. The fifth and sixth uncertainties come from the uncertainties of the experimental data in Eqs. (4.121) and (4.120), respectively. The last four uncertainties come from the non-perturbative corrections, μ_π^2 given by Eq. (4.88), μ_G^2 given by Eq. (4.18), the neglected $\mathcal{O}(1/m_b^3)$ OPE correction and the unsuppressed $u = 1$ renormalon effect, respectively. The uncertainty from μ_G^2 is estimated by combining the uncertainty from the μ_G^2 uncertainty in Eq. (4.18) and the difference between the determinations using $C_{cm}^{\bar{\Gamma}}|_{\rm LO}$ or $C_{cm}^{\bar{\Gamma}}|_{\rm NLO}$. In the second line we combine the uncertainties. While the perturbative uncertainty is at the percent level precision, the uncertainty from $\overline{m}_b$ is dominant among the systematic uncertainties, which reflects the fact that Γ is proportional to the square of $|V_{cb}|$ and the fifth power of $\overline{m}_b$. That is, the relative uncertainties of $|V_{cb}|$ and $\overline{m}_b$ are related by

$$\frac{\delta|V_{cb}|}{|V_{cb}|} \approx -\frac{5}{2} \times \frac{\delta\overline{m}_b}{\overline{m}_b}. \tag{4.124}$$

Therefore, it is important to make $\overline{m}_b$ accurate in order to improve the accuracy of $|V_{cb}|$ determination. We also give the results using the other inputs from the FLAG. The results

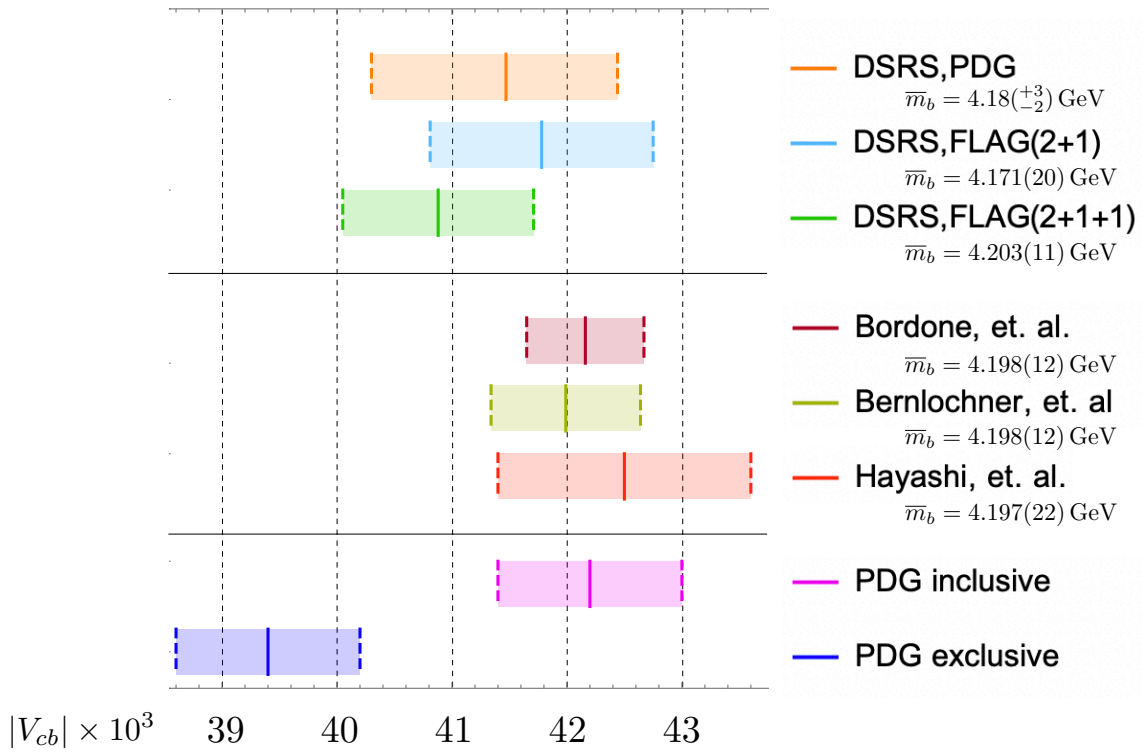

Figure 4.8: Comparison of $|V_{cb}|$ determinations by the DSRS method and previous studies.

are given by

$$\begin{aligned} |V_{cb}| &= 0.04178\,(45)_{\rm PT}\,(69)_{\overline{m}_b}\,(18)_{\overline{m}_c}\,(29)_{\alpha_s}\,(38)_{\mathcal{B}}\,(5)_{\tau_B}\,(10)_{\mu_\pi^2}\,(5)_{\mu_G^2}\,(1)_{1/m_b^3}\,(1)_{\rm sub\,u=1} \\ &= 0.04178\,(97) \quad (\text{from FLAG inputs } N_f = (2+1)), \end{aligned} \tag{4.125}$$

and

$$\begin{aligned} |V_{cb}| &= 0.04088\,(44)_{\rm PT}\,(39)_{\overline{m}_b}\,(33)_{\overline{m}_c}\,(29)_{\alpha_s}\,(37)_{\mathcal{B}}\,(5)_{\tau_B}\,(8)_{\mu_\pi^2}\,(5)_{\mu_G^2}\,(1)_{1/m_b^3}\,(1)_{\rm sub\,u=1} \\ &= 0.04088\,(83) \quad (\text{from FLAG inputs } N_f = (2+1+1)), \end{aligned} \tag{4.126}$$

where the convention of the uncertainties are the same as Eq. (4.123). All the results are consistent with each other within the assigned uncertainties. We can see that the central value of $|V_{cb}|$ is quite sensitive to the shift of the central value of the bottom quark $\overline{\rm MS}$ mass. Nevertheless, all the values are consistent with the inclusive PDG value given by Eq. (1.2), and one of the results, Eq. (4.126), is consistent with the exclusive PDG value given by Eq. (1.1) within the uncertainties. It suggests that how much the value of the bottom quark mass can move should be examined carefully in the other determinations.

Fig. 4.8 shows the comparison of the results of the DSRS method with previous studies. Each line and band width represents the central value and total uncertainty, respectively. First three results are our default determinations using the $\overline{\rm MS}$ mass of the bottom quark, given by Eqs. (4.123), (4.125) and (4.126). The fourth [58] and fifth [59] results are the NNNLO results using the kinetic mass of the bottom quark, given by

Eqs. (4.36) and (4.37), respectively. The sixth one [60] is the NNNLO result using the bottom quark 1S mass, given by Eqs. (4.40). The last two values are the PDG inclusive and exclusive values given by Eqs. (1.2) and (1.1), respectively. The corresponding $\overline{m}_b$ to each scheme is also shown in Fig. 4.8. We note that these determinations use the similar values for $\mathcal{B}$.

Scheme dependence and input parameter dependence

Now we discuss the scheme dependence among the results in Fig. 4.8. Our results of $|V_{cb}|$ using the $\overline{\rm MS}$ mass scheme seems to be smaller than those of the other schemes, but we can confirm the consistency among them as follows.

First we compare our results with the kinetic scheme results. In the determinations using the kinetic mass of the bottom quark m_b^{kin}, Refs. [58, 59] calculated theoretically a variety of the lepton energy moments with OPE corrections up to $\mathcal{O}(1/m_b^4)$. Then $|V_{cb}|$ and the HQET parameters are determined in the global fit by comparison with experimental values. There are several differences from our theoretical formulation. First they used the perturbative expansion in $\alpha_s^{(n_f=4)}$ to calculate the Wilson coefficients, whereas ours is based on the expansion in $\alpha_s^{(n_f=3)}$. Then, the non-perturbative matrix elements such as μ_π^2 are also defined based on the theories with different n_f. In $n_f = 4$ theory, the non-perturbative effects are determined from the low-energy physics by gluons and 4-flavor quarks including the charm quark, but in reality the effect of the charm quark should be decoupled, reflecting the fact that $m_c \gg \Lambda_{\rm QCD}$. Our value of μ_π^2 with $n_f = 3$ is given by Eq. (4.88), which is consistent with zero. It is obtained by comparing with the masses of the B and D mesons. The preference for the $n_f = 3$ theory and its consistency with the result of Ref. [23], which is determined with the same number of flavors and observable settings, support the validity of our μ_π^2 determination results. On the other hand, their values with $n_f = 4$ are given by $\mu_\pi^2 = 0.477 \pm 0.056$ GeV^2 [58] and $\mu_\pi^2 = 0.43 \pm 0.24$ GeV^2[59] [6]. These are the results by fitting the experimental data of the B meson decay in the OPE formula. If we set μ_π^2 to be consistent with zero in the determinations of Refs. [58, 59] , the central value of $|V_{cb}|$ decreases by about 0.5%. Next, the kinetic mass of the bottom quark they used is calculated from the input $\overline{m}_b = 4.198 \pm 0.012$ GeV taken from Ref. [94], which is similar to the $\overline{m}_b$ value used in Eq. (4.126). This value has a small uncertainty, but this may be an underestimate considering that $|V_{cb}|$ is proportional to $(m_b)^{-5/2}$. If they use the PDG values for their determinations, as we do, the consistency can be even better. Therefore, it is expected that the determination values in the $\overline{\rm MS}$ scheme and kinetic scheme will be closer to each other if the value of μ_π^2 decreases and the PDG value of $\overline{m}_b$ is used.

Next, we compare our results with the 1S scheme results. In Ref. [60], the OPE is constructed in the $n_f = 3$ theory and one half of the experimental value of the bottomonium mass is used as the input bottom quark mass to determine $|V_{cb}|$. The $\overline{\rm MS}$ mass of the bottom quark from the 1S ground state of the bottomonium is $\overline{m}_b = 4.197 \pm 0.022$ GeV [21], which is determined by the following equation

$$E_{tot} = 2m_b(\overline{m}_b) + E_{bin}. \tag{4.127}$$

[6] The definition of μ_π^2 in Refs. [58, 59] is based on HQE (heavy quark expansion), which is different from the HQET definition (in the infinite mass limit) by $\mathcal{O}(\Lambda_{\rm QCD}^3/m_b)$.

This equation associates the total energy of the static bottomonium E_{tot} with the perturbative calculation. In Ref. [21], E_{tot} on the left hand side was regarded as the mass of the 1S ground state of the bottomonium $M_{\bar{b}b(1S)}$ ($\bar{b}b(1S) = \Upsilon(1S)\,\text{or}\,\eta_b(1S)$). On the right hand side, $E_{bin} < 0$ is the binding energy calculated perturbatively from the static QCD potential $V(r)$. E_{tot} has a well-behaved perturbative expansion with the $u = 1/2$ renormalon removed by rewriting the pole mass of the bottom quark m_b by the $\overline{\text{MS}}$ mass $\overline{m}_b$. To cancel out the $u = 1/2$ renormalon they use the ε-expansion, which is explained in App. G. We note that they include the non-Coulomb potentials in the calculation of the binding energy, but do not consider the non-perturbative effects to the 1S mass because the latter is smaller or comparable to the current perturbative uncertainty[7]. One important notice is that the spin-dependent part of the QCD potential $V(r)$ has the effect proportional to $\vec{S}^2\delta(\vec{r})$, which contributes to the binding energy E_{bin} as the form proportional to the square of the absolute value of the quarkonium wave-function $|\Psi(0)|^2$ [95]. Here, $\vec{S}$ is the total spin of the bottomonium. If the higher-order perturbative calculation causes the slope of the potential to be steeper in the long-range region [8], the shape of the wave-function changes to become larger as it gets closer to the origin, and the value of $|\Psi(0)|^2$ becomes larger. This increases the value of the hyperfine-splitting $\Delta M_{\bar{b}b(1S)} = |M_{\Upsilon(1S)} - M_{\eta_b(1S)}|$ of the bottomonium mass. It is known that the perturbative calculation of $\Delta M_{\bar{b}b(1S)}$ is considerably smaller than the corresponding experimental value, and it is expected that the higher-order perturbative calculation will increase the consistency between both values [96, 97]. Then the current values of $|V_{cb}|$ determined from the different bottomonium 1S states (Eqs. (4.38) and (4.39)) will be closer to each other as the higher-order perturbative corrections are incorporated. At the same time, the higher-order corrections to $2m_b + V(r)$ (without changing the value where r is small) increases the total energy of the (spin-averaged) bottomonium 1S state, as shown in Fig. 4.9. On the other hand, the left hand side of Eq. (4.127) is fixed because it is experimentally observed one, which consequently leads for the value of corresponding $\overline{m}_b$ to bottomonium mass to decrease. Therefore, this may indicate that the deviation of $|V_{cb}|$ between these schemes is reduced by calculating the higher order corrections to the 1S mass. However, currently it remains an open question whether large non-perturbative corrections exist in the total energy. It also requires the higher-order perturbative calculations in order to answer this question unambiguously and quantitatively.

In summary, it is possible that the somewhat scattered values of $|V_{cb}|$ as in Fig. 4.8 due to differences in the mass schemes will be resolved by using the $n_f = 3$ theory and incorporating higher-order perturbative calculations (and non-perturbative effects). In particular, our results in this thesis and the results of the kinetic scheme use the $\overline{\text{MS}}$ mass as input, and its value should be chosen carefully. In this thesis, we adopt a conservative uncertainty estimate that gives the final result as $|V_{cb}| = 0.04147(^{+98}_{-117})$ determined by

[7] The leading non-perturbative contribution to the bottomonium spectrum is given by the non-local gluon condensate which represents contributions from the ultrasoft scale($\sim m_b\alpha_s^2$) and smaller scales [36]. This contribution is spin independent and is estimated to be smaller than or comparable to the current perturbative uncertainty to each energy level. This feature is further confirmed in the analysis of the static potential [39].

[8] Phenomenologically, it is natural that the gradient of the potential should be steeper to approach the linear potential in the long-range region. Perturbatively, the slope of the potential is expected to be steep based on the estimation of the effect of higher-order perturbative corrections using RG-improvement.

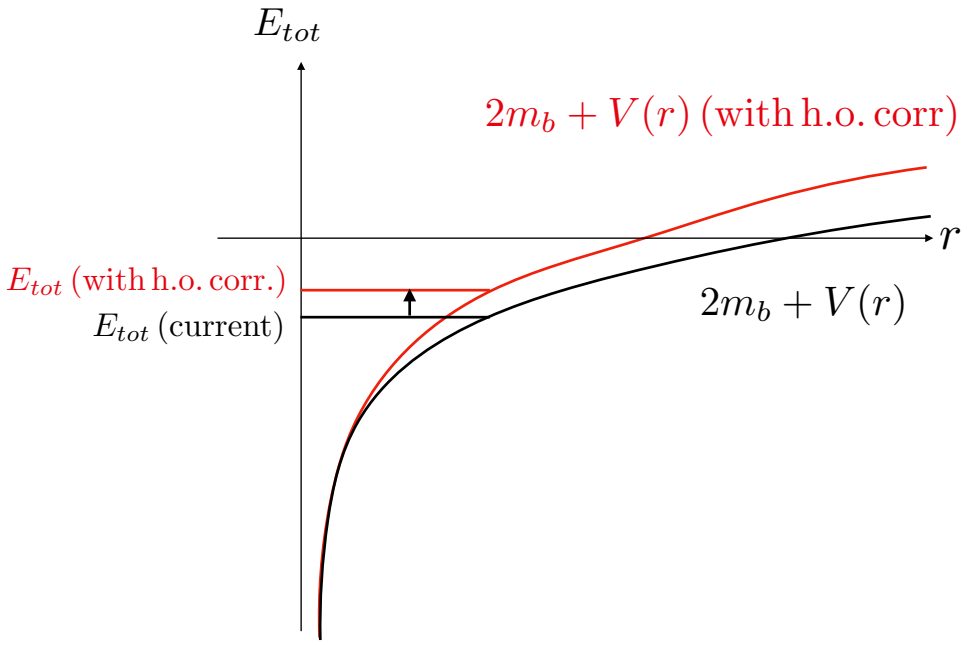

Figure 4.9: Speculation on the mechanism explaining the higher order (h.o.) corrections to $2m_b + V(r)$ increase the total energy of the (spin-averaged) bottomonium 1S state.

using the PDG input values.

Finally, we discuss the experimental input of $\mathcal{B} = \mathcal{B}(B \to X_c \ell \bar{\nu})$. If we use $\mathcal{B} = 10.48\%$ from Eq. (4.122) or $\mathcal{B} = 10.15\%$ [92] in place of the current measurement average $\mathcal{B} = 10.63\%$ from Eq. (4.121), the value of $|V_{cb}|$ decreases by 0.7% or 2.3%, respectively. In particular in the latter case, the values determined from the inclusive process significantly moves in the direction to decrease the discrepancy with the determination from the exclusive process. As with the choice of the input $\overline{\text{MS}}$ mass, better understanding of the input experimental values may help settle the problem on the inconsistency between the inclusive and exclusive determinations. For this purpose, it is essential to investigate whether there is any inconsistency in the two ways of evaluating the experimental branching ratio. The near-future Belle II results will also play an important role. In Ref. [98], the preliminary result of $\mathcal{B}$ is reported as $\mathcal{B} = (9.75 \pm 0.03(\text{stat}) \pm 0.47(\text{sys}))\%$, which is based on the Belle II data collected in the years 2019 and 2020 equivalent to 62.8fb^{-1}. This result is much smaller than those of the BaBar and Belle measurements, and it reduces the discrepancy between the inclusive and exclusive determinations of $|V_{cb}|$. Analysis of the Belle II measurement including the data collected in 2021 is underway, and more precise values will be reported in the near future.

Chapter 5

Conclusions and discussion

Conclusions

In this thesis, we presented a theoretical approach to the goal of realizing high precision QCD from theoretical side. In particular, we focused on the IR renormalons, which cause inevitable uncertainties in perturbative calculations of the Wilson coefficients in the OPE framework. The imaginary part of the Wilson coefficients, which appears by regularizing the divergent behavior of perturbative expansion due to IR renormalons, behaves as an inverse power of the typical scale (with logarithmic corrections). It is expected that the imaginary part of the Wilson coefficients cancel the same-size imaginary part contained in the non-perturbative matrix elements. After the renormalon cancellation, the predictability of the OPE can be successively improved, by higher order perturbative calculations of the Wilson coefficients and determination of the non-perturbative matrix elements by comparing with experimental data.

To use the renormalon-subtracted OPE framework in practice, we developed a new method called DSRS method to separate the renormalon contributions of the Wilson coefficients for general observables. By theoretical requirements of the OPE and the RGE, the form of the imaginary part of the Wilson coefficient due to renormalons is determined except for its normalization. The dual transform, based on the inverse Laplace transform, suppresses the multiple IR renormalons simultaneously in the dual space, where the perturbative expansion shows a good convergence. The renormalons in the original Wilson coefficients can be separated by using the one-parameter (Laplace) integral of the dual-space series. Since the perturbative series is convergent in the dual space, it is possible to successively approximate the Wilson coefficients with the renormalon contribution removed, from a finite number of perturbative coefficients. The Wilson coefficients and non-perturbative matrix elements, from which renormalons are removed in the DSRS method, have the same definitions as in the conventional studies, i.e., in the Principal Value (PV) scheme using the Borel resummation.

We investigated how the theoretical prediction by the DSRS method approaches the actual value using the static QCD potential in the large-β_0 approximation and the simple toy model as examples. The scale dependence becomes more stable as the truncation order of the perturbative expansion increases, and the predicted value at stable scales is confirmed to become closer to the true value by removing the renormalon. Furthermore, we confirmed that the DSRS method can be applied to the perturbative QCD calcula-

tions beyond the large-β_0 approximation. In the latter part of this thesis, we applied this method to the observables of the heavy quark system with the latest perturbative expansion.

The first application is the OPE of the masses of the B and D mesons. The LO term of the OPE is the heavy quark pole mass m_h. The low energy effective field theory called HQET describes the non-perturbative corrections, which contains the uncertainty due to the renormalons of the pole mass of heavy quark. From the quark pole masses m_b and m_c, we separated the $u = 1/2$ and $u = 1$ renormalons, which are canceled by the HQET parameters $\bar{\Lambda}$ and μ_π^2, respectively. The HQET parameters $\left[\bar{\Lambda}\right]$ and $\left[\mu_\pi^2\right]_{\rm PV}$, which are defined in the infinite mass limit and with renormalons removed, are important parameters used to predict multiple observables of the B and D mesons. This is the first time to study the determination of the HQET parameters subtracting the $u = 1/2$ and $u = 1$ renormalons simultaneously. Before the real analysis, we verified that the PV mass results, applying the DSRS method to the pole-$\overline{\rm MS}$ mass relation in the large-β_0 approximation, asymptotically approach the exact values as the order of the perturbative expansion is increased. Then using the DSRS method for the true pole-$\overline{\rm MS}$ mass relation up to $\mathcal{O}(\alpha_s^4)$ (and with estimated α_s^5 coefficient) with the PDG values of $\overline{m}_b$ and $\overline{m}_c$ as inputs, the renormalon-subtracted quark pole masses, called PV masses, are determined as

$$\left[m_b\right]_{\rm PV} = 4.822\,(36)\ {\rm GeV}, \quad \left[m_c\right]_{\rm PV} = 1.468\,(35)\ {\rm GeV}, \tag{5.1}$$

where the uncertainties represent combined systematic uncertainties. Both PV masses have smaller theoretical uncertainties when perturbative calculations of the next order are achieved. This is owing to the removal of renormalon. On the other hand, the uncertainty due to the input value of the $\overline{\rm MS}$ mass, is large in both cases. More precise determination of the $\overline{\rm MS}$ masses is an important task for future precision physics.

Using the results of the PV masses, we determined $\left[\bar{\Lambda}\right]_{\rm PV}$ and $\left[\mu_\pi^2\right]_{\rm PV}$ as

$$\left[\bar{\Lambda}\right]_{\rm PV} = 0.486\,(54)\ {\rm GeV}, \quad \left[\mu_\pi^2\right]_{\rm PV} = 0.05\,(22)\ {\rm GeV}^2, \tag{5.2}$$

where the systematic uncertainties are combined. The size of the (combined) systematic uncertainty for $\left[\bar{\Lambda}\right]_{\rm PV}$ is sufficiently small, reflecting the fact that the IR renormalons of the pole mass are properly removed. $\left[\mu_\pi^2\right]_{\rm PV}$ result has apparently large perturbative uncertainty, but this may be due to the lack of perturbative coefficients in the pole-$\overline{\rm MS}$ mass relation (especially for the charm quark). The results are consistent with the previous studies in the same scheme [23, 45].

As the second application, the semileptonic B decay is investigated. In this analysis, the $u = 1/2$ and $u = 1$ renormalons are subtracted simultaneously, which is the first time to be studied. The $u = 1/2$ renormalon, contained in the LO Wilson coefficient of the inclusive semileptonic decay width, is canceled out by rewriting the pole mass of the bottom quark by the $\overline{\rm MS}$ mass, which is one of the short-distance masses. Although the $\overline{\rm MS}$ mass is not favored in previous studies due to the large infrared-ness between the pole mass and the $\overline{\rm MS}$ mass, in this thesis we found that the convergence of the Wilson coefficients improves when the $u = 1$ renormalon is removed using the DSRS method. This is because subtracting the correct form of the $u = 1$ renormalon, taking into account the deviation from the simple power-type behavior, allows us to construct a dual space in which the perturbative expansion is more convergent. The prediction is consistent with

a calculation that does not subtract the $u = 1$ renormalon using RG-improvement, but confirms that the scale dependence is smaller. The final result of our $|V_{cb}|$ determination using the renormalon-subtracted Wilson coefficient is given by

$$|V_{cb}| = 0.04147\,(^{+98}_{-117}), \tag{5.3}$$

where the uncertainties are combined. We used the PDG values for the theoretical input parameters such as $\overline{m}_b$, $\overline{m}_c$ and α_s. We incorporated the non-perturbative corrections described by two HQET parameters $\left[\mu_\pi^2\right]_{\rm PV}$ and μ_G^2, which are determined from the masses of B and D mesons, and from the hyperfine-splitting of the B mesons, respectively. The experimental inputs of the branching ratio $\mathcal{B}$ and the lifetime τ_B are close to the values used in the previous studies. The uncertainty due to the perturbative calculation is reduced to an accuracy of one percent, due to a highly convergent series constructed using the DSRS method. On the other hand, the uncertainty due to the input parameters, especially the bottom quark mass, is large because $|V_{cb}|$ is proportional to $(\overline{m}_b)^{-5/2}$. If we use the FLAG values of $\overline{m}_b$, the input uncertainty will be smaller, but the result is considered as only a reference point in this thesis.

Our results are consistent with those of the previous studies using other short-distance mass schemes. First we compared the kinetic scheme with the $\overline{\rm MS}$ scheme. Since there is a difference in the number of light quarks n_f between the OPEs of our calculation and those of Refs. [58, 59], the definition of the non-perturbative parameter μ_π^2 is also different. Refs. [58, 59] used the kinetic mass of the bottom quark determined from the FLAG value of $\overline{m}_b$ with a smaller uncertainty, which could lead to an underestimate of the input uncertainty of $|V_{cb}|$. All these observations imply that the consistency between our results and those in kinetic scheme would increase if the value of μ_π^2 decreases and the PDG value of $\overline{m}_b$ is used.

Next the 1S mass scheme was compared with the $\overline{\rm MS}$ mass scheme. We speculated that the contribution to the 1S mass from the higher order potentials (and currently ignored non-perturbative effects) may reduce the value of the $\overline{\rm MS}$ mass corresponding to the same 1S mass. To clarify this, it is necessary to achieve the next order perturbative calculation of the 1S mass spectrum ($M_{\Upsilon(1S)}$ and $M_{\eta_b(1S)}$). Since the naive expectation is that the value of $|V_{cb}|$ using the small $\overline{\rm MS}$ mass is close to the true value corresponding to the bottomonium mass, we took the conservative attitude and determined $|V_{cb}|$ from the PDG inputs as the determination value.

After the above analysis, the determined value of the inclusive $|V_{cb}|$ using the default experimental value of $\mathcal{B}$ is still in tension with the result of the exclusive determination. However, the experimental values of $\mathcal{B}$ by different determination methods may reduce the value of the inclusive $|V_{cb}|$. To verify this effect, it is essential to use the Belle II results to be announced in the near future which improve the accuracy of the background $B \to X_u \ell \bar{\nu}$.

Discussion

We discuss the applicabilities of the DSRS method in the future. First we look into the determination of $\left[m_b\right]_{\rm PV}$ using the 1S states of the bottomonium. Disadvantage of the determination of the PV mass from the $\overline{\rm MS}$ mass is that the input $\overline{\rm MS}$ mass contains a

large uncertainty at present. It is because the $\overline{\rm MS}$ mass is a theoretical parameter, of which precision depends on how we determine its value and what observable we use. The ideal situation is that the PV mass is determined by comparing observables directly. The 1S energy spectrum of a heavy quarkonium has such possibilities. Naively, the right hand side of Eq. (4.127) is a perturbative expansion for $\alpha_s(\overline{m}_b)$, and it seems that the DSRS method can be applied to separate the renormalon. In that case, we can determine $\overline{m}_b$ with renormalons removed by comparing both sides with the experimental value of the 1S mass of the bottomonium on the left hand side, and then we can determine also the PV mass from the formula in this thesis. However, the actual scale of the bottomonium is the Bohr scale $\sim C_F\alpha_s m_b$, and it is difficult to apply the DSRS method to the 1S mass spectrum for the following reason. The perturbative calculation when written in $\alpha_s(\overline{m}_b)$ relies on the ε-expansion explained in App. G, which contains corrections of the form $\alpha_s^n \log^k(\alpha_s)$ that does not appear in the normal perturbation. When the scale is set to the Bohr scale, the perturbative expansion does not have such an exotic form, but even the bottomonium system has a low typical scale of about $1-2$ GeV. At such scales, the number of known perturbative coefficients may not be sufficient to determine the PV mass value accurately, as in the calculations of the charm quark system in this thesis. Furthermore, unlike theoretical quantities such as the pole-$\overline{\rm MS}$ mass relation, the bottomonium mass is an observable, including non-perturbative effects, and such effects would not be negligible in the Bohr scale calculation. In addition to its low scale, the Bohr scale itself is defined in terms of the pole mass, which makes a practical use of the DSRS method difficult because the (hard) Bohr scale has also uncertainty due to the renormalons of the pole mass.

One possible way to calculate the PV mass directly from the 1S mass would be the following. The energy levels of the bottomonium are given as the positions of the poles of the Green function of $H - E_{bin}$ with the Hamiltonian $H = p^2/m_b + V(r)$. Eq. (4.127) is calculated by considering the non-Coulomb potentials as perturbations. On the other hand, the position of the pole can be calculated numerically from the input values of m_b. If the renormalons are removed from $V(r)$ and the pole mass m_b at the Hamiltonian level using the DSRS method, it is expected that the PV mass $\left[m_b\right]_{\rm PV}$ can be determined by numerically varying parameters to reproduce the real bottomonium mass. Although the low Bohr scale cannot be avoided, removing the renormalon at the Hamiltonian level has the advantage that the Bohr scale is well-defined. This is beyond the scope of this thesis, but it would work at least for the bottomonium mass.

It is also possible to determine $|V_{cb}|$ from the other observables, the moments of the semileptonic B decay. In this thesis, the B and D meson masses were used to determine the HQET parameters with renormalons removed, but since there are only two parameters that can be determined for two experimental values, the heavy quark masses had to be used as input parameters. In our determination of $|V_{cb}|$, the uncertainty due to the input bottom quark mass is dominant, and therefore we would like to determine the bottom quark also as a parameter of the theory, from a comparison to experimental values. There are several measurements of the distributions of the lepton energy and invariant hadronic mass in the LHC and Belle II experiments, which provide a large number of observables to compare with the OPE. The HQET parameters and $|V_{cb}|$ have already been determined using the OPE of the moments from the NNNLO-level perturbative calculations in the kinetic scheme. The mass of the bottom quark in addition to the

above have been determined by global fitting at the NNLO level. In the future, using the latest OPE of moments at the NNNLO-level and applying the DSRS method to them, we expect to remove the renormalon and determine $|V_{cb}|$ and HQET parameters as well as the bottom quark mass in the $\overline{\rm MS}$ mass scheme. This investigation would further strengthen the certainty of the OPE and make the determination of $|V_{cb}|$ from the inclusive semileptonic B decay more precise.

Acknowledgements

The work of the author was supported by Grant-in-Aid for JSPS Fellows (No. 21J10226) from MEXT and he also acknowledges support from GP-PU at Tohoku University. This thesis is based on the work in collaboration with Go Mishima, Hiromasa Takaura and Yukinari Sumino. The author thanks all of them for their ungrudging collaboration. He is grateful to Matthias Steinhauser, Shoichi Sasaki and Akimasa Ishikawa for fruitful discussions. He shows special thanks to Yukinari Sumino for giving useful advices throughout his Ph.D. course. Finally, he expresses his gratitude to Mio Takahashi for her dedication and support for his life.

Appendix A

Perturbative coefficients

In this appendix, we collect the perturbative coefficients necessary for the analyses in this paper.

QCD beta function

The QCD β function is known up to $\mathcal{O}(\alpha_s^6)$ (5-loop accuracy) [1].

$$\beta(\alpha_s) = -\sum_{i=0}^{4} b_i \alpha_s^{i+2}, \tag{A.1}$$

$$b_0 = \frac{1}{4\pi}\Big(11 - \frac{2}{3}n_f\Big), \quad b_1 = \frac{1}{(4\pi)^2}\Big(102 - \frac{38}{3}n_f\Big), \tag{A.2}$$

$$b_2 = \frac{1}{(4\pi)^3}\Big(\frac{2857}{2} - \frac{5033}{18}n_f + \frac{325}{54}n_f^2\Big), \tag{A.3}$$

$$b_3 = \frac{1}{(4\pi)^4}\Big[\frac{149753}{6} + 3564\zeta_3 - \Big(\frac{1078361}{162} + \frac{6508}{27}\zeta_3\Big)n_f + \Big(\frac{50065}{162} + \frac{6472}{81}\zeta_3\Big)n_f^2 + \frac{1093}{729}n_f^3\Big], \tag{A.4}$$

$$\begin{aligned} b_4 = \frac{1}{(4\pi)^5}\Bigg[&\frac{8157455}{16} + \frac{621885}{2}\zeta_3 - \frac{88209}{2}\zeta_4 - 288090\zeta_5 \\ &+ n_f\left(-\frac{336460813}{1944} - \frac{4811164}{81}\zeta_3 + \frac{33935}{6}\zeta_4 + \frac{1358995}{27}\zeta_5\right) \\ &+ n_f^2\left(\frac{25960913}{1944} + \frac{698531}{81}\zeta_3 - \frac{10526}{9}\zeta_4 - \frac{381760}{81}\zeta_5\right) \\ &+ n_f^3\left(-\frac{630559}{5832} - \frac{48722}{243}\zeta_3 + \frac{1618}{27}\zeta_4 + \frac{460}{9}\zeta_5\right) + n_f^4\left(\frac{1205}{2916} - \frac{152}{81}\zeta_3\right)\Bigg]. \end{aligned} \tag{A.5}$$

n_f is the number of active quark flavors, and $\zeta_n = \zeta(n) = \sum_{k=1}^{\infty} k^{-n}$ denotes the Riemann zeta function.

Pole-$\overline{\rm MS}$ mass relation

We consider that there are n_l massless and one massive internal quarks, besides the heavy quark h. The relation between pole mass and $\overline{\rm MS}$ mass is given by

$$\frac{m_h}{\overline{m}_h} = 1 + \delta(\overline{m}_h), \tag{A.6}$$

and

$$\delta(\overline{m}_h) = \sum_{n=0}^{\infty} \alpha_s(\overline{m}_b)^{n+1} d_n\big(\overline{m}_c/\overline{m}_b\big), \tag{A.7}$$

where $\alpha_s(\overline{m}_h) = \alpha_s^{(n_l)}(\overline{m}_h)$. The coefficients d_n's are calculated up to d_3 [64, 65, 66, 68, 69, 5, 6, 7]. The internal massive quark effects for $\mathcal{O}(\alpha_s^2)$ and $\mathcal{O}(\alpha_s^3)$ corrections are contained, while those for $\mathcal{O}(\alpha_s^4)$ has not been calculated. The series we used in Chap. 4, including the non-zero m_c corrections up to $\mathcal{O}(\alpha_s^3)$, is given by

$$\frac{m_b}{\overline{m}_b^{(5)}} \approx 1 + 0.424413\,\alpha_s + 1.03744\,\alpha_s^2 + 3.74358\,\alpha_s^3 + 17.4376\,\alpha_s^4, \tag{A.8}$$

where $\alpha_s = \alpha_s^{(3)}(\overline{m}_b)$ with $\overline{m}_b = \overline{m}_b^{(5)}$, and

$$\frac{m_c}{\overline{m}_c^{(4)}} \approx 1 + 0.424413\,\alpha_s + 1.04375\,\alpha_s^2 + 3.75736\,\alpha_s^3 + 17.4376\,\alpha_s^4, \tag{A.9}$$

where $\alpha_s = \alpha_s^{(3)}(\overline{m}_c)$ with $\overline{m}_c = \overline{m}_c^{(4)}$ and non-decoupling bottom effects are included. In obtaining the right-hand sides, we used the inputs $\overline{m}_c^{(4)} = 1.27$ GeV and $\overline{m}_b^{(5)} = 4.18$ GeV. We note that both of $\mathcal{O}(\alpha_s^2)$ and $\mathcal{O}(\alpha_s^3)$ corrections are quite similar to each other, and each series can be approximated well by $\sum_n \alpha_s^{n+1} d_n(\overline{m}_c/\overline{m}_b \to 0)$ with $n_l = 3$, given by

$$\frac{m_h}{\overline{m}_h} \approx 1 + 0.424413\,\alpha_s + 1.04556\,\alpha_s^2 + 3.75086\,\alpha_s^3 + 17.4376\,\alpha_s^4. \tag{A.10}$$

Mass of heavy-light meson

The OPE of its mass M_H based on HQET is given by

$$M_H^{(s)} = m_h + \bar{\Lambda} + \frac{\mu_\pi^2}{2m_h} + A(s) C_{cm}(m_h) \frac{\mu_G^2(m_h)}{2m_h} + \mathcal{O}\left(\frac{\Lambda_{\overline{\rm MS}}^3}{m_h^2}\right), \tag{A.11}$$

where $s\,(= 0,\, 1)$ denotes the spin of H. The Wilson coefficient of a chromo-magnetic term C_{cm} is analytically calculated up to $\mathcal{O}(\alpha_s^3)$ [61], which was used to evaluate $\mu_G^2(\overline{m}_b)$ in Sec. 4.1.3. The numerical values of coefficients of

$$C_{cm} = 1 + \sum_{n=0}^{2} \alpha_s(m_h)^{n+1} c_n^{cm}, \tag{A.12}$$

with $\alpha_s = \alpha_s^{(n_f)}$, are given by

$$c_0^{cm} \approx 0.6897, \tag{A.13}$$

$$c_1^{cm} \approx 2.2186 - 0.1938\, n_f, \tag{A.14}$$

and

$$c_2^{cm} \approx 11.079 - 1.7490\, n_f + 0.0513\, n_f^2. \tag{A.15}$$

Total decay width of inclusive semileptonic B decay

The OPE of the total decay width of $B \to X_c \ell \bar{\nu}$ is given by

$$\Gamma = \frac{G_F^2 |V_{cb}|^2}{192\pi^3} A_{ew} m_b^5 \left[C_{\bar{Q}Q}^{\Gamma} \left(1 - \frac{\mu_\pi^2}{2m_b^2} \right) + C_{cm}^{\Gamma} \frac{\mu_G^2}{m_b^2} + \mathcal{O}\left(\frac{\Lambda_{\overline{\rm MS}}^3}{m_b^3} \right) \right]. \tag{A.16}$$

The leading Wilson coefficient $C_{\bar{Q}Q}^{\Gamma}$ in terms of a pole mass is perturbatively calculated as

$$C_{\bar{Q}Q}^{\Gamma} = \sum_{n=0}^{3} \alpha_s(m_b^2)^n X_n(\rho), \tag{A.17}$$

with $\rho = m_c/m_b$ and $\alpha_s = \alpha_s^{(5)}$. X_0, X_1 and X_2 are analytically calculated [71, 72, 73, 74, 75, 76, 77]. They are given by

$$X_0 = 1 - 8\rho^2 - 12\rho^4 \log(\rho^2) + 8\rho^6 - \rho^8, \tag{A.18}$$

$$\begin{aligned} X_1 = -\frac{2}{3\pi} \Bigg[& -(1-\rho^4)\left(\frac{25}{4} - \frac{239}{3}\rho^2 + \frac{25}{4}\rho^4 \right) + \rho^2 \log(\rho^2) \left(20 + 90\rho^2 - \frac{4}{3}\rho^4 + \frac{17}{3}\rho^6 \right) \\ & + \rho^4 \log^2(\rho^2)(36 + \rho^4) + (1-\rho^4)\left(\frac{17}{3} - \frac{64}{3}\rho^2 + \frac{17}{3}\rho^4 \right) \log(1-\rho^2) \\ & - 4(1 + 30\rho^4 + \rho^8) \log(\rho^2) \log(1-\rho^2) - (1 + 16\rho^4 + \rho^8)(6\mathrm{Li}_2(\rho^2) - \pi^2) \\ & - 32\rho^3(1+\rho^2)(\pi^2 - 4\mathrm{Li}_2(\rho) + 4\mathrm{Li}_2(-\rho) - 2\log(\rho^2) \log\left(\frac{1-\rho}{1+\rho} \right) \Bigg], \end{aligned} \tag{A.19}$$

and

$$\begin{aligned} X_2 \approx & -2.158 - 0.8333\rho + (-65.01 - 39.22\log(\rho) + 0.2701\log^2(\rho))\rho^2 \\ & + (-118.7 - 129.8\log(\rho))\rho^3 + (128.2 - 124.6\log(\rho) - 16.52\log^2(\rho) + 1.081\log^3(\rho))\rho^4 \\ & (-41.65 - 80.98\log(\rho))\rho^5 + (98.42 - 39.30\log(\rho) + 16.77\log^2(\rho))\rho^6 \\ & (-14.86 + 1.954\log(\rho))\rho^7 + (0.09796 - 0.1094\log(\rho))\rho^8 + \mathcal{O}(\rho^9) \end{aligned} \tag{A.20}$$

where we expand X_2 in ρ to avoid a lengthy expression. X_3 is known as the expansion in $\delta = 1 - \rho$ up to $\mathcal{O}(\delta^{20})$ [57].

C_{cm}^{Γ} has been calculated to $\mathcal{O}(\alpha_s)$ order [78, 79, 80, 81]. In this thesis, to determine the central value of $|V_{cb}|$, we use the LO term $C_{cm}^{\Gamma}\big|_{\rm LO}$ given by

$$C_{cm}^{\Gamma}\big|_{\rm LO} = -\frac{1}{2}(3 - 8\rho^2 + 24\rho^4 - 24\rho^6 + 5\rho^8 + 12\rho^4 \log(\rho^2)). \tag{A.21}$$

The NLO term is used for the estimation of uncertainty, which is given by

$$C_{cm}^{\Gamma}\big|_{\rm NLO} \approx -2.42 \times X_0(\bar{\rho})\alpha_s(\overline{m}_b), \tag{A.22}$$

where " $\approx$ " means that we use the numerical value of $C_{cm}^{\Gamma}\big|_{\rm NLO}$ at $\mu = m_b$ since the analytic result is unknown.

To change the flavor of running coupling constant from n_f flavor to $(n_f - 1)$ flavor, we use a flavor threshold relation [99] given by

$$\begin{aligned}\frac{\alpha_s^{(n_f-1)}}{\alpha_s^{(n_f)}} = 1 - \frac{\ell_h}{6\pi}\alpha_s^{(n_f)} + \left(\frac{\ell_h^2}{36} - \frac{19}{24}\ell_h + c_2\right)\left(\alpha_s^{(n_f)}\right)^2 \\ + \left(-\frac{\ell_h^3}{216} - \frac{131}{576}\ell_h^2 + \frac{-6793 + 281(n_f - 1)}{1728}\ell_h + c_3\right)\left(\alpha_s^{(n_f)}\right)^3 + \mathcal{O}(\alpha_s^4),\end{aligned} \tag{A.23}$$

with $\alpha_s = \alpha_s(\mu^2)$, $\mu_h = \overline{m}(\mu_h)$, $\ell_h = \log(\mu^2/\mu_h^2)$ and

$$c_2 = \frac{11}{72}, \quad c_3 = -\frac{82043}{27648}\zeta(3) + \frac{564731}{124416} - \frac{2633}{31104}(n_f - 1). \tag{A.24}$$

In this thesis, we take a scale for matching $\alpha_s^{(5)}$ to $\alpha_s^{(4)}$ as $\mu = \mu_h = \overline{m}_b$, and for matching $\alpha_s^{(4)}$ to $\alpha_s^{(3)}$ as $\mu = \mu_h = \overline{m}_c$.

Appendix B

Relation between Borel transform and Dual transform

In this appendix, we derive a relation between a regularized inverse Borel transform and a regularized inverse dual transform. The relation is used to show equivalence of Eq. (2.25) and Eq. (3.14), which is valid not only in the large-β_0 approximation, but beyond that.

We consider[1] the observable in the dual space $\tilde{X}(\tau) = \tilde{X}^{(k)}(\tau)$ in the $\mathrm{N^kLL}$ approximation for $0 \le k \le 4$, as given by Eq. (3.12) with $\tilde{C}_0$ replaced by $\tilde{X}$. From it, the perturbative coefficients of $X(Q) = \sum_n \alpha_s^{n+1} c_n(L_Q)$ can be computed up to arbitrarily high orders, by inverse dual transformation at each order of expansion in α_s. We assume that the Borel transform of $X(Q)$,

$$B_X(u) = \sum_{n=0}^{\infty} \frac{c_n}{n!} \left(\frac{u}{b_0}\right)^n , \tag{B.1}$$

does not have singularities in the right half u-plane, $\mathrm{Re}\, u > 0$, except on the positive real u-axis.[2] If $|u|$ is smaller than the distance to the renormalon closest to the origin, the series converges and $B_X(u)$ is single-valued. At larger $|u|$, $B_X(u)$ is defined by analytic continuation. For $k = 0$ the closest renormalon is a pole, while for $1 \le k \le 4$ it is a branch point, where the branch cut extends along the real axis to the right [11].

Let us define

$$X_+(Q) = x^{-2au'} \int_{C_-} d\tau^2 \, e^{-\tau^2 x^2} \tilde{X}(\tau) \quad ; \quad x = Q^{-1/a}, \tag{B.2}$$

$$B_{X+}(u) = \oint \frac{dp}{2\pi i} \, e^{up/b_0} \big[X_+(Q)\big]_{\alpha_s \to 1/p} . \tag{B.3}$$

$\tilde{X}$ has a singularity corresponding to the (Landau) singularity of $[\alpha_s(\tau^a)]_{\mathrm{N^kLL}}$ at $\tau > 0$. Along the τ integration contour $C_-(\tau)$ the singularity is circumvented to the lower half

[1] The reason why we limit k to this range is that we do not know the QCD beta function beyond five loops and hence in the argument below the singularity structure in the complex p plane cannot be made definite. In the case within the large-β_0 approximation, where the QCD beta function is given by the LL one, the range of k is not limited.

[2] For $k = 0$ (LL) the assumption indeed holds, see below. Although we believe that this assumption can be checked for $1 \le k \le 4$, up to now we do not know the proof or disproof.

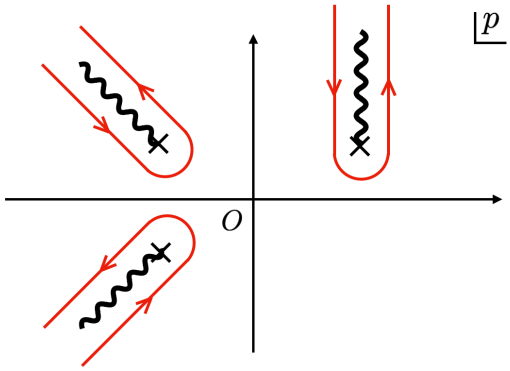

Figure B.1: Schematic diagram of the contour of p integration in eq. (B.3). Each branch cut extends to the direction in which the integral wrapping it converges.

plane. Thus, X_+ is well defined. In the second equation, X_+ is regarded as a function of $\alpha_s \equiv \alpha_s(\mu^2)$ and is rewritten in terms of $p = 1/\alpha_s$. The integral contour of p is taken as a closed path surrounding all the singularities of $\left[X_+(Q)\right]_{\alpha_s \to 1/p}$ counterclockwise; see Fig. B.1. This contour is obtained by a continuous deformation of the closed contour surrounding the origin $p = 0$ in a small $|p|$ region.

In the case that we apply Eqs. (B.2) and (B.3) to the series expansion in $\alpha_s(\mu^2)$ (up to arbitrary order), the expansion of $\tilde{X}(\tau)$ has no singularity at $\tau \in \mathbf{R}_{>0}$. Then, $C_-(\tau)$ can be deformed to the positive real τ axis, and the expansion of $X_+(Q)$ coincides with that of $X(Q)$; the singularities of the expansion of $\left[X(Q)\right]_{\alpha_s \to 1/p}$ are multiple poles at the origin $p = 0$, and the expansion of B_{X+} reduces to Eq. (B.1), which follows readily by the residue theorem. Hence, B_{X+} coincides with B_X for small $|u|$, or in other words, B_{X+} is defined as an analytic continuation of B_X.

We define the regularized Borel resummation representation of $X(Q) = \sum_n c_n(\mu/Q)\alpha_s^{n+1}$ as

$$X(Q)_{\mathrm{BI},+} = \frac{1}{b_0}\int_{C_+} du\, e^{-\frac{u}{b_0\alpha_s}} B_{X+}(u) = i\int_0^\infty ds\, e^{-\frac{is}{\alpha_s}} B_{X+}(ib_0 s)\,, \tag{B.4}$$

where the integration contour of u is rotated to the positive imaginary axis ($u = ib_0 s$)[3].

The reason why we choose the contour $C_-(\tau)$ in Eq. (B.2) rather than $C_+(\tau)$ is as follows. Let us explain in the case that $\tilde{X}(\tau)$ is given by the LL approximation, $\tilde{X} \propto [\alpha_s(\tau^a)]_{\mathrm{LL}}$. (We explain the NLL approximation and beyond later.) Thus,

$$X(Q)_{\mathrm{BI},+} = \frac{x^{-2au'}}{2\pi}\oint dp \int_0^\infty ds\, e^{is(p-1/\alpha_s)} \int_{C_-} d\tau^2\, e^{-\tau^2 x^2} \left[\tilde{X}(\tau)\right]_{\alpha_s \to 1/p}, \tag{B.5}$$

where the integration contour of p surrounds the pole of $\tilde{X}$ at[4] $p = b_0 \log(\mu^2/\tau^{2a})$, which

[3]This equality is invalid if $B_X(u)$ contains singularities in the first quadrant of complex Borel u-plane. We assume that the contribution from such singularities is negligible in the high energy region, while it would be a restriction in the low energy region. For the Adler function, this kind of restriction has been discussed recently [100].

[4]This is the only singularity of $\tilde{X}$ in the LL approximation.

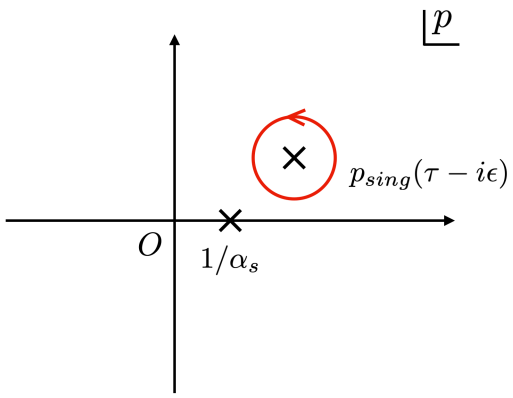

Figure B.2: Singularities and integration contour in the complex p plane, in the LL approximation for $\tilde{X}(\tau)$.

originates from

$$[\alpha_s(\tau^{2a})]_{\rm LL} = \frac{\alpha_s}{1 - b_0 \alpha_s \log(\mu^2/\tau^{2a})}\bigg|_{\alpha_s \to 1/p} = \frac{1}{p - b_0 \log(\mu^2/\tau^{2a})}. \tag{B.6}$$

We would like to integrate over s first. To ensure convergence at $s \to \infty$, the imaginary part of p should be non-negative (Note: $\alpha_s > 0$). By taking the path of τ (slightly) in the lower-half plane, i.e., along $C_-(\tau)$, the pole $p = b_0 \log(\mu^2/\tau^{2a})$ lies in the upper-half p plane, and the entire contour of p can be taken in the upper-half plane. After integration over s, we have

$$X(Q)_{\rm BI,+} = \frac{i x^{-2au'}}{2\pi} \oint dp \frac{1}{p - 1/\alpha_s} \int_{C_-} d\tau^2 \, e^{-\tau^2 x^2} \left[\tilde{X}(\tau)\right]_{\alpha_s \to 1/p}. \tag{B.7}$$

This argument also shows that $B_{X+}(u)$ is a natural integral representation of $B_X(u)$ for u in the upper-half plane.

Next we integrate over p. There are two poles at $p = 1/\alpha_s$ and $p = b_0 \log(\mu^2/\tau^{2a})$. The two poles are well separated as τ moves along $C_-(\tau)$, see Fig. B.2. In fact these two poles coincide only if $\tau^a = \Lambda^{\rm LL}_{\overline{\rm MS}}$ but this is circumvented on $C_-(\tau)$. Hence, the closed contour of p can always be taken to surround only the pole at $p = b_0 \log(\mu^2/\tau^{2a})$. The integrand reduces to zero sufficiently rapidly $\sim 1/|p|^2$ as $|p| \to \infty$. This means that we can take the residue at $p = 1/\alpha_s$ and obtain

$$X(Q)_{\rm BI,+} = \frac{1}{b_0} \int_{C_+} du \, e^{-\frac{u}{b_0 \alpha_s}} B_X(u) = x^{-2au'} \int_{C_-} d\tau^2 \, e^{-\tau^2 x^2} \tilde{X}(\tau). \tag{B.8}$$

This is the relation between the regularized inverse Borel transform and the regularized inverse dual transform, which we set out to derive.[5] Similarly, $X(Q)_{\rm BI,-}$ is given by

[5]In the case that we expand in α_s, regularizations are unnecessary. The difference is that the singularities of $\tilde{X}$ in the p plane stay fixed at the origin, so that we do not need to rotate the integration contour of u but it can be kept on the positive real axis.

changing $C_\pm \to C_\mp$ in Eq. (B.8). We emphasize again that it is crucial that $\tilde{X}(\tau)$ is free of IR renormalons and well-defined (while $X(Q)$ is not).

In the case that $\tilde{X}(\tau)$ is given by the NLL approximation or beyond, the above argument needs to be modified as follows. We set $\tilde{X} = \tilde{X}^{(k)} \propto \sum_{n=0}^{k} \tilde{c}_n(0)\alpha_s(\tau^a)^{n+1}$ for a given $k \in \{1,2,3,4\}$. According to our current knowledge of RGE at N^{k}LL, $\alpha_s(\tau^a)$ diverges at $\tau = \tau_* \in \mathbf{R}$ if the running starts from $\mu > \tau_*^a$ with the initial condition $\alpha_s(\mu) = 1/p$. This causes a singularity on the positive real p-axis for given values of τ and μ. The relation between p and $\alpha_s(\tau^a)$ is determined implicitly by

$$\log\left(\frac{\mu^2}{\tau^{2a}}\right) = -\int_{1/p}^{\alpha_s(\tau^a)} dx\, \frac{1}{\beta(x)}\,, \qquad \beta(\alpha_s) = -\sum_{n=0}^{k} b_n\, \alpha_s^{n+2}\,, \tag{B.9}$$

which can be derived from Eq. (2.2). One can analyze the positions of the singularities of $\left[\tilde{X}(\tau)\right]_{\alpha_s\to 1/p}$ in the complex p plane and find the following feature. If $\tau \in \mathbf{R}_{>0}$, we can choose $^\exists p_{\rm ref} \in \mathbf{R}_{>0}$ independent of τ such that all the singularities except one (let us call it $p_{*,1}$) are located to the left of $p_{\rm ref}$. We can choose α_s such that $1/\alpha_s > p_{\rm ref}$. In the region $\tau^a < \mu$, $p_{*,1}$ is real positive and collides with $1/\alpha_s$ at $\tau = \tau_*$. In this region, if τ is shifted slightly to the lower half plane, $p_{*,1}$ is shifted slightly to the upper half plane. Thus, $p_{*,1}$ plays the role of the only singularity in the LL case if $\tau^a < \mu$, although $p_{*,1}$ is a branch point rather than a pole. In the region $\tau^a > \mu$, $p_{*,1}$ is also located to the left of $p_{\rm ref}$.

We separate the integral along $C_-(\tau)$ of Eq. (B.5) into the regions $\mathrm{Re}\,\tau^a > \mu$ and $\mathrm{Re}\,\tau^a < \mu$. In the latter integral, we further separate the integral corresponding to the contour of p wrapping the branch cut of $p_{*,1}$ from the rest. The branch cut of $p_{*,1}$ is taken to extend to $+i\infty$. For this particular integral, we treat it similarly to the LL case and integrate over s. For the rest of the integrals, rather than integrating over s from 0 to ∞, we integrate over u from 0 to ∞. (Namely, we transform back from s to u, and instead of integrating along the positive imaginary u-axis, we integrate along the positive real u-axis.) The integral over u converges, since $\mathrm{Re}\,p < 1/\alpha_s$ for any p along the contour of p which is closed to the left; see Fig. B.3. After collecting all the integrals, we obtain eq. (B.7) again. The essence of the above procedure is that we can find a path to Eq. (B.7) by an analytic continuation. The remaining procedure is the same as the LL case.

Below we present an analysis of the singularities of $\left[\tilde{X}(\tau)\right]_{\alpha_s\to 1/p}$ in the complex p plane. We consider the case $\tau \in \mathbf{R}_{>0}$. The integral in Eq. (B.9) can be evaluated as

$$\begin{aligned} -\int_{1/p}^{\alpha_s(\tau^a)} dx\, \frac{1}{\beta(x)} &= \int_{1/\alpha_s(\tau^{2a})}^{p} dq\, \frac{q^k}{b_0 q^k + b_1 q^{k-1} + \cdots + b_k} \\ &= \frac{1}{b_0}\left(p - \frac{1}{\alpha_s(\tau^a)}\right) + \sum_{j=1}^{k} R_j \log\left(\frac{p_j - p}{p_j - 1/\alpha_s(\tau^{2a})}\right) = \log\left(\frac{\mu^2}{\tau^{2a}}\right). \end{aligned} \tag{B.10}$$

Here, the complex roots of $-p^{k+2}\beta(1/p) = b_0 p^k + b_1 p^{k-1} + \cdots + b_k = 0$ are denoted as p_j $(1 \le j \le k)$. R_j is the residue of $p^k/[-p^{k+2}\beta(1/p)]$ at $p = p_j$. The roots p_j are logarithmic branch points of $\alpha_s(\tau^a)$, hence, they are singularities of $\left[\tilde{X}(\tau)\right]_{\alpha_s\to 1/p}$. They are branch points independent of τ. The other class of singularities originate from divergence of

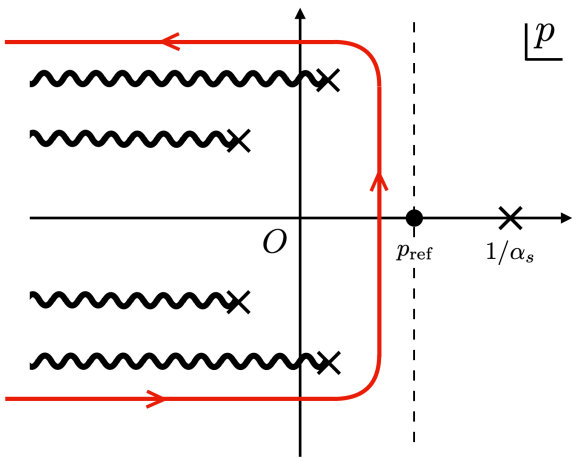

Figure B.3: Contour of p integration surrounding singularities in the p plane. These singularities correspond to all the singularities except $p_{*,1}$ in the region $\tau^a < \mu$, and to all the singularities in the region $\tau^a > \mu$.

$\alpha_s(\tau^a)$, and the positions of those singularities ($p = p_{*,i}$) are determined by

$$\log\left(\frac{\mu^2}{\tau^{2a}}\right) = \int_0^{p_{*,i}} dq\ \frac{q^k}{b_0 q^k + b_1 q^{k-1} + \cdots + b_k}$$
$$= \frac{p_{*,i}}{b_0} + \sum_{j=1}^{k} R_j \log(1 - p_{*,i}/p_j)\,. \tag{B.11}$$

They are branch points, $\alpha_s(\tau^a) \sim (p - p_{*,i})^{-1/(k+1)}$.

When $\tau^a/\mu \simeq 1$, $p_{*,i}$ $(1 \le i \le k+1)$ are located close to the origin and determined approximately by $(k+1)b_k \log(\mu^2/\tau^{2a}) = (p_{*,i})^{k+1}$. In the region $0 < \tau^a < \mu$, we take $p_{*,1}$ as the one corresponding to the Landau singularity τ_*. That is, $p_{*,1}$ is real positive and moves from $+\infty$ to 0 as τ^a is raised from 0 to μ. The behavior of other $p_{*,i}$ as $\tau \to 0$ belongs to either of the following categories:

(a) $p_{*,i}$ goes towards left, i.e., $\mathrm{Re}\, p_{*,i} \to -\infty$ while $\mathrm{Im}\, p_{*,i}/\mathrm{Re}\, p_{*,i} \to 0$.

(b) $p_{*,i} \in \mathbf{R}$ and converges towards one of p_j's which is also real.

(c) $p_{*,i}$ approaches one of p_j's as $p_{*,i}$ rotates around this fixed point infinitely many times (hence it enters the different sheets).

(d) $p_{*,i}$ rotates around one of p_j's infinitely many times (hence it enters the different sheets) as the distance to this fixed point increases.

In the region $\tau^a > \mu$, as $\tau \to \infty$ the behavior of every $p_{*,i}$ (including $p_{*,1}$) belongs to either of the above categories. As an example we show the trajectories of $p_{*,i}$ for $k = 1$ (NLL case) in Fig. B.4.

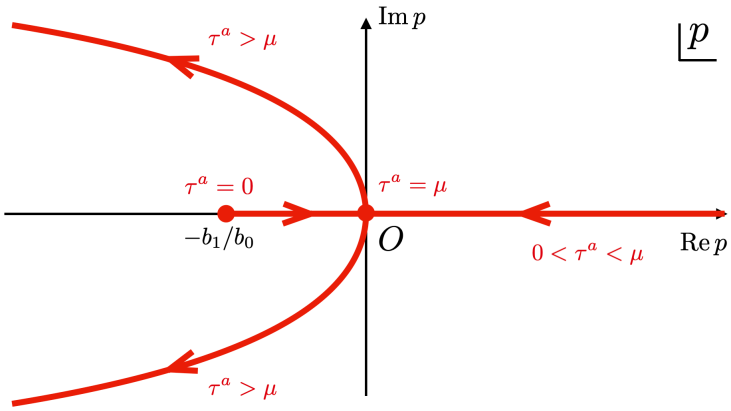

Figure B.4: Trajectories of $p_{*,1}$ and $p_{*,2}$ in the NLL approximation of $\tilde{X}$ $(k = 1)$, as $\tau \in \mathbf{R}$ is raised from 0 to ∞. At $\tau = 0$, $p_{*,1} = +\infty$ and $p_{*,2} = p_1 = -b_1/b_0$.

Appendix C

Including logarithmic corrections to DSRS method

In Chap. 3, we saw the suppression of renormalons of the LO Wilson coefficient in dual space by an appropriate choice of the parameters (a, u'), see Eq. (3.8). It can be extended to a more general case with logarithmic (perturbative) corrections of the renormalons or non-zero values of the anomalous dimensions of the corresponding operators. We demonstrate how these can be incorporated into the DSRS method in this appendix.

For heuristic reasons we present most argument in expansion in $\log(Q_0^2/Q^2)$ with respect to an arbitrary chosen scale $Q = Q_0$. In this way we can start from the limit where we know the answer already (the case without logarithmic corrections). Nonetheless, the expansion in $\log(Q_0^2/Q^2)$ can be resummed using RG. At the end of this appendix we show how to resum $\log(Q_0^2/Q^2)$'s and obtain Q_0 independent expressions.

First, let us consider the case for suppressing only the leading renormalon at $u = u_0$. The imaginary part from the renormalon at $u = u_0$ has the form

$$\delta C_0(Q) = N_{u_0}(b_0\alpha_s(Q^2))^{\gamma_0/b_0}\left(\frac{\Lambda^2_{\overline{\rm MS}}}{Q^2}\right)^{u_0}(1 + \sum_n s_n(1)\alpha_s(Q^2)^{n+1}) \tag{C.1}$$

according to eq. (2.31). We expand $\alpha_s(Q^2)$ in $\log(Q_0^2/Q^2)$ about $Q = Q_0$ using

$$\alpha_s(Q^2) = \sum_{n=0}^{\infty}\frac{\log^n(Q_0^2/Q^2)}{n!}\Big[-\beta(\alpha_s(Q_0^2))\frac{\partial}{\partial\alpha_s(Q_0^2)}\Big]^n\alpha_s(Q_0^2), \tag{C.2}$$

where Q_0 is an arbitrary expansion point.[1] Then δC_0 of eq. (2.31) can be written in the form

$$\delta C_0 = N_{u_0}\Lambda^{2u_0}_{\overline{\rm MS}}\sum_{n=0}^{\infty}q_n\log^n(Q^{-2})Q^{-2u_0} = N_{u_0}\Lambda^{2u_0}_{\overline{\rm MS}}\sum_{n=0}^{\infty}q_n\Big(\frac{\partial}{\partial u_0}\Big)^nQ^{-2u_0}. \tag{C.3}$$

q_n is given by a combination of s_i, $\alpha_s(Q_0^2)$, $\log Q_0^2$, and the coefficients of the beta function and anomalous dimension (b_i and γ_i).

[1] It is natural to take Q_0 within the energy range where we use the OPE, such that $\alpha_s(Q_0)\log(Q_0^2/Q^2)$ can be regarded as a small parameter.

To construct $\tilde{C}_0(\tau)$, define the series $\sum_{m=0}^{\infty} p_m x^m$ by

$$\sum_{m=0}^{\infty} p_m x^m = \frac{1}{\sum_{n=0}^{\infty} q_n x^n} \quad \overset{\text{equiv.}}{\Longleftrightarrow} \quad \sum_{m,n=0}^{\infty} p_m q_n x^{m+n} = 1, \tag{C.4}$$

or,

$$p_0 = 1/q_0\,, \qquad \sum_{i=0}^{N} p_i q_{N-i} = 0 \quad \text{for} \quad N = 1, 2, 3, \cdots\,. \tag{C.5}$$

Then we can define

$$\begin{aligned}
\tilde{C}_0(\tau) &= \sum_m p_m \Big(\frac{\partial}{\partial u'}\Big)^m \frac{1}{2\pi i} \int_{x_0^2 - i\infty}^{x_0^2 + i\infty} dx^2\, e^{\tau^2 x^2} x^{2au'} C_0(x^{-a}) \\
&= \frac{1}{2\pi i} \int_{x_0^2 - i\infty}^{x_0^2 + i\infty} dx^2\, e^{\tau^2 x^2} x^{2au'} \bigg(\sum_{n=0}^{\infty} q_n (2a \log(x))^n \bigg)^{-1} C_0(x^{-a}),
\end{aligned} \tag{C.6}$$

which is a generalized version of Eq. (3.7) with $x = Q^{-1/a}$. Due to the inverse of an infinite sum in the integrand, the renormalon in the integrand behaves a simple power of x, and renormalon in the dual space can be suppressed by the inverse Laplace transform. Actually,

$$\begin{aligned}
\delta\tilde{C}_0(\tau) &= \sum_m p_m \Big(\frac{\partial}{\partial u'}\Big)^m \frac{1}{2\pi i} \int_{x_0^2 - i\infty}^{x_0^2 + i\infty} dx^2\, e^{\tau^2 x^2} x^{2au'} N_{u_0} \Lambda_{\overline{\rm MS}}^{2u_0} \sum_{n=0}^{\infty} q_n \Big(\frac{\partial}{\partial u_0}\Big)^n x^{2au_0} \\
&= N_{u_0} \Lambda_{\overline{\rm MS}}^{2u_0} \sum_{m,n} p_m q_n \Big(\frac{\partial}{\partial u'}\Big)^m \Big(\frac{\partial}{\partial u_0}\Big)^n f\big(a(u_0 + u'); \tau\big) \\
&= N_{u_0} \Lambda_{\overline{\rm MS}}^{2u_0} \sum_{m,n} p_m q_n \Big(\frac{\partial}{\partial u'}\Big)^{m+n} f\big(a(u_0 + u'); \tau\big) \\
&= N_{u_0} \Lambda_{\overline{\rm MS}}^{2u_0} f\big(a(u_0 + u'); \tau\big),
\end{aligned} \tag{C.7}$$

where

$$f(s;\tau) = \frac{1}{2\pi i} \int_{x_0^2 - i\infty}^{x_0^2 + i\infty} dx^2\, e^{\tau^2 x^2} x^{2s} = \frac{1}{(\tau^2)^{1+s}} \frac{1}{\Gamma(-s)}. \tag{C.8}$$

To suppress the renormalon, we can take the same (a, u') as the ones without the logarithmic corrections, e.g., $u' = -u_0$ and $a = 1$. Then $\delta\tilde{C}_0 = 0$ up to an arbitrary order in the $\log(Q_0^2/Q^2)$ expansion. This means that we can construct an appropriate $\tilde{C}_0$ using the sequence c_n and dual transform.

The inverse transform can be constructed as

$$C_0(Q) = x^{-2au'} \sum_{n=0}^{\infty} q_n (2a \log(x))^n \int_0^{\infty} d\tau^2\, e^{-\tau^2 x^2} \tilde{C}_0(\tau)\,. \tag{C.9}$$

In fact, the right-hand side can be written as

$$
\begin{aligned}
& x^{-2au'} \sum_{m,n} p_m q_n \frac{1}{2\pi i} \int_{x_0'^2-i\infty}^{x_0'^2+i\infty} dx'^2 \int_0^\infty d\tau^2\, e^{-\tau^2(x^2-x'^2)} x'^{2au'} (2a\log(x))^n (2a\log(x'))^m C_0(x'^{-a}) \\
&= x^{-2au'} \sum_{m,n} p_m q_n \frac{1}{2\pi i} \int_{x_0'^2-i\infty}^{x_0'^2+i\infty} dx'^2\, \frac{1}{x^2-x'^2} x'^{2au'} (2a\log(x))^n (2a\log(x'))^m C_0(x'^{-a}) \\
&= x^{-2au'} \sum_{m,n} p_m q_n x^{2au'} (2a\log(x))^{m+n} C_0(x^{-a}) \\
&= C(Q),
\end{aligned}
\tag{C.10}
$$

where we set $x'^2 > x^2$ and use the Cauchy's integral theorem in the third line. The formulation in Chap. 3 is a special case where $q_1 = q_2 = \cdots = 0$.

Secondly, we suppress the leading and next-to-leading renormalons simultaneously. For simplicity of calculation, let us assume that they are at $u = u_0,\, u_0+1$, so that we take $a = 1$. For $k = 0, 1$, we write the renormalons as

$$
\delta C_0^{(k)} = N_{u_0+k} \Lambda_{\overline{\rm MS}}^{2(u_0+k)} \sum_{n=0}^{\infty} q_n^{(k)} \Big(\frac{\partial}{\partial u_0}\Big)^n Q^{-2(u_0+k)}. \tag{C.11}
$$

Similarly to the previous case, we define $\tilde{C}_0(\tau)$ as (note that $a = 1$)

$$
\tilde{C}_0(\tau) = \sum_{l=0}^{1} \tau^{2l} \sum_m p_m^{(l)} \Big(\frac{\partial}{\partial u'}\Big)^m \frac{1}{2\pi i} \int_{x_0^2-i\infty}^{x_0^2+i\infty} dx^2\, e^{\tau^2 x^2} x^{2(u'+l)} C_0(x^{-a}). \tag{C.12}
$$

To suppress the renormalons at $u = u_0,\, u_0+1$ simultaneously, the following equations need to be satisfied for $k = 0, 1$:

$$
\delta\tilde{C}_0'^{(k)} = 0 \;\Leftrightarrow\; \sum_{N=0}^{\infty} \left[\sum_{l=0}^{1} \sum_{i=0}^{N} \tau^{2l} p_i^{(l)} q_{N-i}^{(k)} \Big(\frac{\partial}{\partial u'}\Big)^N f(u_0+u'+l+k;\tau) \right] = 0. \tag{C.13}
$$

As a trial analysis, let us truncate the summation at a fixed N and see if we can find a solution for $\{p_i^{(l)}\}$. The condition reads

$$
\tau^{2s+2} \sum_{i=0}^{N} \left[p_i^{(0)} q_{N-i}^{(k)} \Big(\frac{\partial}{\partial s}\Big)^N f(s;\tau) + p_i^{(1)} q_{N-i}^{(k)} \Big(\frac{\partial}{\partial s}\Big)^N \tau^2 f(s+1;\tau) \right] \Bigg|_{s=u_*+u'+k} = 0, \tag{C.14}
$$

for $k = 0, 1$. Let us set $u' = -u_0$. Noting that $f(s;\tau), \tau^2 f(s+1;\tau) \propto 1/\tau^{2s+2}$, the left-hand side is an $(N-1)$th-order polynomial of $\log\tau$, and we write $\tau^2 f(s+1;\tau) = -(s+1) f(s;\tau) = g(s;\tau)$. Hence,

$$
\tau^{2s+2} \sum_{i=0}^{N} \left[p_i^{(0)} \frac{\partial^N f(s;\tau)}{\partial s^N} + p_i^{(1)} \frac{\partial^N g(s;\tau)}{\partial s^N} \right] q_{N-i}^{(k)} \Bigg|_{s=k} = 0, \tag{C.15}
$$

For $N = 0$ the condition is satisfied for arbitrary $(p_0^{(0)}, p_0^{(1)})$ since $f(k;\tau) = g(k;\tau) = 0$ for $k = 0, 1$. For general N, equating each coefficient of $\log^m(\tau)$ to zero in eq. (C.15), there are $2N$ linear equations for $2(N+1)$ variables $\{p_0^{(0)}, p_0^{(1)}\}, \cdots, \{p_N^{(0)}, p_N^{(1)}\}$, which indicates that there is a non-trivial solution for $\{p_i^{(l)}\}$.

We can construct a non-trivial solution in a more sophisticated way as follows. We define

$$G_{k,l}(x) = \sum_n q_n^{(k)} \Big(\frac{\partial}{\partial u_0}\Big)^n x^{2(u_0+u'+l+k)}, \tag{C.16}$$

and $F_l(x)$ satisfying

$$\begin{pmatrix} G_{0,0} & G_{1,0} \\ G_{0,1} & G_{1,1} \end{pmatrix} \begin{pmatrix} F_0(x) \\ F_1(x) \end{pmatrix} = \begin{pmatrix} \alpha_0 \\ \alpha_1 x^2 \end{pmatrix} x^{2(u_0+u')}, \tag{C.17}$$

where α_0, α_1 are x-independent arbitrary coefficients.[2] In particular, α_k, $F_l(r)$ are τ-independent. If we define

$$\tilde{C}_0(\tau) = \sum_{l=0}^{1} \frac{1}{2\pi i} \int_{x_0^2-i\infty}^{x_0^2+i\infty} dx^2\, e^{\tau^2 x^2} x^{2(u'+l)} C_0(x^{-1}) F_l(x)\,, \tag{C.18}$$

we find that $\delta\tilde{C}_0^{(k)}(\tau) = 0$ for $k = 0, 1$.

$$\begin{aligned}
\because \delta\tilde{C}_0^{(k)}(\tau) &= \sum_{l=0}^{1} \frac{1}{2\pi i} \int_{x_0^2-i\infty}^{x_0^2+i\infty} dx^2\, e^{\tau^2 x^2} x^{2(u'+l)} \delta C_0^{(k)}(x^{-1}) F_l(x) \\
&= N_{u_0+k} \Lambda_{\overline{\rm MS}}^{2(u_0+k)} \sum_{l=0}^{1} \frac{1}{2\pi i} \int_{x_0^2-i\infty}^{x_0^2+i\infty} dx^2\, e^{\tau^2 x^2} \sum_{n=0}^{\infty} q_n^{(k)} \Big(\frac{\partial}{\partial u_0}\Big)^n x^{2(u_0+u'+l+k)} F_l(x) \\
&= N_{u_0+k} \Lambda_{\overline{\rm MS}}^{2(u_0+k)} \frac{1}{2\pi i} \int_{x_0^2-i\infty}^{x_0^2+i\infty} dx^2\, e^{\tau^2 x^2} \sum_{l=0}^{1} G_{k,l}(x) F_l(x) \\
&= N_{u_0+k} \Lambda_{\overline{\rm MS}}^{2(u_0+k)} \alpha_k \frac{1}{2\pi i} \int_{x_0^2-i\infty}^{x_0^2+i\infty} dx^2\, e^{\tau^2 x^2} x^{2(u_0+u'+k)} \\
&= N_{u_0+k} \Lambda_{\overline{\rm MS}}^{2(u_0+k)} \alpha_k\, f(u_0+u'+k;\tau) = 0.
\end{aligned} \tag{C.19}$$

The inverse transform is given by

$$C_0(Q) = \frac{x^{-2u'}}{\alpha_k} \sum_n q_n^{(k)} \Big(2\log(x)\Big)^n \int_0^{\infty} d\tau^2\, e^{-\tau^2 x^2} \tilde{C}_0(\tau)\,. \tag{C.20}$$

We can construct it for either $k = 0$ or 1. (The results are the same.) In fact the

[2] These parameters correspond to $\{p_0^{(0)}, p_0^{(1)}\}$. In the case that the matrix on the left-hand side does not have its inverse, we adjust α_0/α_1 such that $F_l(r)$ have a non-trivial solution.

right-hand side can be written as

$$\frac{x^{-2u'}}{\alpha_k}\sum_{l,n} q_n^{(k)}\Big(2\log(x)\Big)^n \frac{1}{2\pi i}\int_{x_0'^2-i\infty}^{x_0'^2+i\infty} dx'^2 \int_0^\infty d\tau^2\, e^{-\tau^2(x^2-x'^2)} x'^{2(u'+l)} C_0(x'^{-1}) F_l(x)$$

$$= \frac{x^{-2(u_0+u'+k)}}{\alpha_k}\sum_l G_{k,l}(x) F_l(x) C_0(x^{-1}) = C_0(Q). \tag{C.21}$$

Finally we present the formulas corresponding to eqs. (C.6), (C.9), (C.16) and (C.20), after resummation of $\log(Q_0^2/Q^2)$'s. According to eqs. (2.31) and (C.3), the relation between the expansion coefficients in $\log(Q_0^2/Q^2)$ and in $\alpha_s(Q^2)$ is given by

$$\sum_{n=0}^\infty q_n \log^n(Q^{-2}) = (b_0\alpha_s(Q^2))^{\gamma_0/b_0}\sum_{m=0}^\infty s_m(1)\,\alpha_s(Q^2)^m\,. \tag{C.22}$$

Then it is readily seen that the following expression is equivalent to eq. (C.6):

$$\tilde{C}_0(\tau) = \int_{x_0^2-i\infty}^{x_0^2+i\infty}\frac{dx^2}{2\pi i}\,\frac{e^{\tau^2x^2}\,x^{2au'}C_0(x^{-a})}{(b_0\alpha_s(x^{-2a}))^{\gamma_0/b_0}\sum_m s_m(1)\,\alpha_s(x^{-2a})^m}\,. \tag{C.23}$$

This is an RG invariant expression. To obtain an explicit expression of $\tilde{C}_0(\tau)$ up to N^{k}LL, we express the integrand in expansion in $\alpha_s(\mu^2)$, dual transform order by order in $\alpha_s(\mu^2)$ up to the k-th order, and then set $\mu = \tau^a$. Eq. (C.9) can be written as

$$C_0(x^{-a}) = x^{-2au'}\,(b_0\alpha_s(x^{-2a}))^{\gamma_0/b_0}\sum_m s_m(1)\,\alpha_s(x^{-2a})^m\int_0^\infty d\tau^2\,e^{-\tau^2x^2}\tilde{C}_0(\tau)\,. \tag{C.24}$$

Similarly the relation between the expansion coefficients in the case with two renormalons reads

$$\sum_{n=0}^\infty q_n^{(k)}\log^n(Q^{-2}) = (b_0\alpha_s(Q^2))^{\delta_k}\sum_{m=0}^\infty s_m^{(k)}(1)\,\alpha_s(Q^2)^m\,, \tag{C.25}$$

where $\delta_k = \gamma_0^{(k)}/b_0$. The following formulas achieve resummation of logarithms in eqs. (C.16) and (C.20):

$$G_{k,l}(x) = (b_0\alpha_s(x^{-2}))^{\delta_k}\sum_m s_m^{(k)}(1)\,\alpha_s(x^{-2})^m\,x^{2(u_0+u'+l+k)}, \tag{C.26}$$

$$C_0(Q) = \frac{x^{-2u'}}{\alpha_k}\,(b_0\alpha_s(x^{-2}))^{\delta_k}\sum_m s_m^{(k)}(1)\,\alpha_s(x^{-2})^m\int_0^\infty d\tau^2\,e^{-\tau^2x^2}\tilde{C}_0(\tau)\,. \tag{C.27}$$

We anticipate that the formulation presented in this appendix can be extended to the case $a \neq 1$ and $k = 2, 3, 4, \cdots$.

Appendix D

Resummation of UV renormalons in DSRS method

In this appendix, we give the definition of the resummation formula for UV renormalons in the large-β_0 approximation, which is used in the third analysis of Sec. 3.3. In the formula, we introduce a new parameter $\bar{u}$ to suppress UV renormalons. $\tilde{C}_0(\tau)$ can be expressed by the following one-parameter integral form,

$$\begin{aligned}
\tilde{C}_0(\tau) &= \frac{1}{(\tau^2)^{1+au'}} \sum_{n=0}^{\infty} \alpha_s(\mu^2)^{n+1} \tilde{c}_n(L_\tau) \\
&= \frac{1}{(\tau^2)^{1+au'}} \frac{\Gamma(a(\bar{u}+\hat{H}))}{\Gamma(a(\bar{u}+\hat{H}))} \sum_{n=0}^{\infty} \alpha_s(\mu^2)^{n+1} \tilde{c}_n(L_\tau) \\
&= \frac{1}{(\tau^2)^{1+au'}} \int_0^\infty d\zeta\, \zeta^{a(\bar{u}+\hat{H})-1} e^{-\zeta} \sum_{n=0}^{\infty} \alpha_s(\mu^2)^{n+1} \tilde{c}'_n(L_\tau) \\
&= \frac{1}{(\tau^2)^{1+au'}} \int_0^\infty d\zeta\, \zeta^{a\bar{u}-1} e^{-\zeta} \sum_{n=0}^{\infty} \alpha_s(\tau^{2a}\zeta^{-a})^{n+1} \tilde{c}'_n,
\end{aligned} \tag{D.1}$$

where $\tilde{c}'_n$'s can be read from the following relation

$$\sum_{n=0}^{\infty} \alpha_s(\mu^2)^{n+1} \tilde{c}'_n = \frac{1}{\Gamma(a(\bar{u}+\hat{H}))\Gamma(-a(u'+\hat{H}))} \sum_{n=0}^{\infty} \alpha_s(\mu^2)^{n+1} c_n. \tag{D.2}$$

It can be seen that the UV renormalons of $\sum_{n=0}^{\infty} \alpha_s(\mu^2)^{n+1} \tilde{c}'_n$ at $u = -\bar{u}, -\bar{u}-1/a, -\bar{u}-2/a, \cdots$ are suppressed by the $1/\Gamma(a(\bar{u}+\hat{H}))$ factor. In the fourth line of Eq. (D.1), we use the RG running formula given by

$$(\mu^2/\mu'^2)^{\hat{H}} \alpha_s(\mu^2) = \alpha_s(\mu'^2), \tag{D.3}$$

with $\mu^2/\mu'^2 = \zeta^a$.

Then $\left[C_0\right]_\pm$ with UV renormalons resummed is calculated by

$$\begin{aligned}
\left[C_0(Q)\right]_\pm &= x^{-2au'} \int_{C_\mp} d\tau^2\, e^{-\tau^2 x^2} \tilde{C}_0(\tau) \\
&= x^{-2au'} \int_{C_\mp} d\tau^2\, e^{-\tau^2 x^2} \frac{1}{(\tau^2)^{1+au'}} \int_0^\infty d\zeta\, \zeta^{a\bar{u}-1} e^{-\zeta} \sum_{n=0}^\infty \alpha_s(\tau^{2a}\zeta^{-a})^{n+1} \tilde{c}'_n \\
&= x^{-2au'} \int_0^\infty d\zeta\, \zeta^{a(\bar{u}-u')-1} e^{-\xi} \int_{C_\mp} d\tau^2\, e^{-\zeta\tau^2 x^2} \frac{1}{(\tau^2)^{1+au'}} \sum_{n=0}^\infty \alpha_s(\tau^{2a})^{n+1} \tilde{c}'_n \\
&= x^{-2au'} \int_{C_\mp} \frac{d\tau^2}{(\tau^2)^{1+au'}} \frac{\Gamma(a(\bar{u}-u'))}{(1+\tau^2x^2)^{a(\bar{u}-u')}} \sum_{n=0}^\infty \alpha_s(\tau^{2a})^{n+1} \tilde{c}'_n. \qquad \text{(D.4)}
\end{aligned}$$

We note that the above formula cannot extend to the case beyond large-β_0 approximation because the accurate asymptotic behavior due to UV renormalons is unclear.

Appendix E

Derivation of Eq. (4.51)

According to our paper [35][1], $\delta_G(\overline{m}_h)$ is expressed by the one-parameter integral form after the mass renormalization as

$$\begin{aligned}\delta_G(\overline{m}_h) &= \lim_{M\to\infty}\left[\int_0^{M^2}\frac{d\tau}{\pi\tau}\,\mathrm{Im}\,\overline{W}_m\!\left(\frac{\tau}{\overline{m}_h^2}\right)\,\alpha_{\beta_0}(\tau^2) - f_{\mathrm{UV}}\right]\\ &= \int_0^{\infty}\frac{d\tau}{\pi\tau}\,\left[\mathrm{Im}\,\overline{W}_m\!\left(\frac{\tau}{\overline{m}_h^2}\right) - \frac{3C_F}{4}\,\theta(\tau - e^{5/3}\overline{m}_h^2)\right]\alpha_{\beta_0}(\tau^2),\end{aligned} \tag{E.1}$$

where

$$\overline{W}_m(s) = -\frac{C_F}{4\pi}\int_0^1 dx\,\left[(2+2x)\log\left(x^2+s\,x-s-i0\right)+2x\right], \tag{E.2}$$

and α_{β_0} is defined by Eq. (3.2). Eq. (E.1) is ill-defined due to the Landau pole of α_{β_0}, which causes the IR renormalons of $\delta_G(\overline{m}_h)$ in analogy of the DSRS method. The renormalon-free part of δ_G with the same convention as the Borel resummation is obtained by taking a principal value of Eq. (E.1). Furthermore, the imaginary part of $\overline{W}_m$ is calculable in the analytic form as

$$\begin{aligned}\mathrm{Im}\,\overline{W}_m(s) &= \frac{C_F}{4\pi}\,\mathrm{Im}\left[-\alpha^2\log(-1+\alpha)+2\alpha\log(-\alpha)+\alpha^2\log(\alpha)+\big(\alpha\to\beta\big)\right]\\ &= \frac{C_F}{8}\Big(-s^2+(s-2)\sqrt{4s+s^2}\Big),\end{aligned} \tag{E.3}$$

where α and β are roots of the equation $x^2+sx-s-i0=0$. α and β are given by,

$$\alpha = \frac{-s-\sqrt{4s+s^2}}{2},\quad \beta = \frac{-s+\sqrt{4s+s^2}}{2}, \tag{E.4}$$

which follows $-1<\mathrm{Re}\,\alpha<0$, $\mathrm{Im}\,\alpha<0$, $0<\mathrm{Re}\,\beta<1$ and $0<\mathrm{Im}\,\beta<1$. We can see that

$$\lim_{s\to\infty}\mathrm{Im}\,\overline{W}_m(s) = \frac{3C_F}{4}, \tag{E.5}$$

[1]We found a misprint in Eq. (21) of Ref. [35], in which a factor π in the denominator of the second term is unnecessary.

which is canceled by the step function term in Eq. (E.1). Using Eq. (E.3), the principal value of the integral (E.1) is calculated as

$$\begin{aligned}\left[\delta_G(\overline{m}_h)\right]_{\rm PV} &= \frac{C_F}{4\pi b_0}\int_{0,{\rm PV}}^{e^{5/3}} d\tau\,\frac{\tau+(2-\tau)\sqrt{1+4/\tau}}{2}\,\frac{1}{\log(\tau\,\overline{m}_h^2/\Lambda'^2_{\overline{\rm MS}})}\\ &+\frac{C_F}{4\pi b_0}\int_{e^{5/3}}^{\infty} d\tau\left(\frac{\tau+(2-\tau)\sqrt{1+4/\tau}}{2}-\frac{3}{\tau}\right)\frac{1}{\log(\tau\,\overline{m}_h^2/\Lambda'^2_{\overline{\rm MS}})}. \qquad \text{(E.6)}\end{aligned}$$

Appendix F

Renormalon cancellation in $B \to X_c \ell \bar{\nu}$ in the large-β_0 approximation

In this appendix, we explain how the LO renormalon ($u = 1/2$) in the inclusive semileptonic B decay width is canceled by rewriting the quark pole mass by the $\overline{\rm MS}$ mass in the large-β_0 approximation. It can be proved by using a one-parameter integral representation discussed in Sec. 2.2. The total decay width $\Gamma = \Gamma(B \to X_c \ell \bar{\nu})$ in the large-β_0 approximation is calculated as

$$\Gamma = N_\Gamma m_b^5 f_1(\rho) \left[1 + C_F \int_0^\infty \frac{d\tau}{2\pi\tau} w_\gamma(\tau/m_b^2,\, \rho) \alpha_{\beta_0}(\tau^2) \right], \tag{F.1}$$

with

$$N_\Gamma = \frac{G_F^2 |V_{cb}|^2}{192\pi^3}, \tag{F.2}$$

$$f_1(\rho) = 1 - 8\rho^2 - 12\rho^4 \log(\rho^2) + 8\rho^6 - \rho^8 \tag{F.3}$$

and $\rho = m_c/m_b$. All-order corrections are resummed to the running coupling constant

$$\alpha_{\beta_0}(\tau^2) = \frac{\alpha_s(\mu^2)}{1 - b_0 \alpha_s(\mu^2) \log(\mu^2\, e^{5/3}/\tau)}. \tag{F.4}$$

$w_\gamma(\tau/\overline{m}_b^2,\, \rho)$ is a structure function of the LO loop diagrams with τ being a square of the momentum of the internal gluon. From Eq. (3.2) of Ref. [19], the function $w_\gamma(\tau/m_b^2, \rho)$ for small τ can be read as

$$w_\gamma(\tau/m_b^2, \rho) = h_1(\rho) \frac{\sqrt{\tau}}{m_b} + \mathcal{O}(\tau/m_b^2), \tag{F.5}$$

where

$$\begin{aligned} h_1(\rho) = \frac{1}{f_1(\rho)} \big(& 5 - 16\rho - 24\rho^2 - 24\rho^3 + 24\rho^4 + 48\rho^5 - 8\rho^6 - 8\rho^7 + 3\rho^8 \\ & - 48\rho^3 \log(\rho^2) - 12\rho^2 \log(\rho^2) \big). \end{aligned} \tag{F.6}$$

Eq. (F.5) implies that Γ expressed in terms of the pole mass m_h has the $u = 1/2$ renormalon. Now, Γ is expressed by rewriting m_h by the $\overline{\rm MS}$ mass $\overline{m}_h$ to explicitly see the cancellation of the $u = 1/2$ renormalon. The relation between the pole mass and the $\overline{\rm MS}$ mass is given by

$$m_h = \overline{m}_h \left[1 + \int_0^\infty \frac{d\tau}{2\pi\tau} w_m(\tau/\overline{m}_b^2) \alpha_{\beta_0}(\tau^2) \right], \tag{F.7}$$

where w_m in $1/m_b$ expansion can be read from Eq. (E.6) as

$$w_m(\tau/\overline{m}_b^2) = -C_F \frac{\sqrt{\tau}}{\overline{m}_b} + \mathcal{O}(\tau/\overline{m}_b^2). \tag{F.8}$$

Sources of $u = 1/2$ renormalon in Eq. (F.1) are identified as m_b^5, $f_1(\rho)$ and w_γ. Their expansion forms in $1/\overline{m}_h$ are given by

$$\begin{aligned} m_b^5 &= \overline{m}_b^5 \left[1 + 5 \int_0^\infty \frac{d\tau}{2\pi\tau} w_m(\tau/\overline{m}_b^2) \alpha_{\beta_0}(\tau^2) + \mathcal{O}(\Lambda_{\rm QCD}^2/\overline{m}_b^2) \right] \\ &= \overline{m}_b^5 \left[1 - \frac{5C_F}{\overline{m}_b} \int_0^\infty \frac{d\tau}{2\pi\tau} \sqrt{\tau} \alpha_{\beta_0}(\tau^2) + \mathcal{O}(\Lambda_{\rm QCD}^2/\overline{m}_b^2) \right], \end{aligned} \tag{F.9}$$

$$\begin{aligned} f_1(\rho) &= f_1(\bar\rho) \left[1 + \frac{f_1'(\bar\rho)}{f_1(\bar\rho)} \bar\rho \int_0^\infty \frac{d\tau}{2\pi\tau} \Big(w_m(\tau/\overline{m}_c^2) - w_m(\tau/\overline{m}_b^2) \Big) \alpha_{\beta_0}(\tau^2) + \mathcal{O}(\Lambda_{\rm QCD}^2/\overline{m}_h^2) \right] \\ &= f_1(\bar\rho) \left[1 - \frac{C_F}{\overline{m}_b} \frac{f_1'(\bar\rho)}{f_1(\bar\rho)} (1-\bar\rho) \int_0^\infty \frac{d\tau}{2\pi\tau} \sqrt{\tau} \alpha_{\beta_0}(\tau^2) + \mathcal{O}(\Lambda_{\rm QCD}^2/\overline{m}_h^2) \right], \end{aligned} \tag{F.10}$$

and

$$\begin{aligned} C_F \int_0^\infty \frac{d\tau}{2\pi\tau} w_\gamma(\tau/m_b^2,\, \rho) \alpha_{\beta_0}(\tau^2) &= C_F \int_0^\infty \frac{d\tau}{2\pi\tau} h_1(\rho) \frac{\sqrt{\tau}}{m_b} \alpha_{\beta_0}(\tau^2) + \mathcal{O}(\Lambda_{\rm QCD}^2/m_h^2) \\ &= \frac{C_F}{\overline{m}_b} h_1(\bar\rho) \int_0^\infty \frac{d\tau}{2\pi\tau} \sqrt{\tau} \alpha_{\beta_0}(\tau^2) + \mathcal{O}(\Lambda_{\rm QCD}^2/\overline{m}_h^2), \end{aligned} \tag{F.11}$$

where $\bar\rho = \overline{m}_c/\overline{m}_b$ and we use

$$\rho/\bar\rho = 1 + \int_0^\infty \frac{d\tau}{2\pi\tau} \Big(w_m(\tau/\overline{m}_c^2) - w_m(\tau/\overline{m}_b^2) \Big) \alpha_{\beta_0}(\tau^2) + \mathcal{O}(\Lambda_{\rm QCD}^2/\overline{m}_h^2). \tag{F.12}$$

Finally we obtain

$$\Gamma = N_\Gamma \overline{m}_b^5 f_1(\bar\rho) \left[1 + \frac{F_{1/2}(\bar\rho)}{\overline{m}_b} \int_0^\infty \frac{d\tau}{2\pi\tau} \sqrt{\tau} \alpha_{\beta_0}(\tau^2) + \mathcal{O}(\Lambda_{\rm QCD}^2/\overline{m}_h^2) \right], \tag{F.13}$$

with

$$F_{1/2}(\bar\rho) = -5C_F - C_F \frac{f_1'(\bar\rho)}{f_1(\bar\rho)} (1-\bar\rho) + C_F h_1(\bar\rho) = 0, \tag{F.14}$$

which indicates for Γ to be free from the $u = 1/2$ renormalon after rewriting a pole mass to $\overline{\rm MS}$ mass. It is non-trivial that the $\rho = m_c/m_b$ dependence of Γ is essentially important for this excellent cancellation. In the limit $m_c \to 0$, in which the B meson decays to the up-type hadrons and $\ell\bar\nu$, the second term in Eq. (F.14) vanishes.

Appendix G

Determination of $|V_{cb}|$ at N^{3}LO level using 1S state mass of bottomonium

In this appendix, we explain the detailed calculation of the Wilson coefficient in the $|V_{cb}|$ determination at N^{3}LO level using 1S state mass of bottomonium $M_{\bar{b}b(1\mathrm{S})}$. The perturbative calculated part of 1S mass in terms of the pole mass m_b is given by

$$\frac{M_{\bar{b}b(1\mathrm{S})}}{2m_b} = 1 + \sum_{n=1}^{3} \varepsilon^n e_n\big(\overline{m}_c/M_{\bar{b}b(1\mathrm{S})}, \alpha_s\big), \tag{G.1}$$

where we use the ε-expansion [25, 26] instead of the usual α_s expansion. The ε-expansion is a convenient framework which can treat the $u = 1/2$ renormalon properly, whereas the order counting in α_s is not appropriate in the situation that the typical scale or the Bohr radius of the bottomonium depends on α_s as $(\frac{1}{2}C_F\alpha_s m_b)^{-1}$. Each coefficient of ε depends on α_s. The parameter ε is finally set to one. For the mass relation Eq. (G.1), we basically use the results in ref. [101] but we consider the internal charm mass effects beyond the linear approximation in $\overline{m}_c/M_{\bar{b}b(1\mathrm{S})}$ using the results in ref. [7]. For the charm quark, we use the relation between the pole and the MS masses up to the $\mathcal{O}(\alpha_s^3)$ order given in App. A. We include non-decoupling effects of the bottom quark using the results in ref. [7], although the effects turned out to be small as in App. A.

In this analysis, the LO Wilson coefficient of the decay width is also given in the ε-expansion as

$$C^{\Gamma}_{\bar{Q}Q}(m_c/m_b, \alpha_s) = \sum_{n=0}^{3} \varepsilon^n \alpha_s (m_b^2)^n X_n(\rho), \tag{G.2}$$

where coefficient X_n is given in App. A. We make a remark on the $u = 1/2$ renormalon cancellation in the product $m_b^5 C^{\Gamma}_{\bar{Q}Q}$ Since the Wilson coefficient $C^{\Gamma}_{\bar{Q}Q}$ is calculated by treating the charm quark as massive, its renormalon uncertainty is actually that of three-flavor QCD. To cancel the renormalon in the product $m_b^5 C^{\Gamma}_{\bar{Q}Q}$, the renormalon uncertainty of m_b should also be that of three-flavor QCD. We therefore need to consider internal charm mass effects on the mass relation for consistency. Related to this, we consider the three-flavor running coupling constant $\alpha_s = \alpha_s^{(3)}$ as it is natural in this situation.

Using Eq. (G.1), we rewrite m_b in Eq. (G.2) in terms of $M_{\bar{b}b(1\mathrm{S})}/2$. In this process we use the flavor threshold relation in App. A to express the series in terms of $\alpha_s^{(3)}$. The

charm quark pole mass m_c is expressed in terms of $\overline{m}_c$. Then we obtain

$$m_b^5 C_{\bar{Q}Q}^{\Gamma}(m_c/m_b, \alpha_s) = m_{1\mathrm{S}}^5 \sum_{n=0}^{3} \varepsilon^n X_n^{1\mathrm{S}}\big(\overline{m}_c/m_{1\mathrm{S}}, \alpha_s\big), \tag{G.3}$$

with $m_{1\mathrm{S}} = M_{\bar{b}b(1\mathrm{S})}/2$. After rewriting the quark pole masses, the ε-expansion shows a good convergence. Using $M_{\bar{b}b(1\mathrm{S})} = M_{\Upsilon(1\mathrm{S})} = 9.46030$ GeV and the PDG values of $\overline{m}_c$ and α_s as inputs, we obtain

$$\sum_{n=0}^{3} \varepsilon^n X_n^{1\mathrm{S}}\big(\overline{m}_c/m_{1\mathrm{S}}, \alpha_s\big) = 0.5903 - 0.0836\varepsilon - 0.0281\varepsilon^2 - 0.0070\varepsilon^3, \tag{G.4}$$

and using $M_{\bar{b}b(1\mathrm{S})} = M_{\eta_b(1\mathrm{S})} = 9.3987$ GeV, we obtain

$$\sum_{n=0}^{3} \varepsilon^n X_n^{1\mathrm{S}}\big(\overline{m}_c/m_{1\mathrm{S}}, \alpha_s\big) = 0.5863 - 0.0797\varepsilon - 0.0294\varepsilon^2 - 0.0073\varepsilon^3. \tag{G.5}$$

The detailed procedure of the determination of $|V_{cb}|$ is explained in Ref. [60].

Bibliography

[1] P. A. Baikov, K. G. Chetyrkin and J. H. Kühn, "Higgs Decay, Z Decay and the QCD Beta-Function," Acta Phys. Polon. B **48** (2017), 2135 [arXiv:1711.05592 [hep-ph]].

[2] C. Anzai, Y. Kiyo and Y. Sumino, "Static QCD Potential at Three-Loop Order," Phys. Rev. Lett. **104** (2010), 112003 [arXiv:0911.4335 [hep-ph]].

[3] A. V. Smirnov, V. A. Smirnov and M. Steinhauser, "Three-Loop Static Potential," Phys. Rev. Lett. **104** (2010), 112002 [arXiv:0911.4742 [hep-ph]].

[4] R. N. Lee, A. V. Smirnov, V. A. Smirnov and M. Steinhauser, "Analytic Three-Loop Static Potential," Phys. Rev. D **94** (2016) no.5, 054029 [arXiv:1608.02603 [hep-ph]].

[5] P. Marquard, A. V. Smirnov, V. A. Smirnov and M. Steinhauser, "Quark Mass Relations to Four-Loop Order in Perturbative QCD," Phys. Rev. Lett. **114** (2015) no.14, 142002 [arXiv:1502.01030 [hep-ph]].

[6] P. Marquard, A. V. Smirnov, V. A. Smirnov, M. Steinhauser and D. Wellmann, "$\overline{\text{Ms}}$-On-Shell Quark Mass Relation Up to Four Loops in QCD and a General Su(N) Gauge Group," Phys. Rev. D **94** (2016) no.7, 074025 [arXiv:1606.06754 [hep-ph]].

[7] M. Fael, K. Schönwald and M. Steinhauser, "Exact Results for Z_m^{OS} and Z_2^{Os} with Two Mass Scales and Up to Three Loops," JHEP **10** (2020), 087 [arXiv:2008.01102 [hep-ph]].

[8] D. J. Gross and A. Neveu, "Dynamical Symmetry Breaking in Asymptotically Free Field Theories," Phys. Rev. D **10** (1974), 3235

[9] B. E. Lautrup, "On High Order Estimates in Qed," Phys. Lett. B **69** (1977), 109-111

[10] G. 't Hooft, "Can we make sense out of "Quantum Chromodynamics?"", lectures given at the "Ettore Majorana" Int. School of Subnuclear Physics, Erice, July 1977.

[11] M. Beneke, "Renormalons," Phys. Rept. **317**, 1 (1999). [hep-ph/9807443].

[12] U. Aglietti and Z. Ligeti, "Renormalons and Confinement," Phys. Lett. B **364** (1995), 75 [arXiv:hep-ph/9503209 [hep-ph]].

[13] M. Beneke and V. M. Braun, "Heavy Quark Effective Theory Beyond Perturbation Theory: Renormalons, the Pole Mass and the Residual Mass Term," Nucl. Phys. B **426** (1994), 301-343 [arXiv:hep-ph/9402364 [hep-ph]].

[14] I. I. Y. Bigi, M. A. Shifman, N. G. Uraltsev and A. I. Vainshtein, "The Pole mass of the heavy quark: Perturbation theory and beyond," Phys. Rev. D **50**, 2234-2246 (1994) [arXiv:hep-ph/9402360 [hep-ph]].

[15] A. Pineda, "Heavy Quarkonium And Nonrelativistic Effective Field Theories," Ph.D. Thesis (1998).

[16] A. H. Hoang, M. C. Smith, T. Stelzer and S. Willenbrock, "Quarkonia and the pole mass," Phys. Rev. D **59**, 114014 (1999) [arXiv:hep-ph/9804227 [hep-ph]].

[17] M. Beneke, "A Quark mass definition adequate for threshold problems," Phys. Lett. B **434**, 115-125 (1998) [arXiv:hep-ph/9804241 [hep-ph]].

[18] M. Neubert and C. T. Sachrajda, "Cancellation of Renormalon Ambiguities in the Heavy Quark Effective Theory," Nucl. Phys. B **438** (1995), 235-260 [arXiv:hep-ph/9407394 [hep-ph]].

[19] P. Ball, M. Beneke and V. M. Braun, "Resummation of Running Coupling Effects in Semileptonic B Meson Decays and Extraction of —V(Cb)—," Phys. Rev. D **52** (1995), 3929-3948 [arXiv:hep-ph/9503492 [hep-ph]].

[20] A. A. Penin and N. Zerf, "Bottom Quark Mass from Υ Sum Rules to $\mathcal{O}(\alpha_s^3)$," JHEP **04** (2014), 120 [arXiv:1401.7035 [hep-ph]].

[21] Y. Kiyo, G. Mishima and Y. Sumino, "Determination of M_C and M_B from Quarkonium 1S Energy Levels in Perturbative QCD, " Phys. Lett. B **752** (2016) 122 Erratum: [Phys. Lett. B **772** (2017) 878] [arXiv:1510.07072 [hep-ph]].

[22] M. Beneke, A. Maier, J. Piclum and T. Rauh, "Nnnlo Determination of the Bottom-Quark Mass from Non-Relativistic Sum Rules," PoS **RADCOR2015** (2016), 035 [arXiv:1601.02949 [hep-ph]].

[23] A. Bazavov *et al.* [Fermilab Lattice, MILC and TUMQCD], "Up-, Down-, Strange-, Charm-, and Bottom-Quark Masses from Four-Flavor Lattice QCD," Phys. Rev. D **98** (2018) no.5, 054517 [arXiv:1802.04248 [hep-lat]].

[24] C. Peset, A. Pineda and J. Segovia, "The Charm/Bottom Quark Mass from Heavy Quarkonium at N^3LO," JHEP **09** (2018), 167 [arXiv:1806.05197 [hep-ph]].

[25] A. H. Hoang, Z. Ligeti and A. V. Manohar, "B Decays in the Upsilon Expansion," Phys. Rev. D **59** (1999), 074017 [arXiv:hep-ph/9811239 [hep-ph]].

[26] A. H. Hoang, Z. Ligeti and A. V. Manohar, "B Decay and the Upsilon Mass," Phys. Rev. Lett. **82** (1999), 277-280 [arXiv:hep-ph/9809423 [hep-ph]].

[27] A. Alberti, P. Gambino, K. J. Healey and S. Nandi, "Precision Determination of the Cabibbo-Kobayashi-Maskawa Element V_{cb}, " Phys. Rev. Lett. **114** (2015) no. 6, 061802 [arXiv:1411.6560 [hep-ph]].

[28] A. Bazavov, N. Brambilla, X. Garcia Tormo, i, P. Petreczky, J. Soto and A. Vairo, "Determination of α_s from the QCD static energy," Phys. Rev. D **86** (2012), 114031 [arXiv:1205.6155 [hep-ph]].

[29] K. G. Wilson, "Nonlagrangian Models of Current Algebra," Phys. Rev. **179** (1969) 1499.

[30] A. H. Mueller, "On the Structure of Infrared Renormalons in Physical Processes at High-Energies," Nucl. Phys. B **250** (1985), 327-350

[31] M. Neubert, "Scale setting in QCD and the momentum flow in Feynman diagrams," Phys. Rev. D **51**, 5924 (1995) [hep-ph/9412265].

[32] M. Beneke and V. M. Braun, "Naive non-abelianization and resummation of fermion bubble chains," Phys. Lett. B **348** (1995) 513 [hep-ph/9411229].

[33] Y. Sumino, "Static QCD potential at $r < \Lambda_{\rm QCD}^{-1}$: Perturbative expansion and operator-product expansion," Phys. Rev. D **76**, 114009 (2007) [arXiv:hep-ph/0505034 [hep-ph]].

[34] G. Mishima, Y. Sumino and H. Takaura, "Subtracting Infrared Renormalons from Wilson Coefficients: Uniqueness and Power Dependences on Λ_{QCD}," Phys. Rev. D **95** (2017) no.11, 114016 [arXiv:1612.08711 [hep-ph]].

[35] Y. Hayashi and Y. Sumino, "UV contributions to energy of a static quark-antiquark pair in large β_0 approximation," Phys. Lett. B **795** (2019), 107-112 [arXiv:1904.02563 [hep-ph]].

[36] N. Brambilla, A. Pineda, J. Soto and A. Vairo, "The Infrared behavior of the static potential in perturbative QCD," Phys. Rev. D **60**, 091502 (1999) [arXiv:hep-ph/9903355 [hep-ph]].

[37] Y. Sumino and H. Takaura, "On Renormalons of Static QCD Potential at $u = 1/2$ and 3/2," JHEP **05** (2020), 116 [arXiv:2001.00770 [hep-ph]].

[38] H. Takaura, T. Kaneko, Y. Kiyo and Y. Sumino, "Determination of α_s from static QCD potential with renormalon subtraction," Phys. Lett. B **789**, 598-602 (2019) [arXiv:1808.01632 [hep-ph]].

[39] H. Takaura, T. Kaneko, Y. Kiyo and Y. Sumino, "Determination of α_s from static QCD potential: OPE with renormalon subtraction and lattice QCD," JHEP **04**, 155 (2019) [arXiv:1808.01643 [hep-ph]].

[40] Y. Hayashi, Y. Sumino and H. Takaura, "New method for renormalon subtraction using Fourier transform," Phys. Lett. B **819** (2021), 136414 [arXiv:2012.15670 [hep-ph]].

[41] Y. Hayashi, Y. Sumino and H. Takaura, "Renormalon subtraction in OPE using Fourier transform: Formulation and application to various observables," JHEP **02** (2022), 016 [arXiv:2106.03687 [hep-ph]].

[42] Y. Hayashi, "Renormalon Subtraction Using Fourier Transform: Analyses of Simplified Models," JHEP **06** (2022), 157 [arXiv:2112.14408 [hep-ph]].

[43] T. Lee, "Surviving the renormalon in heavy quark potential," Phys. Rev. D **67**, 014020 (2003) [arXiv:hep-ph/0210032 [hep-ph]].

[44] C. Ayala, X. Lobregat and A. Pineda, "Superasymptotic and Hyperasymptotic Approximation to the Operator Product Expansion," Phys. Rev. D **99** (2019) no.7, 074019 [arXiv:1902.07736 [hep-th]].

[45] C. Ayala, X. Lobregat and A. Pineda, "Hyperasymptotic Approximation to the Top, Bottom and Charm Pole Mass," Phys. Rev. D **101** (2020) no.3, 034002 [arXiv:1909.01370 [hep-ph]].

[46] C. Ayala, X. Lobregat and A. Pineda, "Determination of $\alpha(M_z)$ from an Hyperasymptotic Approximation to the Energy of a Static Quark-Antiquark Pair," [arXiv:2005.12301 [hep-ph]].

[47] H. Takaura, "Formulation for renormalon-free perturbative predictions beyond large-β_0 approximation," JHEP **10**, 039 (2020) [arXiv:2002.00428 [hep-ph]].

[48] E. Eichten and B. R. Hill, "An Effective Field Theory for the Calculation of Matrix Elements Involving Heavy Quarks," Phys. Lett. B **234** (1990), 511-516

[49] H. Georgi, "An Effective Field Theory for Heavy Quarks at Low-Energies," Phys. Lett. B **240** (1990), 447-450

[50] B. Grinstein, "The Static Quark Effective Theory," Nucl. Phys. B **339** (1990), 253-268

[51] T. Mannel, W. Roberts and Z. Ryzak, "A Derivation of the Heavy Quark Effective Lagrangian from QCD," Nucl. Phys. B **368** (1992), 204-217

[52] M. Neubert, "Heavy Quark Symmetry," Phys. Rept. **245** (1994), 259-396 [arXiv:hep-ph/9306320 [hep-ph]].

[53] A. V. Manohar and M. B. Wise, "Heavy Quark Physics," Camb. Monogr. Part. Phys. Nucl. Phys. Cosmol. **10** (2000) 1.

[54] R. L. Workman *et al.* [Particle Data Group], "Review of Particle Physics," PTEP **2022**, 083C01 (2022)

[55] A. Crivellin and S. Pokorski, "Can the Differences in the Determinations of V_{ub} and V_{cb} Be Explained by New Physics?," Phys. Rev. Lett. **114** (2015) no.1, 011802 [arXiv:1407.1320 [hep-ph]].

[56] M. Fael, M. Rahimi and K. K. Vos, "New Physics Contributions to Moments of Inclusive $b \to c$ Semileptonic Decays," [arXiv:2208.04282 [hep-ph]].

[57] M. Fael, K. Schönwald and M. Steinhauser, "Third Order Corrections to the Semileptonic $b \to c$ and the Muon Decays," Phys. Rev. D **104** (2021) no.1, 016003 [arXiv:2011.13654 [hep-ph]].

[58] M. Bordone, B. Capdevila and P. Gambino, "Three Loop Calculations and Inclusive V_{cb}," Phys. Lett. B **822** (2021), 136679 [arXiv:2107.00604 [hep-ph]].

[59] F. Bernlochner, M. Fael, K. Olschewsky, E. Persson, R. van Tonder, K. K. Vos and M. Welsch, "First Extraction of Inclusive V_{cb} from q^2 Moments," JHEP **10** (2022), 068 [arXiv:2205.10274 [hep-ph]].

[60] Y. Hayashi, Y. Sumino and H. Takaura, "Determination of $|V_{cb}|$ using N^{3}LO perturbative corrections to $\Gamma(B \to X_c \ell \nu)$ and 1S masses," Phys. Lett. B **829** (2022), 137068 [arXiv:2202.01434 [hep-ph]].

[61] A. G. Grozin, P. Marquard, J. H. Piclum and M. Steinhauser, "Three-Loop Chromomagnetic Interaction in HQET," Nucl. Phys. B **789** (2008), 277-293 [arXiv:0707.1388 [hep-ph]].

[62] M. E. Luke and A. V. Manohar, "Reparametrization Invariance Constraints on Heavy Particle Effective Field Theories," Phys. Lett. B **286** (1992), 348-354 [arXiv:hep-ph/9205228 [hep-ph]].

[63] T. Mannel and K. K. Vos, "Reparametrization Invariance and Partial Re-Summations of the Heavy Quark Expansion," JHEP **06**, 115 (2018) [arXiv:1802.09409 [hep-ph]].

[64] R. Tarrach, "The Pole Mass in Perturbative QCD," Nucl. Phys. B **183** (1981), 384-396

[65] N. Gray, D. J. Broadhurst, W. Grafe and K. Schilcher, "Three Loop Relation of Quark (Modified) Ms and Pole Masses," Z. Phys. C **48**, 673-680 (1990)

[66] K. G. Chetyrkin and M. Steinhauser, "Short Distance Mass of a Heavy Quark at Order α_s^3," Phys. Rev. Lett. **83** (1999), 4001-4004 [arXiv:hep-ph/9907509 [hep-ph]].

[67] K. G. Chetyrkin and M. Steinhauser, "The Relation Between the Ms-bar and the On-Shell Quark Mass at Order α_s^3," Nucl. Phys. B **573** (2000), 617-651 [arXiv:hep-ph/9911434 [hep-ph]].

[68] K. Melnikov and T. v. Ritbergen, "The Three Loop Relation Between the Ms-bar and the Pole Quark Masses," Phys. Lett. B **482** (2000), 99-108 [arXiv:hep-ph/9912391 [hep-ph]].

[69] K. Melnikov and T. van Ritbergen, "The Three Loop On-Shell Renormalization of QCD and QED," Nucl. Phys. B **591** (2000), 515-546 [arXiv:hep-ph/0005131 [hep-ph]].

[70] C. Ayala, G. Cvetič and A. Pineda, "The Bottom Quark Mass from the $\Upsilon(1S)$ System at Nnnlo," JHEP **09** (2014), 045 [arXiv:1407.2128 [hep-ph]].

[71] M. E. Luke, M. J. Savage and M. B. Wise, "Charm Mass Dependence of the $O(\alpha_s^2 n_f)$ Correction to Inclusive $B \to X_c e \nu_e$Decay," Phys. Lett. B **345** (1995), 301-306 [arXiv:hep-ph/9410387 [hep-ph]].

[72] M. Trott, "Improving Extractions of —V(Cb)— and M(B) from the Hadronic Invariant Mass Moments of Semileptonic Inclusive B Decay," Phys. Rev. D **70** (2004), 073003 [arXiv:hep-ph/0402120 [hep-ph]].

[73] V. Aquila, P. Gambino, G. Ridolfi and N. Uraltsev, "Perturbative Corrections to Semileptonic B Decay Distributions," Nucl. Phys. B **719** (2005), 77-102 [arXiv:hep-ph/0503083 [hep-ph]].

[74] A. Pak and A. Czarnecki, "Mass Effects in Muon and Semileptonic $b \to c$ Decays," Phys. Rev. Lett. **100** (2008), 241807 [arXiv:0803.0960 [hep-ph]].

[75] A. Pak and A. Czarnecki, "Heavy-To-Heavy Quark Decays at NNLO," Phys. Rev. D **78** (2008), 114015 [arXiv:0808.3509 [hep-ph]].

[76] K. Melnikov, "$O(\alpha_s^2)$ Corrections to Semileptonic Decay $b \to c\ell\nu$," Phys. Lett. B **666** (2008), 336-339 [arXiv:0803.0951 [hep-ph]].

[77] M. Dowling, J. H. Piclum and A. Czarnecki, "Semileptonic Decays in the Limit of a Heavy Daughter Quark," Phys. Rev. D **78** (2008), 074024 [arXiv:0810.0543 [hep-ph]].

[78] I. I. Y. Bigi, N. G. Uraltsev and A. I. Vainshtein, "Nonperturbative Corrections to Inclusive Beauty and Charm Decays: QCD Versus Phenomenological Models," Phys. Lett. B **293** (1992), 430-436 [erratum: Phys. Lett. B **297** (1992), 477-477] [arXiv:hep-ph/9207214 [hep-ph]].

[79] B. Blok, L. Koyrakh, M. A. Shifman and A. I. Vainshtein, "Differential Distributions in Semileptonic Decays of the Heavy Flavors in QCD," Phys. Rev. D **49** (1994), 3356 [erratum: Phys. Rev. D **50** (1994), 3572] [arXiv:hep-ph/9307247 [hep-ph]].

[80] A. V. Manohar and M. B. Wise, "Inclusive Semileptonic B and Polarized $Lambda_b$ Decays from QCD," Phys. Rev. D **49** (1994), 1310-1329 [arXiv:hep-ph/9308246 [hep-ph]].

[81] A. Alberti, P. Gambino and S. Nandi, "Perturbative Corrections to Power Suppressed Effects in Semileptonic B Decays," JHEP **01** (2014), 147 [arXiv:1311.7381 [hep-ph]].

[82] I. I. Y. Bigi, M. A. Shifman, N. G. Uraltsev and A. I. Vainshtein, "Sum Rules for Heavy Flavor Transitions in the SV Limit," Phys. Rev. D **52** (1995), 196-235 [arXiv:hep-ph/9405410 [hep-ph]].

[83] I. I. Y. Bigi, M. A. Shifman, N. Uraltsev and A. I. Vainshtein, "High Power n of m_b in Beauty Widths and $n = 5 \to \infty$ Limit," Phys. Rev. D **56** (1997), 4017-4030 [arXiv:hep-ph/9704245 [hep-ph]].

[84] P. Ball, M. Beneke and V. M. Braun, "Resummation of $(\beta_0\alpha_s)^N$ Corrections in QCD: Techniques and Applications to the Tau Hadronic Width and the Heavy Quark Pole Mass," Nucl. Phys. B **452** (1995), 563-625 [arXiv:hep-ph/9502300 [hep-ph]].

[85] M. Neubert, "Exploring the Invisible Renormalon: Renormalization of the Heavy Quark Kinetic Energy," Phys. Lett. B **393** (1997), 110-118 [arXiv:hep-ph/9610471 [hep-ph]].

[86] H. Takaura, "Renormalons in Static QCD Potential: Review and Some Updates," Eur. Phys. J. ST **230** (2021) no.12-13, 2593-2600 [arXiv:2106.01194 [hep-ph]].

[87] Y. Aoki *et al.* [Flavour Lattice Averaging Group (FLAG)], "Flag Review 2021," Eur. Phys. J. C **82** (2022) no.10, 869 [arXiv:2111.09849 [hep-lat]].

[88] C. W. Bauer, Z. Ligeti, M. Luke, A. V. Manohar and M. Trott, "Global Analysis of Inclusive B Decays," Phys. Rev. D **70** (2004), 094017 [arXiv:hep-ph/0408002 [hep-ph]].

[89] Y. S. Amhis *et al.* [HFLAV], "Averages of b-Hadron, c-Hadron, and τ-lepton Properties as of 2018," Eur. Phys. J. C **81** (2021) no.3, 226 [arXiv:1909.12524 [hep-ex]].

[90] P. Urquijo *et al.* [Belle], "Moments of the Electron Energy Spectrum and Partial Branching Fraction of $B \to X_c e\bar{\nu}$ Decays at Belle," Phys. Rev. D **75** (2007), 032001 [arXiv:hep-ex/0610012 [hep-ex]].

[91] B. Aubert *et al.* [BaBar], "Measurement and Interpretation of Moments in Inclusive Semileptonic Decays $\bar{B} \to X_c \ell \bar{\nu}$," Phys. Rev. D **81** (2010), 032003 [arXiv:0908.0415 [hep-ex]].

[92] J. P. Lees *et al.* [BaBar], "Measurement of the Inclusive Electron Spectrum from B Meson Decays and Determination of —Vub—," Phys. Rev. D **95** (2017) no.7, 072001 [arXiv:1611.05624 [hep-ex]].

[93] A. H. Mahmood *et al.* [CLEO], "Measurement of the B-Meson Inclusive Semileptonic Branching Fraction and Electron Energy Moments," Phys. Rev. D **70** (2004), 032003 [arXiv:hep-ex/0403053 [hep-ex]].

[94] S. Aoki *et al.* [Flavour Lattice Averaging Group], "FLAG Review 2019: Flavour Lattice Averaging Group (FLAG)," Eur. Phys. J. C **80**, no.2, 113 (2020) [arXiv:1902.08191 [hep-lat]].

[95] Y. Kiyo and Y. Sumino, "Full Formula for Heavy Quarkonium Energy Levels at Next-To-Next-To-Next-To-Leading Order," Nucl. Phys. B **889** (2014), 156-191 [arXiv:1408.5590 [hep-ph]].

[96] S. Recksiegel and Y. Sumino, "Fine and Hyperfine Splittings of Charmonium and Bottomonium: an Improved Perturbative QCD Approach," Phys. Lett. B **578** (2004), 369-375 [arXiv:hep-ph/0305178 [hep-ph]].

[97] B. A. Kniehl, A. A. Penin, A. Pineda, V. A. Smirnov and M. Steinhauser, "$M(\eta_b)$ and α_s from Nonrelativistic Renormalization Group," Phys. Rev. Lett. **92** (2004), 242001 [erratum: Phys. Rev. Lett. **104** (2010), 199901] [arXiv:hep-ph/0312086 [hep-ph]].

[98] F. Abudinén *et al.* [Belle-II], "Measurement of the Inclusive Semileptonic B Meson Branching Fraction in 62.8 Fb^{-1} of Belle II Data," [arXiv:2111.09405 [hep-ex]].

[99] K. G. Chetyrkin, B. A. Kniehl and M. Steinhauser, "Strong Coupling Constant with Flavor Thresholds at Four Loops in the $\overline{\mathrm{MS}}$ Scheme," Phys. Rev. Lett. **79** (1997), 2184-2187 [arXiv:hep-ph/9706430 [hep-ph]].

[100] A. H. Hoang and C. Regner, "Borel Representation of τ Hadronic Spectral Function Moments in Contour-Improved Perturbation Theory," Phys. Rev. D **105** (2022) no.9, 096023 [arXiv:2008.00578 [hep-ph]].

[101] A. H. Hoang, "Bottom Quark Mass from Upsilon Mesons: Charm Mass Effects," [arXiv:hep-ph/0008102 [hep-ph]].